4-2019

The Role of Inflammatory Pathways in Development, Growth, and Metabolism of Skeletal Muscle in IUGR Offspring; Blood Gene Expression of Inflammatory Factors as Novel Biomarkers for Assessing Stress and Wellbeing in Exotic Species.

Robert J. Posont
University of Nebraska-Lincoln, rjposont3@gmail.com

The Role of Inflammatory Pathways in Development, Growth, and Metabolism of Skeletal Muscle in IUGR Offspring; Blood Gene Expression of Inflammatory Factors as Novel Biomarkers for Assessing Stress and Wellbeing in Exotic Species.

Robert Posont
University of Nebraska-Lincoln, rjposont3@gmail.com

THE ROLE OF INFLAMMATORY PATHWAYS IN DEVELOPMENT, GROWTH, AND METABOLISM OF SKELETAL MUSCLE IN IUGR OFFSPRING; BLOOD GENE EXPRESSION OF INFLAMMATORY FACTORS AS NOVEL BIOMARKERS FOR ASSESSING STRESS AND WELLBEING IN EXOTIC SPECIES.

by

Robert J. Posont

A THESIS

Presented to the Faculty of

The Graduate College at the University of Nebraska

In Partial Fulfillment of Requirements

For the Degree of Master of Science

Major: Animal Science

Under the Supervision of Professor Dustin T. Yates

Lincoln, Nebraska

April 2019

THE ROLE OF INFLAMMATORY PATHWAYS IN DEVELOPMENT, GROWTH, AND METABOLISM OF SKELETAL MUSCLE IN IUGR OFFSPRING; BLOOD GENE EXPRESSION OF INFLAMMATORY FACTORS AS NOVEL BIOMARKERS FOR ASSESSING STRESS AND WELLBEING IN EXOTIC SPECIES.

Robert Joseph Posont, M.S.

University of Nebraska, 2019

Advisor: Dustin Yates

Our first study identified the effects of maternal inflammation-induced intrauterine growth restriction (**MI-IUGR**) on growth and muscle glucose metabolism in offspring supplemented with curcumin. MI-IUGR lambs exhibited asymmetric growth restriction at birth and 30d of age, but normal glucose-stimulated insulin secretion. Hindlimb glucose oxidation was reduced by MI-IUGR and not improved by curcumin supplementation. *Ex vivo* muscle glucose oxidation was reduced by MI-IUGR but improved somewhat by curcumin. These finding indicate that fetal programming responses to MI contribute to neonatal growth and metabolic deficits. Neonatal curcumin supplementation had minimal effect on growth deficits but may improve glucose metabolism.

Our second study identified programmed mechanistic changes that explain intrinsic functional deficits in myoblasts from maternal hyperthermia-induced IUGR fetal sheep. Myoblasts were incubated with TNFα, TNFα with IKK inhibitor (**IKKi**), or IL6. Proliferation in IUGR myoblasts was less than controls in basal and IL6-spiked media. IKKi decreased proliferation in all myoblasts, but more in IUGR myoblasts. IUGR myoblasts differentiated less than controls, and TNFα further reduced their

differentiation. TNFα increased *TLR4* mRNA in all myoblasts, but more in IUGR myoblasts. *TNFR1* and *ULK2* mRNA was greater in IUGR myoblasts. *IL6* and *TNFR1* mRNA and c-Fos protein were greater in IUGR semitendinosus muscle, but IκB content was reduced. These results demonstrate intrinsic enhancement of inflammatory signaling and IKK pathways in IUGR myoblasts, which coincided with reduced functional capacity.

A final study assessed stress-responsive mRNA biomarkers in blood. MI at mid-gestation altered blood mRNA expression in pregnant rats and fetuses. Blood *TNFR1* was increased in IUGR fetuses, but not when dams received meloxicam. Fetal *IL6R* and maternal *TNFR1* were reduced by IUGR with or without meloxicam. We also designed ddPCR probes/primers to assess stress-responsive transcripts including cytokines/receptors in blood from elephants, cheetahs, and giraffes. These studies demonstrate stress-induced changes in blood transcriptomes of animals, which represent novel stress biomarkers.

Acknowledgements

The pursuit of scientific research is far from an individual effort. Rarely is a paper published with only a single name, and the research presented in this thesis is no exception to the rule. These pages hold thousands of data points obtained over two years. This is thanks, in no small part, to the individuals listed below.

Firstly, my advisor Dr. Dustin Yates and his wife Lily deserve more thanks than I could ever convey in words alone. It amazes me to this day that Dr. Yates was willing to offer me a position in his lab, but for some reason he decided to take a chance on me. His patience and encouragement during my M.S. program despite my inclination to turn in papers that had as much in common with a certain Tolstoy novel in their length and scientific content than a true manuscript have shaped me into a confident and independent researcher. Dr. Yates' constant support and dedication to my success have allowed me to grow as a researcher and as a person. Dr. Yates and his wife Lily made me feel like I was part of a family…rather than simply a lab. From the opportunities he has offered me to the support of the entire Yates' family and the time that they have all dedicated to my success it has been my sincerest pleasure to be a part of his lab. I will forever be grateful for the time I've spent under his tutelage.

I'd like to thank my lab-mates Caitlin Cadaret, Joslyn Beard, Rachel Gibbs, Rebecca Swanson, and Taylor Barnes for their tireless support. These individuals have dedicated an immense amount of their time and energy to ensure my success. They lost many an hour of sleep feeding lambs at 4am and entire days at a time to make sure that the 40 metabolic studies and 20 necropsies in the second chapter were successful. Very few people would be willing to give up visiting their families for the holidays or entire weekends to support research. I will never be able to thank them enough for their support and will forever be indebted to them for their help during these past two years.

I entered into this position naïve to research and this document would have not been possible if not for the support and patience of our lab manager Kristin Beede. Kristin spent countless hours in the lab teaching me everything from basic concepts to day-long protocols as I worked toward this degree. She constantly put the needs of our work above her own and sacrificed her time to make sure that my projects were completed. Any research with live animals is prone to ever changing plans, but Kristin was ready to adapt and more than once her forethought saved a study. She remains one of my best resources for research techniques, and it has been my pleasure to learn from and work alongside her these past two years.

I would also like to thank my committee members Dr. Jessica Petersen and Dr. Jason Herrick for their willingness to support me as I pursued this degree. Their guidance helped me to understand my research and their dedication to my education has allowed me to build my confidence as a researcher and achieve my goals. Dr. Petersen was integral in helping me design cross-species primers and her patience as I worked to design my primers was greatly appreciated. Dr. Herrick's enthusiastic support of my intended future research was critical to my success. Without his collaboration and

continued support, the final chapter of this thesis would not have been possible. It has been my pleasure to work with both of these individuals during my M.S. career, and I look forward to collaborating with them in the future.

I would be remiss if I didn't acknowledge and thank Ms. Lisa Graham, Mr. Gary Brown, and Dr. David Lovejoy. In 8th grade we seldom consider what our future career might be. Mr. Brown's enthusiasm for science and engaging teaching methods introduced me to the concept in a way that challenged my idea of what the future might hold. Similarly, I would not be where I am today without the support of Ms. Lisa Graham. Without her support as I sought an education outside Nebraska, I may never have attended the University of Toronto during my undergraduate career. Finally, I would like to extend my thanks to Dr. David Lovejoy. Between his frequent Star Trek references, and humorous anecdotes, I found a passion for endocrinology during my time at UofT, and his course on stress, physiology and reproduction is the reason I pursued my degree in this field.

Finally, I would like to acknowledge and thank my parents. They have worked tirelessly to provide me with the opportunity to pursue my goals and supported me at every step in my life. From conversations over Sunday crepes to week long fishing trips they have listened to me blather on about my passions, hopes and dreams, and now my research. They sacrificed countless hours of their lives outside of their full-time jobs to support me in every facet of my life, and even in retirement continue to make sure that I have every opportunity to succeed. These two individuals were my advisors long before I entered into academia and remain the two most important role models in my life. While I might not be following in either of their footsteps, I will forever strive to be half the amazing and successful human beings that they are today. There is not enough superfluous language, nor space in this document to express how much they mean to me. Without their love and support I would not be where I am or who I am today. Regardless, of what my future might hold it is my sincerest hope that I can continue to make them proud and achieve the goals they have given me the opportunity to pursue.

Table of Contents

List of Figures

List of Tables

Chapter 1: Literature Review

Introduction

Intrauterine growth restriction (IUGR) is a leading cause of perinatal morbidity and mortality in both humans and animals (Alisi et al., 2011). Impaired growth and development can result from a plethora of maternal stressors such as obesity, inflammation, malnutrition, and environmental stress (Valsamakis et al., 2006). Previous studies have linked IUGR to disproportionately reduced skeletal muscle growth during prenatal development (Padoan et al., 2004; Yates et al., 2014). IUGR offspring present with reduced muscle mass and increased risk of developing metabolic disorders at all stages of life (Godfrey and Barker, 2000; Yates et al., 2018). These offspring continue to demonstrate deficits in skeletal muscle growth throughout their lifespan (Greenwood et al., 2000). Regardless of maternal insult, fetal growth restriction is usually caused by reduced nutrient transfer to the fetus due to placental insufficiency leading to IUGR (PI-IUGR) (Baschat, 2004; Cox and Marton, 2009). This leads to a poor *in utero* environment during development and subjects the fetus to chronic hypoxemia, hypoglycemia, hypertension, and hyperlactatemia (Thorn et al., 2011). In response, adaptations occur in the fetal tissues to repartition nutrients to vital organs, leading to impaired skeletal muscle growth and changes in leukocyte cell populations and phenotypes (Godfrey and Barker, 2000; Martinez et al., 2014; Yates et al., 2018). These adaptations, although beneficial *in utero,* lead to impaired metabolic function and restricted skeletal muscle growth capacity throughout the lifespan. This “thrifty phenotype” was first described by Hales and Barker (1992), who originally linked fetal

adaptations that lower birthweight to an increased risk of developing metabolic diseases in adulthood. Epidemiological and seminal research studies describe the health outcomes of these adaptations (Joyce et al., 2001; Sharma et al., 2016; Camacho et al., 2017b). However, little is known about the underlying molecular mechanisms, particularly the role that inflammation and other stress system signaling pathways play in the development of these adaptions and the resulting IUGR phenotype.

Fetal Skeletal Muscle Growth and Development

Forty-percent of total body mass in the uncompromised term fetus is comprised of skeletal muscle, which is found predominantly in the hindlimbs, neck and trunk areas (Bentzinger et al., 2012; Felber et al., 2013; Brown, 2014). Muscle fibers are composed from myoblasts that fuse during early prenatal development to form singular fibers with multiple peripherally-located nuclei (Zammit et al., 2006; McCarthy et al., 2011). This differentiates skeletal muscle from both cardiac and smooth muscle. Due to the presence of actin and myosin filaments, which are responsible for the contraction and function, skeletal muscle appears straited. This organ is highly metabolic, relying on both internal and external stores of glucose and fatty acids for energy (Bentzinger et al., 2012; Felber et al., 2013). Skeletal muscle is active throughout life and after birth continues to undergo growth *via* hypertrophy, whereby existing fibers incorporate new myonuclei via additional myoblast fusion (McCarthy et al., 2011). Hyperplasia, which is the formation of new fibers from resident satellite stem cell populations is rare after birth in most species, making the initial populations of fibers and myoblasts established *in utero* a crucial point in development (Bentzinger et al., 2012).

Myogenesis

Skeletal muscle plays a crucial role in glucose homeostasis and the metabolic health of an individual, making its proper development and growth an imperative part of development (Felber et al., 2013; Brown, 2014). Skeletal muscle develops in stages, which together form a process known as myogenesis. Myogenesis begins during embryogenesis with the migration of somatic mesoderm progenitor cells, which terminally differentiate into myoblasts upon arrival at the various sites of skeletal muscle formation (Bentzinger et al., 2012). These cells undergo stepwise proliferation, differentiation, and fusion to form the polynuclear myofibers that make up skeletal muscle (Mitchell et al., 2002). Initial development produces primary myofibers, which become the scaffolding for subsequent skeletal muscle fibers. This occurs early on in development and is typically completed halfway through the first trimester of pregnancy (Sambasivan and Tajbakhsh, 2007). Late in the first trimester, secondary myofibers form along these initial primary fibers but, unlike primary fibers, may not run the full length of the developing muscle (Wilson et al., 1992). Early in the third trimester of pregnancy, tertiary fibers appear around the existing primary and secondary fibers, completing the myogenic process (Bentzinger et al., 2012). Together, these stages of myogenesis (**Figure 1-1**) establish all myofiber populations before birth in most mammals, thus fiber number remains static postnatal. Further growth occurs via fiber hypertrophy and requires the incorporation of resident myoblasts to increase myonuclear content and nuclear protein synthetic capacity as illustrated in **Figure 1-1**.

Myogenic regulators of skeletal muscle growth

Throughout the myogenic process, the transcription factors shown in **Figure 1-1** are expressed at specific stages, allowing this process to be tightly regulated. Initial activation of myoblasts involves the expression of two paired-box (Pax) transcription factors, *Pax3* and *Pax7*, the latter of which acts as markers for these cells (Sambasivan and Tajbakhsh, 2007; Bentzinger et al., 2012). *Pax3* is critical for the migration and establishment of the founder cell populations early in development, however it is not exclusively expressed by skeletal muscle myoblasts (Bentzinger et al., 2012). Alternatively, *Pax7* is exclusive to myoblast populations and is responsible for establishing satellite cell pools and secondary fibers during the later stages of development and is one of the preferred markers for myoblast populations after birth along with myogenic factor 5 (myf5) (Seale et al., 2000; Soto et al., 2017). These pools of satellite cells are normally quiescent after birth acting as a reserve population capable of proliferating after injury regenerating muscle in a process known as hypertrophy (Morgan and Partridge, 2003). Terminal differentiation of myoblasts requires the sequential expression of a series of transcription factors belonging to the basic-Helix-Loop-Helix (bHLH) family: myogenic differentiation factor 1 (myoD), myf5, and myogenin (Molkentin et al., 1995; Soto et al., 2017). Early in development, dermomyotome cells mature into a primitive muscle structure known as the myotome, which expresses high levels of myf5 followed by increased levels of myoD, marking them as active muscle stem cells and initiating the transformation from stem cell to muscle progenitor cells (Rudnicki et al., 1993; Bentzinger et al., 2012). The initial expression of myf5 within these cell populations is typically coincident with the

expression of *Pax7* and proliferating cell nuclear antigen (PCNA) (Yates et al., 2014). This expression profile marks these progenitor cells as active myoblasts destined for proliferation and differentiation (Punch et al., 2009; Bentzinger et al., 2012). Terminal differentiation of myoblasts during late gestation and postnatal begins with the onset of myoD expression committing these myoblasts to differentiation (Brown, 2014; Yates et al., 2014). As myogenin expression then increases, myoblasts begin to fuse and form the myofibers that comprise skeletal muscle (Brown, 2014; Yates et al., 2014). Increased myogenin expression causes differentiated myoblasts and myofibers to begin expressing the type III intermediate filament known as desmin, which is responsible for the structural development of the contractile unit of skeletal muscle called the sarcomere (Paulin and Li, 2004). Both desmin and myogenin continue to be expressed by fetal skeletal muscle throughout the gestational period and in postnatal skeletal muscle, marking the continued fusion of myoblasts and myonuclear accumulation of myofibers (Andrés and Walsh, 1996; Paulin and Li, 2004; Brown, 2014). Newly formed fibers also begin to express myosin heavy chain (MyHC) isoforms, marking them as functional units capable of contractile motion (Brown, 2014). MyHC help to further classify the muscle fiber type and function within heterogeneous populations present in most skeletal muscles, as discussed in the next section (Yates et al., 2016). Together, these transcription factors and structural proteins serve as biomarkers for distinct stages of the myogenic progression of myoblasts during development and postnatal during hypertrophy (**Figure 1-1**).

Skeletal muscle growth late in gestation and postnatal must rely on existing myoblast populations that reside adjacent to the muscle fibers and facilitate myofiber

hypertrophy (Allen et al., 1979; Yates et al., 2014). During proliferation, a sub-population of myoblasts does not differentiate or fuse to form fibers, instead becoming populations of satellite cells, quiescent skeletal muscle stem cells (Morgan and Partridge, 2003). These are present adjacent to muscle fibers between the sarcolemma and the endomysium throughout the lifespan of the organism (Yates et al., 2014; Soto et al., 2017). Upon injury, upregulation of muscle growth, mechanical activities such as exercise, or cell death, satellite cells may become activated. Most newly-activated satellite cells then proliferate and differentiate before fusing with existing muscle fibers, thus adding nuclei and increasing protein synthesis capacity (Anderson et al., 2006; Brown, 2014). A subset remains Pax7-positive/ myoD- negative and re-establish satellite cell populations in a process known as self-renewal. Thus, populations of satellite cells are maintained by asymmetric divisions and stored within the stem cell niche of the muscle itself, providing the mechanism for growth of skeletal muscle fibers (Zammit et al., 2004; Jones and Wagers, 2008; Yates et al., 2014). Myoblasts that commit to differentiation demonstrate an increase in myoD expression (Bismuth and Relaix, 2010). High levels of myoD cause myoblasts to exit the cell cycle, allowing most of the cells to differentiate (Zammit et al., 2004; Brown, 2014). Subsequent upregulation of myogenin by myoD induces terminal differentiation, whereby myoblasts become capable of fusing with myofibers (Brown, 2014; Yates et al., 2014; Soto et al., 2017). These two mechanisms allow for the maintenance of the muscle stem cell pool, while also maintaining a readily available source of satellite cells for muscle growth. The number of satellite cells present typically decreases with age, making the proper development and size of initial populations crucial to future skeletal muscle growth capacity (Morgan and Partridge, 2003; Brown, 2014).

Perturbations in the establishment of this population during fetal development will have lifelong negative consequences for muscle mass and the metabolic health of the individual.

Skeletal Muscle Fiber Types, Metabolic Phenotypes, and Relative Abundances

Skeletal muscle in mammalian species have heterogeneous populations of skeletal muscle fibers consisting of four different types, each with their own metabolic phenotypes and contractile characteristics (Spangenburg and Booth, 2003; Yates et al., 2016). Fiber type categories are defined by their metabolic phenotypes, twitch speed, and strength of contraction upon stimulation (Schiaffino and Reggiani, 2011; Brown, 2014). The proportions of fiber types within a muscle group can change over time based on the influence that the environment or other extrinsic factors have on the metabolic, or functional, demand of the muscle (Schiaffino and Reggiani, 2011; Yates et al., 2016). Fiber types are identified by MyHC isoforms that are indicative of the fibers metabolic activity, which can be broadly classified as either fast or slow twitch (Spangenburg and Booth, 2003; Yates et al., 2016). Type I skeletal muscle fibers are the slow-twitch fiber found throughout the body. These fibers are characterized by their red color due to the high content of myoglobin and can be identified by expression of the MyHC-I isoform (Schiaffino and Reggiani, 2011; Yates et al., 2016). Type I fibers exhibit high rates of oxidative metabolism, increased mitochondria. and myoglobin content, larger nerve terminals and motor endplate areas, a less developed sarcoplasmic reticulum, and higher cytosolic free calcium (Schiaffino and Reggiani, 2011; Wang and Pessin, 2013). These fibers favor oxidative phosphorylation as their primary metabolic pathway and, as their name implies, contract slowly and generate less mechanical force relative to other fiber

types (Spangenburg and Booth, 2003)**.** Type I fibers are more fatigue resistant due to a greater content of mitochondria and thicker Z lines, which mark the boundaries of individual sarcomeres where thin actin fibers attach (Schiaffino and Reggiani, 2011).

Type II fast-twitch fibers can be delineated into three subgroups, which are Type IIa, IIx, and IIb (Wang and Pessin, 2013). Type IIa fibers represent an intermediary population between Type I and the other Type II fibers. These fibers are anatomically red in color and maintain a higher content of mitochondria than other Type II fibers, relying on both oxidative and glycolytic pathways to generate energy for their contractile force (Schiaffino and Reggiani, 2011). Type IIa fibers can be distinguished from the other fast-twitch types by their high levels of succinate dehydrogenase (SDH) activity, the presence of slow twitch motor units, and expression of MyHC-IIa (Spangenburg and Booth, 2003; Schiaffino and Reggiani, 2011). In pigs and rodents, Type IIb fibers are anatomically white in color due to the low amounts of mitochondria and myoglobin they contain. They express the MyHC-IIb isoform (Schiaffino and Reggiani, 2011). These fibers are defined as a fast-fatiguing, glycolytic populations that rely primarily on ATPase activity and present with low levels of SDH activity (Schiaffino and Reggiani, 2011). They are predominantly found in the lower extremities or hindlimbs and can generate a large contractile force. They are quick to fatigue due to the low abundance of myoglobin and capillary content (Spangenburg and Booth, 2003; Wang and Pessin, 2013). Humans, cattle, sheep, and most other non-litter bearing mammals express the mRNA transcript for Type IIb myosin but cannot produce the MyHC-IIb protein (Schiaffino and Reggiani, 2011). Type IIx fast-twitch fibers are an intermediary population of fibers that are instead expressed by these mammals (Schiaffino and Reggiani, 2011). These fibers are

anatomically white and rely on glycolytic metabolism to generate energy for contractile force (Larsson et al., 1991). They have contractile shortening velocities similar to Type IIa fibers, but present with less of ATPase and SDH activity and less resistance to fatigue relative to Type IIa fibers (Larsson et al., 1991). Type IIx fibers are identified by their expression of MyHC-IIx (Schiaffino and Reggiani, 2011). In addition to morphological and contractile differences fiber types can also be categorized by their metabolic phenotypes. Type I fibers demonstrate the greatest rate of insulin-stimulated glucose uptake making them the most insulin-sensitive of the fiber types (Yates et al., 2016). Type IIx fibers demonstrate the lowest insulin-stimulated glucose uptake rates with Type IIa fibers representing an intermediate population between Type I and Type IIx myofibers (Yates et al., 2016).

Skeletal Muscle Glucose Metabolism

Insulin regulation of skeletal muscle glucose utilization

Skeletal muscle accounts for approximately 40% of total body mass in most mammals but it is responsible for upwards of 65% of total glucose consumption and 85% of insulin-stimulated glucose metabolism (Felber et al., 2013; Brown, 2014). Glucose is the primary source for energy production within skeletal muscle, and the maintenance of homeostatic levels is primarily facilitated by insulin-sensitive skeletal muscle (Mizgier et al., 2014). Systemic glucose consumption is regulated in part by the action of insulin, with increased circulating levels associated with higher rates of glucose uptake into skeletal muscle (Leney and Tavaré, 2009). Increased circulating blood glucose stimulates the production and secretion of insulin from pancreatic β-cells, leading to inhibition of hepatic gluconeogenesis and stimulation of glucose uptake by skeletal muscle for

utilization or storage (Aronoff et al., 2004). Changes in uptake rates are facilitated by insulin-dependent translocation of GLUT-4 transporters expressed by skeletal muscle, which rapidly translocate from the cytoplasm to the plasma membrane following insulin stimulation (Limesand et al., 2007; Leney and Tavaré, 2009; Pinto-Junior et al., 2018). Skeletal muscle also expresses low levels of GLUT-1 transporters, which are ubiquitously expressed throughout the body and operate in an insulin-independent manner (Ebeling et al., 1998; Limesand et al., 2007).

Metabolic pathways for glucose utilization

Beginning in late gestation, increased blood glucose levels in the body lead to the release of insulin, stimulating uptake of glucose by skeletal muscle (Hay et al., 1988). After uptake, glucose can be utilized by a number of different metabolic pathways shown in **Figure 1-2**. The relative activity of each pathway is dependent on the fiber type composition of the muscle. Upon entry into the cell, glucose is converted to the metabolic intermediate glucose-6-phosphate, which is then utilized via one of three major pathways (Jensen and Richter, 2012). Initial formation of Glucose-6-phosphate (G-6-P) is mediated by the enzyme Hexokinase II (HK2), an irreversible step in skeletal muscle (Petersen and Shulman, 2002; Jensen and Richter, 2012). G-6-P can be stored as the polysaccharide glycogen, providing the muscle with stores of energy that can be rapidly mobilized and utilized later. Glucose utilized for immediate metabolization will undergo the process of glycolysis. Glucose within this pathway is metabolized via a series of enzymatic interactions to two 3-carbon pyruvate molecules (Bouché et al., 2004). This process generates a relatively small amount of ATP and NADH (Bouché et al., 2004). Under aerobic conditions, pyruvate will enter into the mitochondria where it is utilized in the

TCA cycle to generate large amounts of NADH and $FADH_2$. These high-energy electron carriers are then utilized by the electron transport chain for oxidative phosphorylation (Nelson et al., 2008). The process of oxidative phosphorylation is more time consuming than glycolysis, however it represents a much more efficient use of glucose by producing approximately 36 net ATP per glucose molecule compared to the approximately 2 net ATP produced by glycolysis (Nelson et al., 2008). Under nutrient poor conditions such as those experience by a PI-IUGR fetus, a large amount of pyruvate will instead be metabolized into lactate (Bouché et al., 2004). Unlike glucose, lactate can then be secreted by skeletal muscle to help maintain energy substrate levels within the body (Bouché et al., 2004). Lactate excreted from skeletal muscle can travel to the liver, where it is reformed into glucose via gluconeogenesis in a process called the Cori cycle (Cori, 1931). Lactate can also be utilized by cardiac muscle as a source of energy under nutrient or oxygen restricted conditions (Kemppainen et al., 2002). A reduction in glucose oxidation coincident with an increase in the less efficient glycolytic lactate production is commonly associated with increases in adrenergic and inflammatory activity. It is also a characteristic of individuals with metabolic syndrome (Bouché et al., 2004; Limesand et al., 2007; Cadaret et al., 2017).

Metabolic regulation by insulin and IGF-I pathways

Insulin is the primary regulator of blood glucose concentrations. This protein hormone is secreted by the β cells located in the islets of Langerhans within the pancreas (Fu et al., 2013). Pancreatic β cells sense changes in blood glucose concentrations and release insulin in corresponding amounts to maintain homeostatic levels within the blood. Tissues and organs with high energy requirements, such as skeletal muscle rely on

glucose as their primary source of energy and skeletal muscle stores it as glycogen for rapid metabolism during periods of high energy output (Horowitz et al., 2001; Mizgier et al., 2014). The insulin signaling cascade for skeletal muscle is shown in **Figure 1-3**. First, insulin binds to its tyrosine kinase receptor, leading to the phosphorylation of the downstream docking proteins, insulin receptor substrates (IRS) (Krook et al., 2000). IRS-1 and IRS-2 are the primary types found in skeletal muscle (Krook et al., 2000; Boucher et al., 2014). Their phosphorylation by IR leads to the activation of the key signaling mediator phosphatidylinositol 3-kinase (PI3K) (Krook et al., 2000; Sarbassov et al., 2005). PI3K is responsible for the transmitting activation signals of multiple pathways involved in glucose transport and metabolism within skeletal muscle. The canonical PI3K-mediated pathway is the activation of 3-phosphphoinositide-dependent protein kinase 1 (PDK-1) and its subsequent phosphorylation of the AGC protein kinase family including Akt1, p70 ribosomal S6 kinase (S6K), and protein kinase C (PKC) (Pearce et al., 2010). Phosphorylation of Thr308 leads to the partial activation of Akt1, which is a key mediator of metabolism within skeletal muscle (Sarbassov et al., 2005). This initial phosphorylation leads to the translocation of Akt1 to the plasma membrane (Dan et al., 2016) where further activation occurs by the additional phosphorylation of a serine residue (S437) by the mammalian target of rapamycin (mTOR) complex-2 (Sarbassov et al., 2005; Dan et al., 2016). Activation of Akt inhibits protein degradation by inactivating forkhead box O (Foxo) via phosphorylation and also stimulates glycogen and protein synthesis within skeletal muscle (Sano et al., 2003; Boucher et al., 2014). Akt also stimulates glucose uptake via activation of the mammalian target of rapamycin complex 1 (mTORC1) and increases lipolysis via phosphorylation of peroxisome proliferator

activated receptor gamma coactivator 1-alpha (PGC-1α) (Takaishi et al., 1999; Sano et al., 2003; Düvel et al., 2010; Boucher et al., 2014).

Insulin-like growth factors (IGF-I, IGF-II) along with growth hormone are the primary mediators of tissue growth and differentiation (Dupont and LeRoith, 2001; Boucher et al., 2010). However, studies have demonstrated that these are pleiotropic hormones with differing tissue-specific effects (Baker et al., 1993; Westwood et al., 2001). Similar to insulin, binding of IGF to their tyrosine receptor complexes leads to the activation of downstream signaling cascades, beginning with the phosphorylation of IRS, which then activates the PI3K-Akt1 pathway (Boucher et al., 2010). Although they utilize similar pathways as insulin downstream of receptor binding, IGF-I and II stimulate a wide range of cellular functions associated with growth and differentiation distinct from those of insulin (Coolican et al., 1997; Boucher et al., 2010). IGF-II is implicit in development and growth of the placenta, and IGF-I concentrations in fetal blood are directly correlated with *in utero* growth and birthweight (Brice et al., 1989; Ogilvy-Stuart et al., 1998). However, the downstream activation of mTORC1 and FoxO3 mediated pathways is still achieved by IGF-receptor binding. This elicits insulin-like effects on protein cycling and glucose metabolism, suggesting that IGFs work synergistically with insulin (Di Cola et al., 1997). Normal signal transduction of insulin and IGF pathways (**Figure 1-3**) is crucial for fetal skeletal muscle growth, fetal development, and metabolism (Rosenthal and Cheng, 1995; Thorn et al., 2011).

The Immune System

Hematopoiesis and Fetal Development

Like myogenesis, the development of the immune system is a highly-ordered process that occurs in progressive stages throughout gestation (Pagenkemper and Diemert, 2014). Hematopoetic stem cells (HSC) begin developing in the yolk sac early in embryogenesis, with the first functional cells appearing late in the first trimester of pregnancy (Mikkola et al., 2006). The definitive origins of HSC populations remains unclear, but functional populations can be detected within the yolk sac, aortagonadmesonephros region (AGM), and placenta by the end of the first trimester (Ciriza et al., 2013). The placenta plays a critical role in the development of HSC by facilitating rapid expansion and even *in situ* generation of new cells (Mikkola et al., 2006). This occurs during mid-gestation in mice with an almost 15-fold increase in HSC numbers compared to the AGM populations (Mikkola et al., 2005; Mikkola et al., 2006). Regardless of their site of origin, the fetal liver is the main site of expansion and differentiation of HSC before they migrate to their respective immunological organs (Ciriza et al., 2013). Immunological cells and their products are scarce in early development to avoid premature activation and allow for these cells to mature during development (Ygberg and Nilsson, 2012). High intrauterine production of pro-inflammatory cytokines can be associated with growth restriction and, if severe, abortion (Ygberg and Nilsson, 2012). However, both naive innate and adaptive immune cells are present in appreciable amounts by birth (Ygberg and Nilsson, 2012; Simon et al., 2015).

After birth, the cells of the immune system and all of the cellular elements of blood arise from progenitor cells in the bone marrow termed pluripotent hematopoietic

stem cells (pHSC) (Janeway Jr. et al., 2001). Innate and adaptive immune responses depend on the activities of leukocytes, which facilitate the complex interactions between these two overlapping arms of the immune system. Together, these two evolutionarily conserved systems coordinate to protect the body from infectious agents, confer lifelong immunity, and serve as a robust defense to the wide range of pathogenic microorganisms present in the postnatal environment (Janeway Jr. et al., 2001).

The Innate Immune Response

The majority of cells in the innate immune system shown in **Figure 1-4,** arise from a pHSC-derivative population of progenitors known as the common myeloid progenitors (CMP) (Janeway Jr. et al., 2001). The skin and mucosal epithelia also provide an additional first line of defense against infection and are considered to be part of this system (Gleeson et al., 1982; Nikolovski et al., 2008). CMP-derived progenitor cells termed granulocyte/macrophage progenitor cells (GMP) form the entire population of innate immune cells with the exception of lymphoid progenitor-derived natural killer (NK) cells (Janeway Jr. et al., 2001). Most leukocytes within the innate immune system perform phagocytosis, the process of engulfing pathogens (Janeway Jr. et al., 2001). These are identified *via* cell-surface pattern recognition receptors such as the members of the toll-like receptor family (TLR), which serve to bridge the gap between innate and adaptive immune responses (Alberts et al., 2002). This group of cells is collectively known as phagocytes and act as a non-specific defense against pathogens *via* recognition of pathogen associated molecules (PAMP) (Alberts et al., 2002). The subpopulation of phagocytes known as monocyte/macrophages are involved in metabolic regulation via interactions with endocrine pathways involved in metabolism (Alberts et al., 2002;

Cadaret et al., 2017). Macrophages are tissue resident phagocytes that play a critical role in pathogen recognition and inflammatory modulation (Meshkani and Vakili, 2016; Cadaret et al., 2017). Monocytes are circulating populations of bone marrow derived cells that patrol the lymphatic and circulatory system (Alberts et al., 2002). After recruitment to sites of infection or inflammation, monocytes infiltrate tissue and become macrophages, leading to the combined terminology monocyte/macrophage (Alberts et al., 2002). Together with dendritic cells (DC), monocyte/macrophages represent a critical link between the innate and adaptive immune systems by acting as professional antigen presenting cells (APCs) (Alberts et al., 2002). APC are responsible for presenting processed epitopes in the presence of co-signaling factors such as major histocompatibility complexes I and II (MHC-I/II) to naïve T-cells (Triozzi and Aldrich, 1997; Oehler et al., 1998; Alberts et al., 2002). This MHC-I/II signaling cascade leads to the activation of the adaptive immune component and a conserved antigen-specific immune response. Monocyte/macrophage activity, TLR signaling pathways, and central signaling vis NF$\boldsymbol{\kappa}$B are universal to all host's innate defense system (Janeway et al., 2001a). The conservation of these pathways across mammalian species, vertebrates, and many non-vertebrates allows research on these critical pathways to be applied to most species.

The Adaptive Immune Response

Unlike the innate immune response, the adaptive immune system (**Figure 1-4**) is specific to particular pathogens (Alberts et al., 2002). It is responsible for the clearance of cells presenting processed PAMP and for long-lived protection against future infection by specific pathogens (Janeway Jr. et al., 2001; Alberts et al., 2002). The two major cell

types involved in adaptive immunity are T-cells and B-cells, collectively classified as lymphocytes (Janeway et al., 2001b). Lymphocytes arise from the common lymphoid progenitor (CLP) within bone marrow where B-cell maturation also occurs (Janeway Jr. et al., 2001). Alternatively, T-cells migrate to the thymus before maturation can occur (Zinkernagel, 1978). The differences in maturation sites give rise to the differential classification. The adaptive immune system relies on clonal selection (CST), a theory first posited in the early 1950s by Drs. Burnet and Talmage (Talmage, 1957). Mammals and some non-mammalian species, first generate a large and diverse population of lymphocytes that undergo commitment within primary lymphoid organs (Talmage, 1957). These cells then undergo rapid clonal expansion upon activation by a particular antigen specific to their cell surface receptor (Talmage, 1957; Alberts et al., 2002). Since its initial introduction, CST has been adapted to fit more recent findings regarding the response and development of lymphocytes. These include the phenomenon of somatic hypermutation in B-cell populations and self/non-self tolerance (Silverstein, 2002).

T-cell populations can be separated into two categories, which together comprise the cellular response of the adaptive immune system (Janeway Jr. et al., 2001). Cluster of differentiation 8 (CD8)-positive cells known as cytotoxic T-cells facilitate the destruction of infected non-self cells and contribute to the memory response (Busch et al., 1998). CD4-positive T-cells are called helper T-cells and can be sub-categorized by their cytokine expression profiles and roles within the immune system into Th1, Th2, Th17, and Treg populations (Zhu et al., 2010). This diverse population of cells mediates a number of critical functions of the immune system, such as B-cell antibody production, $CD8^+$ activity, macrophage regulation, orchestration of systemic immune response,

suppression of the immune response, and regulation of the magnitude and length of the immune response (Mosmann et al., 1986; Zhu et al., 2010). Activation of naive $CD4^+$ and $CD8^+$ populations requires a co-stimulatory MHC/ T-cell receptor (TCR)-dependent signal from the above professional antigen-presenting cells. However, once memory cells have been generated, they can be directly activated by their respective antigen. Similar to innate immunity, the adaptive immune response is conserved across vertebrate species (Flajnik and Kasahara, 2010).

Cytokines and Chemokines

The immune and inflammatory response is tightly regulated and diverse. Cells can elicit differential effects based on location within the body, type of activation signal, and acute vs. chronic responsivity (Janeway Jr. et al., 2001). The precision of inflammatory responses are controlled in large part by extracellular mediators known as cytokines and chemokines (Turner et al., 2014). These chemical messengers allow small numbers of immune cell types to mediate a diverse and complex systemic immune response (Lata and Raghava, 2008). Upon binding, cytokines and chemokines stimulate subsequent intracellular signaling mechanisms modulating acute or chronic inflammation (Lata and Raghava, 2008; Turner et al., 2014). Furthermore, changes in the expression profiles of these signaling molecules have been implicated in stress responsivity, depression and anxiety, and pathologies like type II diabetes and metabolic syndrome (Sassoon et al., 1988; Vogelzangs et al., 2016; Akash et al., 2018; Yates et al., 2018).

Cytokines are small secreted proteins that serve as the chemical messengers for the immune system. They have the ability to mediate systemic and local inflammation, hematopoiesis, and immune responsivity (Lata and Raghava, 2008). Cytokines are

canonically categorized as pro-inflammatory or anti-inflammatory, but recent studies have demonstrated that cytokines can have pleiotropic effects depending upon the target receptors they bind, and external co-signaling factors like glucocorticoids and growth factors (Al-Shanti et al., 2008; Muñoz-Cánoves et al., 2013; Morey et al., 2015). Generally accepted pro-inflammatory cytokines include the interleukin-1 (IL-1) family, interleukin-6 (IL-6), tumor necrosis factor alpha (TNFα), and interferon gamma (IFNγ) (Turner et al., 2014). These cytokines signal *via* specific receptors that are responsible for signal modulation and downstream effects (**Figure 1-5**). The major anti-inflammatory cytokines are interleukin-4 (IL-4), interleukin-10 (IL-10), and the pleiotropic IL-6 (Cassatella et al., 1993; Muñoz-Cánoves et al., 2013). Similar to the inflammatory cytokines, anti-inflammatory cytokines signal *via* specific families of receptors with different downstream effects based on the cell type and context of activation (Ho et al., 1993; Nelms et al., 1999) as shown in **Figure 1-5**. Dysfunctional expression of cytokines has been implicated in the development of pathologies such as anxiety, depression, and type II diabetes (Vogelzangs et al., 2016; Akash et al., 2018).

Chemokines are a conserved subset of cytokines primarily responsible for the recruitment of circulating effector leukocytes (Moser et al., 2004). They also play roles in immunological surveillance and in leukocyte development (Moser et al., 2004). Chemokines are categorized broadly into two groups; chemotactic or homeostatic (Constantin et al., 2000). Similar to cytokines, chemokines are also dual-functional and create increasing gradients to recruit leukocytes within circulation to their target (Constantin et al., 2000; Turner et al., 2014). Chemokines and chemokine receptors (**Figure 1-5**) are critical for the tissue-specific responsivity of the immune system, as well

as proper growth and development of tissues. (Turner et al., 2014; Quinn et al., 2017). The best characterized chemokine in mammals is the pro-inflammatory interleukin 8, also known as CXCL8 (Hammond et al., 1995). Similar to its pro-inflammatory cytokine kin, it signals *via* activation of two different G-protein coupled receptors (GPCRs), responsible for the recruitment of leukocytes to sites of inflammation and acts as an angiogenic factor in humans (Hammond et al., 1995; Heidemann et al., 2003) (**Figure 1-5**). Chemokine Receptor 4 (CXCR4) and its ligand (CXCL12) have been shown to play a role in placental growth as well as vascular development in the growing fetus demonstrating the pleiotropy of these signaling molecules (Quinn et al., 2017).

Effects of Curcumin and Systemic Stress on Cytokine Regulation of Skeletal Muscle

Cytokines play a critical role in the regulation of tissues and organs throughout the body including skeletal muscle, adipose tissue, and pancreatic β-cells (Andersson et al., 2001; Al-Shanti et al., 2008; Hansen et al., 2010). Cytokine activity is coordinated by circulating and tissue resident leukocytes and lymphocytes (Fan and Rudensky, 2016; Holzlechner et al., 2017). Immune cells residing within the tissue possess the ability to self-renew (Hashimoto et al., 2013), and differential expression of surface markers delineate them from circulating immune cells, which are bone marrow derived (Hashimoto et al., 2013). Meshkani & Vakili (2016) reviewed the literature showing that tissue resident macrophages contribute to metabolic homeostasis and that abnormal population profiles are associated with development of metabolic syndrome and type II diabetes.

Tissue Resident Macrophages

A review by Martinez & Gordon (2014) concludes that tissue resident macrophages are dynamic cells capable of differential activation depending on systemic and local signals. Resident macrophages are categorized into two main phenotypes shown in **Figure 1-6**. M1 macrophages are classically activated by IFNγ, Lipopolysaccharide (LPS), TNFα, or granulocyte macrophage colony-stimulating factor (GM-CSF) (Chow et al., 1999; Hansen et al., 2008; Kayagaki et al., 2013). TLR4-MyD88 signaling pathways or inflammasome activation within these cells stimulates production of inflammatory factors including TNFα, IL-6, IL-1β, CCL2, and CCL10 (Kayagaki et al., 2013; Martinez and Gordon, 2014). M2 macrophages are considered to be alternatively activated by IL-4, IL-10, glucocorticoids, and TLR signaling (Sironi et al., 2006). This population can be further classified by activation signal and downstream effects into either M2a (IL-4 activated), b (TLR/IgG/Inflammasome complex activated), or c (IL-10 and glucocorticoid activated) groups (Edwards et al., 2006; Sironi et al., 2006). Regardless of initial activating signal, cells are associated with a predominantly anti-inflammatory response. M2 populations are unique in their ability to recognize and respond at the systemic level, while also being responsible for the local resolution of the inflammatory response. It should be noted that these M0/M1/M2 macrophage phenotypes are dynamic (Lavin et al., 2014). These classifications represent a snapshot of populations in a constant state of flux as they respond to systemic and local signals during development and after maturation (Lavin et al., 2014; Martinez and Gordon, 2014).

Cytokine Regulation of Skeletal Muscle

Skeletal muscle growth, development, and function are regulated in part by cytokine signaling (Spangenburg and Booth, 2003; Al-Shanti et al., 2008; Muñoz-Cánoves et al., 2013). Recent studies in our lab demonstrate that cytokines affect both insulin signaling and insulin-independent glucose metabolism within skeletal muscle (Cadaret et al., 2017). Previous research demonstrates that skeletal muscle is capable of secreting cytokines and growth factors in response to tissue injury, exercise, and other stimuli (Pedersen and Febbraio, 2008). IL-6, TNFα, and IGF-I secreted by skeletal muscle have since been recognized as myokines and represent a source of muscle growth and metabolic regulation (Pedersen and Febbraio, 2008; Henningsen et al., 2010; Schnyder and Handschin, 2015). Thus, skeletal muscle is a highly metabolic endocrine organ capable of secreting a number of myokines with autocrine, paracrine, and endocrine effects. Two multifunctional cytokine/myokines most commonly associated with the regulation of skeletal muscle are TNFα and IL-6 (Al-Shanti et al., 2008).

TNFα is a pleiotropic cytokine with abnormal expression involved in inflammatory skeletal muscle disorders and insulin resistance, and normal expression essential for proper skeletal muscle development and growth (Al-Shanti et al., 2008; Tüzün, et al., 2006). Abnormal TNFα expression is commonly associated with the pathology of type II diabetes, muscle wasting, and pro-inflammatory responses in skeletal muscle (Li and Reid, 2000; Tüzün et al., 2006; Akash et al., 2018). Skeletal muscle expresses tumor necrosis factor receptor 1 (TNFR1) and TNFR2 (Hsu et al., 1996). Most inflammatory effects of TNFα are due to activation of the NF***κ***B and JNK1 pathways by TNFR1 signaling cascades (**Figure 1-6**), leading to the induction of inflammation,

apoptosis, autophagy, and insulin resistance (Li and Reid, 2000; Plomgaard et al., 2005; Yang et al., 2015). Activation of TNFR1 leads to the recruitment of adaptor proteins such as tumor necrosis factor receptor-associated factors (TRAF), tumor necrosis factor-associated death domain (TRADD), and receptor interacting serine/threonine kinases (RIPK) (Hsu et al., 1996). These adaptor proteins activate IKK, which induces NFκB, JNK1, and autophagy-associated pathways (Hsu et al., 1996; Criollo et al., 2010; Ting and Bertrand, 2016). NFκB and autophagy-associated pathway activation by TNFR1 is dependent on TRAF2 (Puimège et al., 2014; Yang et al., 2015). Other downstream pathways of TNFR1 affecting apoptosis and protein metabolism in skeletal muscle are TRAF2-independent, signaling instead *via* TRADD-mediated pathways (Hsu et al., 1996; Guttridge et al., 1999) The activation of NFκB by TNFα is context-dependent within skeletal muscle and is involved in the regulation of cell survival and growth (Mourkioti and Rosenthal, 2008a). TNFR1-mediated activation of the JNK1/AMPK pathways via TRAF2 has similarly been shown to increase rates of mitophagy, autophagy, and reactive oxygen species (ROS) production (Yan et al., 2012; Yang et al., 2015). Thus, TNFα-mediated pathways play a multifaceted role in the development and growth of skeletal muscle.

IL-6 is another pleiotropic cytokine/myokine that binds a membrane bound receptor (IL6R) complexed with a homodimer of gp130 (Schroers et al., 2005). Studies indicate that IL6R is only expressed in its membrane-bound form on hepatocytes and leukocytes within the body in a classical manner (Keller et al., 2005; Wolf et al., 2014). However, gp130 is expressed by almost every cell within the body (Schroers et al., 2005; Wolf et al., 2014). These findings led to the discovery of a second soluble form of IL6R,

termed sIL6R (Schroers et al., 2005). sIL6R complexes first with its ligand IL-6 and then with a homodimer of gp130 (Schroers et al., 2005). The soluble version of IL6R is produced via alternative splicing of mRNA in a number of cell types including skeletal muscle (Keller et al., 2005; Wolf et al., 2014). This allows IL-6 to affect most cell types via both classical and trans-signaling (Keller et al., 2005; Wolf et al., 2014). Classical signaling is associated with the anti-inflammatory regenerative effects of IL6, and trans-signaling has been implicated in the pro-inflammatory cascades that contribute to autoimmune disease, metabolic dysfunction, and sepsis (Rose-John, 2012; Wolf et al., 2014; Garbers et al., 2015). Activation of both receptor types leads to the association of Janus kinases (JAK) JAK1 and JAK2 with gp130 (**Figure 1-6**) (Stahl et al., 1994). These recruit signal transducer and activator of transcription (STAT)-1 and STAT3 to be phosphorylated and translocated to the nucleus, where they up-regulate transcription of genes involved in the IL-6 response (Hemmann et al., 1996). Inhibition of this pathway occurs via negative feedback from JAK/STAT-induced suppressor of cytokine signaling-3 (SOCS3), allowing the cell to return to its basal state (Babon et al., 2014). JAK-mediated phosphorylation events can also activate the MAPK pathways and interact with the PI3K pathway (Heinrich et al., 2003), which has multifunctional effects on skeletal muscle. IL-6 produced during muscle contraction increases satellite cell proliferation in adult skeletal muscle and prevents premature differentiation in developing myocytes (Sun et al., 2007). However, IL-6 also interferes with IGF-1 signaling, increases age-related muscle atrophy, and promotes some inflammatory disorders (Bartoccioni et al., 1994; De Benedetti et al., 1997; Bonetto et al., 2012).

Curcuminoid effects on skeletal muscle growth and cytokine signaling

Turmeric root, and its bioactive polyphenol curcumin represent a topic of intensive research. A review of recent research by Hewlings & Kalman (2017) summarizes how this extract of *Curcuma longa* plants may help manage inflammatory and oxidative conditions. The anti-inflammatory effects of curcumin have been attributed to its role as a NFκB inhibitor (Mourkioti and Rosenthal, 2008b). The NFκB pathway can be activated by the inflammatory cytokine TNFα to suppress myogenesis and stimulate proteolysis promoting, loss of muscle protein (Mourkioti and Rosenthal, 2008b). However, it also enhances satellite cell proliferation and promotes cell survival (Guttridge et al., 1999; Li and Reid, 2000; Mourkioti and Rosenthal, 2008b). Inhibition of this pathway by curcuminoids may mediate some of the detrimental effects of cytokines on skeletal muscle growth.

Stress-induced modulation of cytokine expression

Recent work has begun to assess systemic immunological responses to different stressors and psychological pathologies. Reviews of this research indicate the differential effects of stress type and magnitude on immune function, with differences in cytokine secretion, antibody production, and cytokine expression pattern switching occurring in circulating leukocytes (Padgett and Glaser, 2003; Morey et al., 2015). Circulating leukocytes express glucocorticoid (GR) and catecholamine (ADR) receptors that upon binding modulate the function of NFκB, regulating cytokine production and gene expression (Padgett and Glaser, 2003). Glucocorticoid (GC) binding to GR under high stress conditions has been shown to modulate cytokine production by suppression of NFκB and downregulating pro-inflammatory cytokine gene expression, favoring a

Th2/M2 anti-inflammatory phenotype instead (Reichardt et al., 2001). However, GC also sensitize the innate immune system and upregulate inflammation through activation of the NLRP3 inflammasome (Busillo et al., 2011). Furthermore, under periods of chronic stress GR levels are decreased in part due to cytokine over-stimulation of the HPA-axis (Liu et al., 2017). The catecholamines epinephrine (E) and norepinephrine (NE) modulate immune function primarily through the actions of β_2 adrenergic receptors (ADRβ2) and the subsequent synthesis of cyclic-AMP (cAMP) (Reichardt et al., 2001). ADRβ2 appears to be preferentially expressed on Th1/M1 pro-inflammatory immune cells in circulation and within tissues (Bellinger et al., 2008) Acute stimulation by catecholamines leads to increased expression of inflammatory cytokines but has an overall inhibitory effect similar to GCs (Bellinger et al., 2008). More recently, studies have connected stress-induced cytokine expression and inflammation to behavioral pathologies including anxiety and depression (Henry et al., 2008; Peng et al., 2012). Together, this represents a promising new avenue of research regarding stress modulated immunology, and its role in behavior. However, it is necessary to first understand the role that inflammatory cytokines play in muscle growth and metabolic health outcomes.

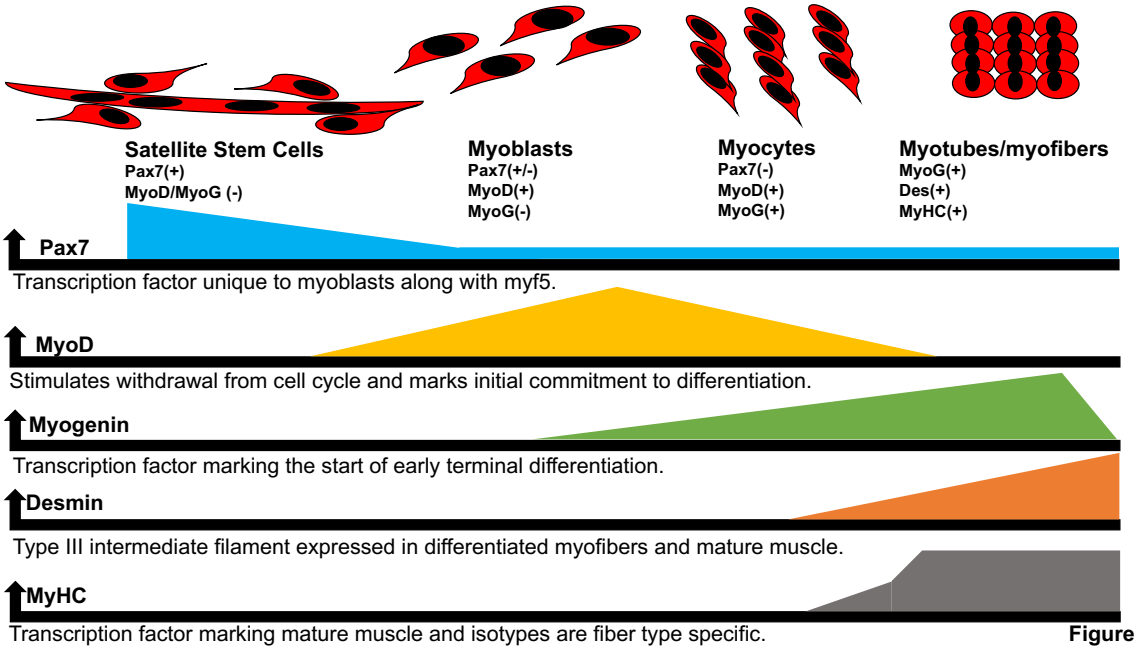

Figure 1-1. **Myogenic progression markers from precursor cells to mature muscle fibers**

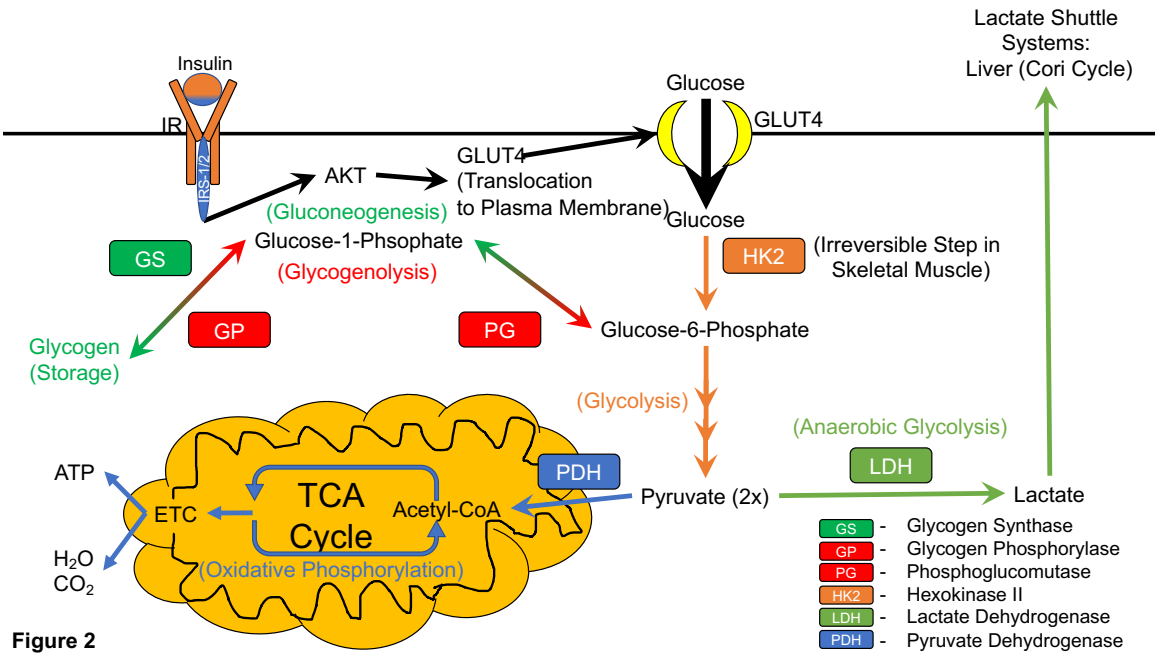

Figure 1-2. **Schematic illustrating the major pathways by which glucose is metabolized in skeletal muscle.**

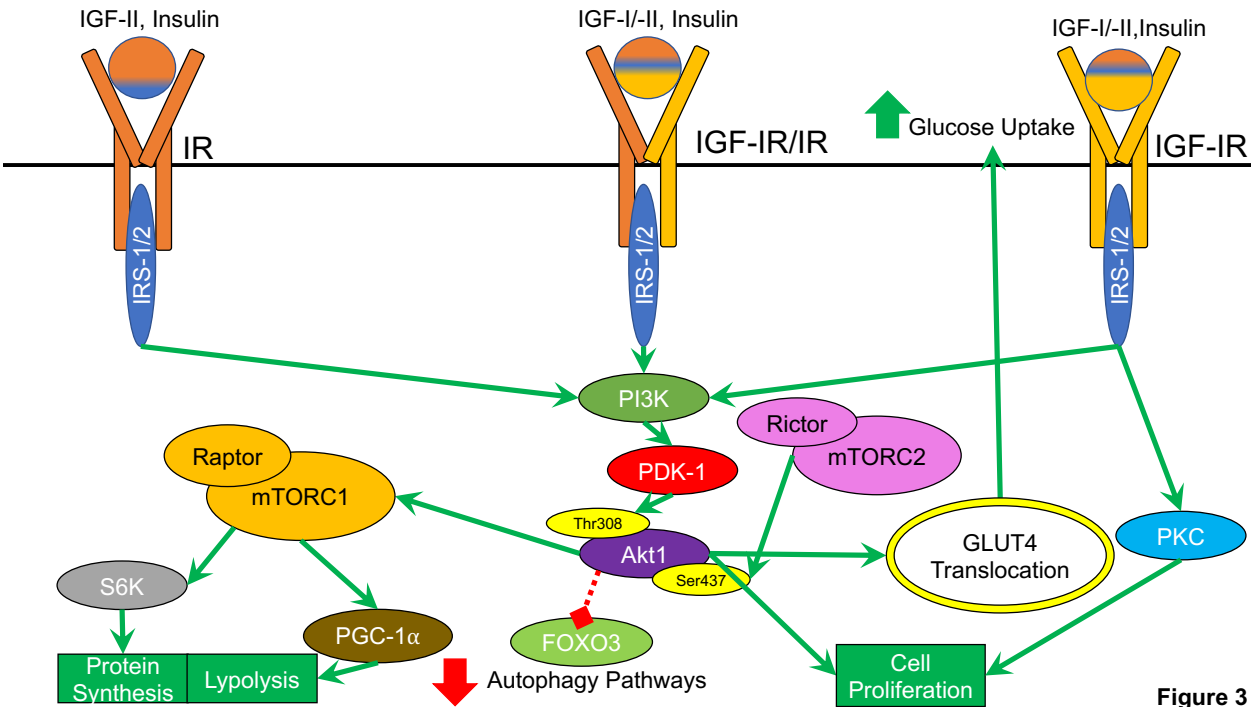

Figure 1-3. **Schematic of the pathways activated and effects of ligand binding to Insulin Receptor (IR), Insulin-like Growth Factor I Receptor/Insulin Receptor Heterodimer (IGF-IR/IR), and Insulin-like Growth Factor I Receptor (IGF-IR) by Insulin, IGF-I and IGF-II.**

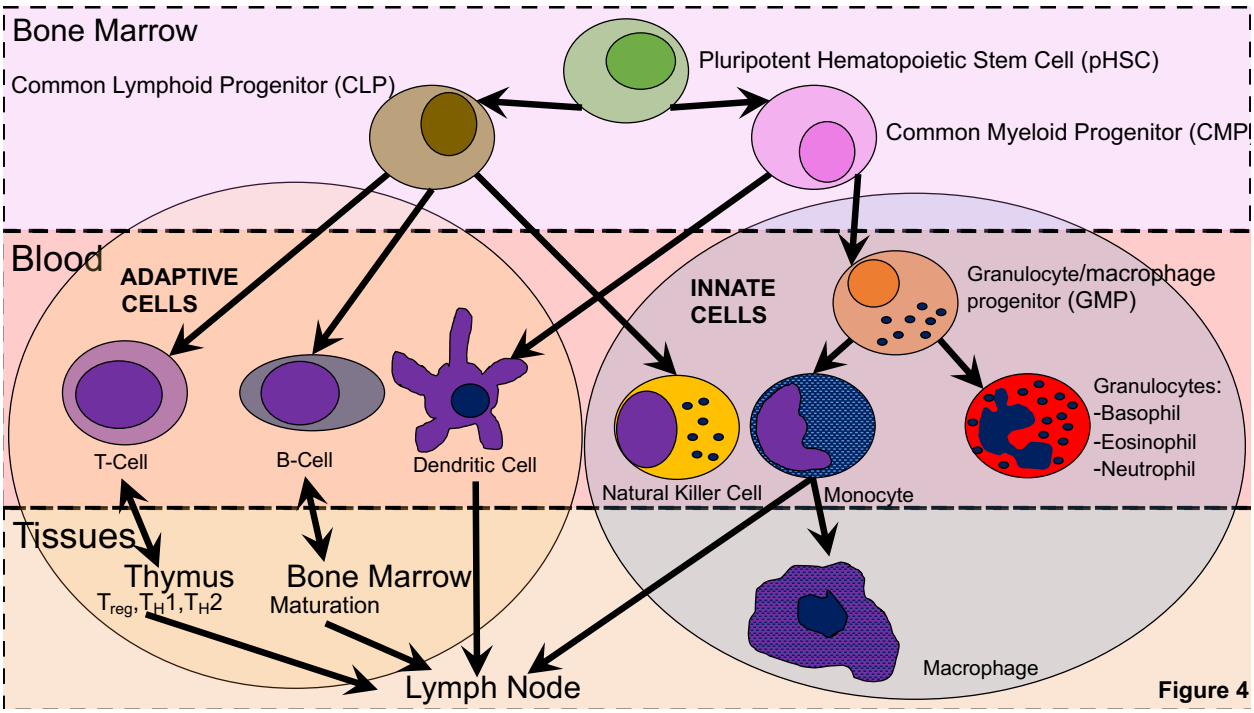

Figure 1-4. **Immune cell development and site of maturation from precursor cells to terminally differentiated populations.**

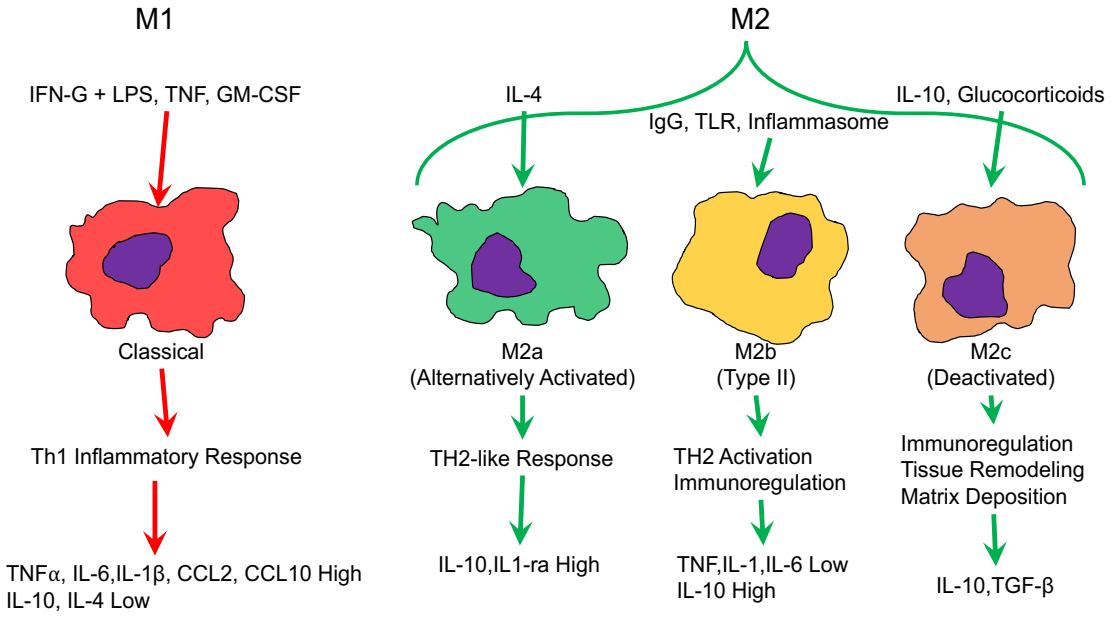

Figure 1-5. **Schematic of activation signals and the different effects on inflammation and immunoregulation of M1 and M2 macrophages.**

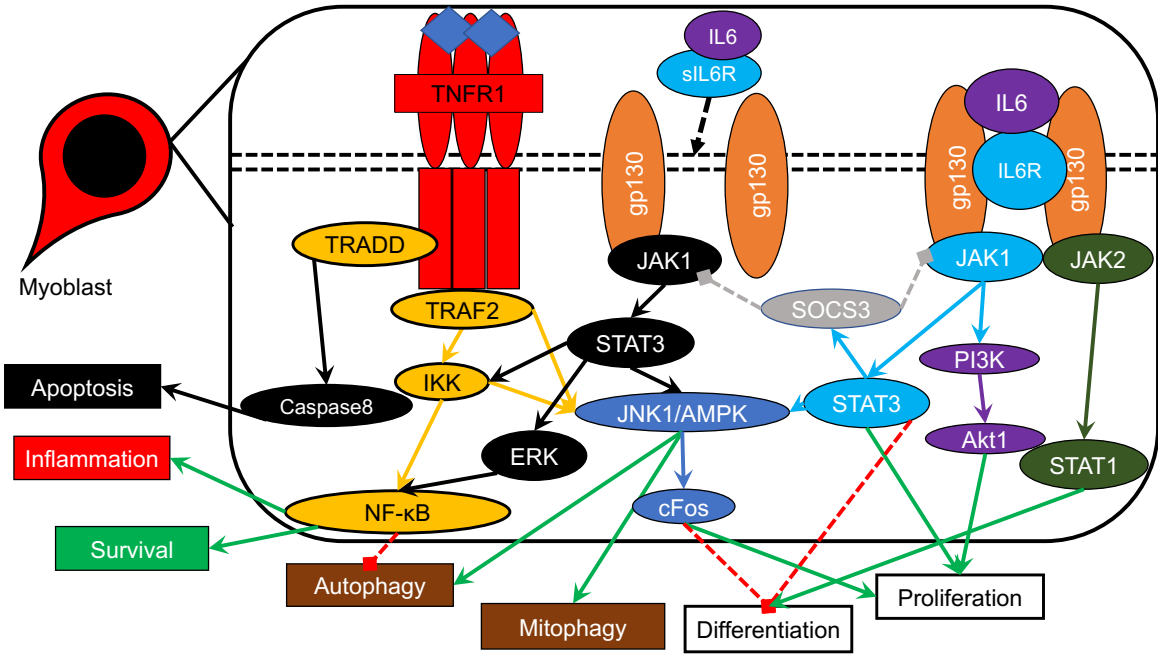

Figure 6

Figure 1-6. **Diagram of Tumor Necrosis Factor alpha (TNFA) and Interleukin 6 (IL-6) signaling pathways and downstream effects on growth and survival in myoblasts.**

Chapter 2: Maternofetal inflammation at 0.7 gestation in ewes leads to mild intrauterine growth restriction and impaired glucose metabolism in offspring at 30d of age.

Abstract

Intrauterine growth restriction (**IUGR**) leads to lifelong deficits in growth of offspring as well as an increased risk for metabolic disorders. These effects may be due in part to intrinsic inflammatory system programming that occurs in response to chronic exposure to stress *in utero*. Recent studies by our lab demonstrate that maternal inflammation during either mid- or late-gestation induces an IUGR phenotype in fetal rats and sheep, respectively. Turmeric root extract and its main polyphenol component curcumin have antioxidant and anti-inflammatory properties. The objective of this study was to determine whether sustained maternal inflammation at 0.7 gestation induces fetal IUGR and programmed inflammatory system responses that persist in lambs at 30 days of age, and whether these lead to deficits in growth and metabolism. We further sought to determine whether these effects could be mitigated by daily oral curcumin supplementation of the lambs. Timed-mated Polypay ewes were injected with bacterial endotoxin (MI-IUGR) or saline (controls) on the 100^{th},104^{th},107^{th},110^{th}, and 113^{th} day of gestational age (dGA; term~145 dGA). A subset of MI-IUGR lambs received a daily oral supplement of curcumin mixed in piperine and corn oil (MI-IUGR+C), and all other lambs received the piperine/corn oil carrier only. In MI-IUGR ewes, total white blood cells (**WBC**) decreased ($P < 0.05$) immediately after each injection before subsequently

increasing ($P < 0.05$). Rectal temperatures increased ($P < 0.05$) after each injection before returning to normal, demonstrating a canonical inflammatory response. Lambs were weaned 24 hours after birth. Birthweights of MI-IUGR lambs tended to be less ($P < 0.1$) than controls, and females tended to be lighter ($P < 0.1$) than males. Abdominal circumference / body weight (**BW**) and cannon bone length / BW were greater ($P < 0.05$) in MI-IUGR lambs at birth indicating asymmetric growth restriction. Day30 BW of MI-IUGR lambs was less ($P < 0.05$) than controls, but MI-IUGR+C BW did not differ from controls. MI-IUGR males tended to be lighter ($P < 0.1$) at 30d than males from the other groups. Average daily gain (**ADG**) was less ($P < 0.05$) in MI-IUGR and MI-IUGR+C compared to controls for males but not for females. Head circumference growth over the 30d period was greater ($P < 0.05$) in MI-IUGR and MI-IUGR+C females and less ($P < 0.05$) in MI-IUGR and MI-IUGR+C males compared to respective controls. Abdominal circumference growth was greater ($P < 0.05$) in MI-IUGR+C females and less ($P < 0.05$) in MI-IUGR+C males compared to controls. Brain weight / BW was greater ($P < 0.05$) in MI-IUGR and MI-IUGR+C males compared to control males and was greater ($P < 0.05$) in MI-IUGR males compared to MI-IUGR+C males, indicating persistent asymmetric growth. Glucose-stimulated insulin secretion determined by square-wave hyperglycemic clamp did not differ among groups. Hindlimb insulin-stimulated glucose oxidation was less ($P = 0.01$) in MI-IUGR and MI-IUGR+C compared to control hindlimbs. Hindlimb Insulin-stimulated glucose uptake did not differ among groups. *Ex vivo* primary skeletal muscle glucose uptake was less ($P < 0.05$) in MI-IUGR muscle compared to control and MI-IUGR+C. *Ex vivo* glucose oxidation was less ($P < 0.05$) in MI-IUGR and MI-IUGR+C muscle compared to controls and was less ($P < 0.05$) in MI-IUGR lambs

compared to MI-IUGR+C. Insulin increased ($P < 0.05$) *ex vivo* glucose uptake and glucose oxidation ($P < 0.05$) in primary skeletal muscle in all groups. TNFα increased ($P < 0.05$) glucose uptake in MI-IUGR muscle. The results of this study demonstrate that sustained maternal inflammation at 0.7 gestation caused fetal programming that affected postnatal growth and glucose metabolism of MI-IUGR offspring. Future research to determine what the mechanisms for inflammatory programming observed in MI-IUGR offspring is warranted to understand how these inflammatory system changes arise and contribute to the IUGR phenotype. Supplementation of curcumin in this study had minimal effects on deficits in growth but was able to partially improve skeletal muscle glucose oxidation. Further research is needed at different dosages, frequencies, and routes of administration, as curcumin may represent a potential treatment for improving metabolic outcomes in MI-IUGR offspring.

Introduction

Intrauterine growth restriction (IUGR) leads to lifelong deficits in growth and metabolic function of offspring, which increases risk for metabolic disorders (Hales and Barker, 2013). Fetuses adapt to adverse *in utero* environments by repartitioning nutrients to critical organs (i.e., brain, heart, lungs) and away from skeletal muscle (Yates et al., 2012; Yates et al., 2018). This fetal programming is beneficial *in utero* but leads to persistent reductions in muscle mass and glucose metabolism that prove detrimental to glucose homeostasis in offspring (DeFronzo et al., 1981). Recent studies done by our lab demonstrate that maternal inflammation during both mid- and late-gestation may induce programmed inflammatory responses that impair muscle growth and glucose metabolism in fetal rats and sheep (Cadaret et al., 2017; Cadaret et al., 2018). This could be due to altered responsiveness of skeletal muscle to cytokines and other inflammatory changes that disrupt insulin action and glucose metabolism (Cadaret et al., 2017; Cadaret et al., 2018; Posont et al., 2018). Curcumin is the main bioactive polyphenol in extracts of the root of *Curcuma longa* and has anti-inflammatory and anti-oxidative properties in humans and animals (Hewlings and Kalman, 2017; Mariely Jaguezeski et al., 2018). The bioavailability of curcumin alone is relatively low in the digestive tract, but is increased by co-administration with piperine and corn oil (Jenkins and Fotouhi, 1990; Shoba et al., 1998). We hypothesize that the maternal inflammation-induced fetal programming responses we previously observed in MI-IUGR fetuses contribute to growth and metabolic deficits in MI-IUGR offspring at 30d, and that supplementation with curcumin may mitigate their effects. Therefore, the objective of this study was to determine if sustained maternal inflammation induced by the administration of LPS during late-

gestation produces MI-IUGR offspring and fetal programming responses that impair growth and metabolism at 30 days after birth. We further sought to determine if daily oral supplementation of curcumin could mitigate the effects on growth and metabolism in MI-IUGR offspring.

Materials and Methods

Animals and Experimental Design

All procedures were approved by the Institutional Animal Care and Use Committee at the University of Nebraska-Lincoln. Studies were performed at the University of Nebraska-Lincoln Animal Science Complex, which is an AAALAC International accredited institution. Timed-mated Polypay ewes were treated (i.v.) with saline (control, $n = 8$) or 0.1 μg/ kg BW of bacterial lipopolysaccharide (**LPS**; $n = 12$; *E. coli* O55:B5; MilliporeSigma) in saline every third day from dGA 100 to 115 to produce maternal inflammation-induced IUGR (**MI-IUGR**) lambs. Rectal temperatures were recorded and complete blood counts (**CBC**, HemaTrue Veterinary Chemistry Analyzer, Heska) were performed for total and differential white blood cell (**WBC**) concentrations on blood samples collected at 0, 3, 6, 12, 24, and 48hr after each injection of LPS. After vaginal birth, lambs were weighed and measurements were taken for head circumference (**HC**), abdominal circumference (**AC**), crown-rump length (**CRL**), and cannon bone length (**CB**). Lambs received colostrum within 12hr of brith. After 24 ± 2 hours, lambs were weaned and transitioned to *ad libitum* milk replacer (DuMOR) prepared according to manufacturer recommendations. Daily intake was recorded. Lambs were weighed daily and body measurements were taken every week. Beginning at weaning a subset of MI-IUGR lambs (**MI-IUGR+C**; $n = 6$) received daily oral supplement of curcumin (95%

pure HPLC-verified; Bulk Supplements) mixed with commercial corn oil (1ml for first three days, and 1.5ml after until necropsy at d30 ± 2) and 20 mg/kg BW of piperine (95% pure HPLC-verified; Z-natural foods). All other lambs received corn oil and piperine carrier only. At 25 ± 2 days, indwelling catheters and a perivascular blood flow probe were surgically placed in hindlimb femoral arteries and veins as previously described (Cadaret et al., 2018). Blood samples were subsequently collected daily from an arterial catheter and CBC and blood gas, glucose, and lactate concentrations (**ABL**, ABL90 FLEX blood gas analyzer, Radiometer) were performed. Glucose-stimulated insulin secretion (**GSIS**) and hyperinsulinemic-euglycemic clamp (**HEC**) studies were performed at day 28 ± 2 and 29 ± 2 respectively. Lambs were euthanized at 30 ± 2 days of age via a double barbiturate overdose. Organ weights were recorded and flexor digitorum superficialis muscles were isolated for *ex vivo* metabolic studies.

Lamb GSIS Studies

β-cell function was determined using a square-wave hyperglycemic clamp performed at day 28 ± 2 of age in control (n = 8), MI-IUGR (n = 6), and MI-IUGR+C (n = 6) lambs as previously described (Yates et al., 2012; Camacho et al., 2017a). Three baseline samples were collected at 5-min intervals prior to an intravenous dextrose bolus (150mg/kg). This bolus was followed by continuous variable-rate infusion of 33% dextrose solution targeting a steady-state glucose concentration of ~2-fold baseline value. After 30 minutes of steady-state hyperglycemia three additional blood samples were collected at 5-min intervals. Blood collected in EDTA syringes was centrifuged (14,000 x *g*, 2min, 4ºC) to isolate plasma. Insulin concentrations were determined in duplicate via ELISA (Ovine Insulin, Alpco). Intra- and inter-assay CV were 14.75% and 13.11%

respectively. Samples collected in heparin-coated syringes were analyzed for blood gas, glucose, and lactate using an ABL90 FLEX (Radiometer).

Lamb Hindlimb Glucose Metabolism Studies

Hindlimb-specific glucose utilization and oxidation rates at baseline and during hyperinsulinemic euglycemic clamp (**HEC**) were determined in control, MI-IUGR, and MI-IUGR+C lambs on day 29 ± 2 of age as described previously (Cadaret et al., 2018). Lambs were first bolused (1mL, i.v.) with U-[^{14}C]-glucose tracer (18.75 μCi/mL; Perkin-Elmer) prior to constant infusion (1ml/hr). Arterial and venous blood were collected simultaneously at 5-min intervals (4 total draws) in heparin-coated syringes and EDTA syringes after 40-min of infusion. Lambs were then bolused with glucose (150mg/kg) and insulin (1500 mU; Humulin-R, Eli Lilly) before infusion (glucose, variable rate; insulin 500mU/mL, 5mL/hr) to produce stead state HEC. After HEC was achieved for 2hrs, simultaneous venous and arterial samples were again collected at 5-min intervals as described above. To measure glucose oxidation, whole blood (0.3mL) was added in triplicate to micro-centrifuge tubes containing 2 M HCl and suspended inside a sealed 20-mL scintillation vial containing 1 M NaOH. HCl facilitates the release of CO_2 from blood, which is then captured by the NaOH. After a 24-hr incubation at room temperature, the micro-centrifuge tube was removed and UltimaGold scintillation fluid (Perkin-Elmer) was added to each vial. Concentrations of ^{14}C from each blood sample was quantified using a Beckman-Coulter 1900 TA LC counter. Hindlimb glucose utilization rate was calculated as the difference in glucose concentration between arterial and venous samples normalized to the femoral blood flow rate and hindlimb weight at necropsy. Glucose oxidation rates were quantified from the difference between venous

and arterial ^{14}C specific activities normalized to femoral blood flow rate and hindlimb weight at necropsy. The amount of glucose oxidized in nmol was calculated from blood ^{14}C using the specific activity of the infused radiolabeled glucose.

Primary Skeletal Muscle Glucose Metabolism

Glucose uptake and oxidation was quantified in primary skeletal muscle from control, MI-IUGR, and MI-IUGR+C lambs as previously described (Cadaret et al., 2017). The flexor digitorum superficialis muscle of each lamb was collected tendon-to-tendon and dissected longitudinally into ~800mg strips. Isolated flexor digitorum superficialis muscles were washed in phosphate buffered saline (PBS; pH7.4) and pre-incubated for 1hr at 37ºC in Krebs-Henseleit bicarbonate buffer (**KHB**) containing no additives (basal), insulin (5mU/mL Humulin-R), or tumor necrosis factor alpha (TNFα) (20 ng/mL; MilliporeSigma). Muscle strips were then washed for 20-min in zero glucose treatment-spiked KBH. Glucose uptake was measured by incubating muscle strips in treatment-spiked KHB containing 1 mM [^{3}H]2-deoxyglucose (300µCi/mmol) and 1mM [^{14}C]-mannitol (1.25µCi/mmol) for 20min. Glucose oxidation was measured by incubation in treatment-spiked KHB containing [^{14}C-U]D-glucose (0.25µCi/mmol) for 2 hrs, before capturing $^{14}CO_2$ in 1M NaOH for 2 hrs.

Serum Curcumin Quantification

Jugular blood draws were taken from MI-IUGR+C lambs 3hr after supplementation with curcumin every third day after birth until the HEC was performed at day 29 ± 2 of age. Blood collected in EDTA tubes (~1mL) was analyzed for WBC. Blood collected in 3mL Heparin coated tubes (~2mL) was centrifuged (3,500 x *g*, 15 min, 4ºC) to isolate serum and stored at -80ºC. These samples were then sent to the

Proteomics and Metabolomics Facility (PMF; UNL Center for Biotechnology Core Facility) where the three bioactive curcuminoids curcumin, bisdemethoxycurcumin, and demethoxycurcumin were measured using liquid chromatography with tandem mass spectrometry (**LC-MS/MS**).

Statistical Analysis

All data were analyzed using the Mixed procedure in SAS (SAS Institute, Cary NC) with lamb as the experimental unit. *In vivo* and *ex vivo* data were analyzed for effects due to experimental groups, period (or incubation condition), and the interaction. Period/condition was treated as a repeated variable. For *in vivo* metabolic studies, samples within each period were averaged for each lamb. Similarly, technical replications were averaged for each lamb in *ex vivo* studies. Morphometric and CBC data were analyzed for effects due to treatment in maternal data and effects due to experimental groups, sex, and the interaction in neonates. All data are presented as means ± SEM.

Results

Maternal CBC Response

Maternal total WBC and differential WBC values for monocytes and granulocytes decreased ($P < 0.05$) by 3 hr in MI-IUGR ewes after each LPS injection before increasing ($P < 0.05$) by ~24hr and subsequently normalizing by ~72hr over the period between each injection (**Figure 2-1A, 2-1B**, and **2-1C** respectively). Differential WBC for lymphocytes decreased ($P < 0.05$) by 3hr and normalized by ~24hr (**Figure 2-1D**) Rectal temperatures increased ($P < 0.05$) by 3hr and normalized by ~9hr (**Figure 2-1E**).

Neonatal CBC Response

Neonatal total WBC and differential WBC values for monocytes and granulocytes differed ($P < 0.01$) by day across all groups to varying degrees (**Figure 2-2A, 2-2B, 2-2C,** and **2-2D**).

Lamb Growth Metrics

MI-IUGR (n=12) birthweight tended to be less ($P < 0.1$) than controls (n=8) but cannon bone length/bodyweight and abdominal circumference/bodyweight was greater ($P < 0.05$) than controls (**Figure 2-3**). In males, MI-IUGR (n=4) and MI-IUGR+C (n=3) bodyweight tended to be less ($P < 0.1$) than controls (n=3) at 30d and MI-IUGR bodyweight tended to be less ($P < 0.1$) than MI-IUGR+C males. At 30 days, abdominal circumference/bodyweight and cannon bone length/body weight was greater ($P < 0.05$) in MI-IUGR lambs than controls (**Figure 2-4**) and ADG, head circumference growth, and abdominal circumference growth was less ($P < 0.05$) in MI-IUGR and MI-IUGR+C than control males (**Figure 2-5**). In females, MI-IUGR (n=2) and MI-IUGR+C (n=3) head circumference growth was greater ($P < 0.05$) than controls (n=5) and abdominal

circumference growth was greater ($P < 0.05$) in MI-IUGR+C compared to both other groups (**Figure 2-5)**. Lung weight/ bodyweight was greater ($P = 0.01$) in MI-IUGR lambs compared to controls and less ($P= 0.01$) in MI-IUGR+C lambs regardless of sex (**Figure 2-6A**) In males, brain weight/ bodyweight was greater ($P < 0.05$) in MI-IUGR and MI-IUGR+C compared to controls and greater ($P < 0.05$) in MI-IUGR compared to MI-IUGR+C (**Figure 2-6B**).

Glucose-Stimulated Insulin Secretion

GSIS studies did not reveal any significant differences between groups (**Figure 2-7**). Baseline hindlimb glucose uptake and oxidation rates did not differ between groups, nor did plasma insulin.

Hindlimb Glucose Metabolism

Under HEC conditions, hindlimb insulin-stimulated glucose oxidation was less ($P = 0.01$) in MI-IUGR and MI-IUGR+C lambs compared to controls (**Figure 2-8**). There were no differences in hindlimb insulin-stimulated glucose uptake between groups.

Ex Vivo Primary Skeletal Muscle Metabolism

Glucose uptake by primary skeletal muscle from MI-IUGR lambs was less ($P < 0.05$) than that of control and MI-IUGR+C muscle (**Figure 2-9A**). MI-IUGR skeletal muscle glucose uptake was increased ($P < 0.05$) by incubation with TNFα compared to basal. Incubation with insulin increased glucose uptake in all groups. In all media, glucose oxidation rates were less ($P < 0.05$) in MI-IUGR and MI-IUGR+C muscle compared to control muscle and in MI-IUGR skeletal muscle compared to MI-IUGR+C skeletal muscle (**Figure 2-9B**). Insulin increased glucose oxidation rates in all groups.

Discussion

The results of this study demonstrate that sustained maternal inflammation during late gestation produces IUGR and fetal programming responses in skeletal muscle that impair glucose metabolism in offspring at 30d. It further demonstrates that supplementation of curcumin has minimal effects on growth deficits but may be able to mitigate the changes in skeletal muscle glucose oxidative metabolism. MI-IUGR lambs were smaller at birth than their control counterparts but had greater abdominal circumference and cannon bone length to body weight ratios than controls, which is indicative of asymmetrical fetal growth. At 30d, MI-IUGR lambs had greater abdominal circumference and cannon bone length by bodyweight ratios and MI-IUGR males had lower bodyweights compared to both control and MI-IUGR+C lambs, which indicate that asymmetrical growth continues after birth in MI-IUGR lambs but is tempered by supplementation with curcumin. Growth rates in males were slower in MI-IUGR lambs receiving curcumin or placebo compared to controls, but growth rates in females did not differ among groups. Consistent with asymmetrical growth, the brain and lung weights relative to BW in all MI-IUGR males were greater than controls, but this size differential was tempered when MI-IUGR were supplemented with curcumin. We previously found that chronic maternal inflammation during late gestation leads to asymmetric fetal growth rates (Cadaret et al., 2018), and the morphometric and organ spring differences observed in the present study show that these intrinsic growth characteristics persist in the neonate. Interestingly, female growth characteristics appeared to be less affected than males. Such differences between sexes are not unprecedented as, recent studies have reported differences between sexes in growth during early life in humans (Alur, 2019) and IUGR

lambs (Hunter et al., 2015). This could represent a survival advantage in females after periods of maternal stress and inflammation, but more research is warranted to understand why this sex-specific dimorphism occurs and how it mitigates growth deficits after intrauterine growth restriction in females.

Supplementation with curcumin had minimal effects on deficits in growth characteristics in this study. If programmed inflammatory responses are indeed contributing to the asymmetrical growth observed in MI-IUGR lambs, then this minimal effect on growth may be due to the anti-inflammatory properties of curcumin. The observed minor improvements and mitigation of asymmetrical growth characteristics in this study could be due to curcumins ability to reduce inflammatory signaling pathways in peripheral tissues and reduce circulating inflammatory cytokines (Hewlings and Kalman, 2017). This would mitigate the effects of some of these inflammatory programming responses on peripheral tissue growth characteristics and temper the growth deficits as we observed in this study. This effect may instead be due to curcumins ability to reduce serum free fatty acids, decrease blood glucose, and modulate the expression of genes involved in lipoprotein metabolism in patients that suffer from metabolic syndrome, which could lead to the alleviation of some of the nutrient repartitioning inherent in asymmetrical growth (Na et al., 2013; Hewlings and Kalman, 2017). Thus, the observed improvements in growth could instead be due to shifts in fatty acid metabolism and reductions in serum free fatty acids which has been shown to improve insulin resistance (Na et al., 2013), rather than alleviating the inflammatory responses that contribute to the initial deficits in metabolism. This would instead involve shifts away from the nutrient repartitioning responses that contribute to asymmetrical growth in

IUGR-offspring by modulating fatty acid metabolism and transport allowing for some minimal improvements in growth as we observed. Further research is clearly warranted to determine how curcumin is able to mitigate some of the deficits in growth observed in the current study and what mechanism are involved.

Glucose-stimulated insulin secretion was neither impaired by MI-IUGR programming, nor improved by curcumin supplementation. These findings contrast with the results of our fetal study using the same model for IUGR and indicate that late-gestation sustained maternal inflammation induces conditions that suppress β-cell function *in utero* but not fetal programming that impairs β-cell functional capacity after birth. Previous studies using placental insufficiency to create IUGR have demonstrated that impaired β-cell function and islet development is due to hypercatecholaminemia in IUGR fetuses (Macko et al., 2016; Boehmer et al., 2017). These β-cell deficits persist in the PI-IUGR born lamb (Camacho et al., 2017a). Adrenergic function was not measured in the present study, but we would not expect changes in adrenergic function in a model of maternal inflammation as these effects are due to a sustained inflammatory response and are not likely to illicit the fetal stress response and hypercatecholaminemia observed in models of placental insufficiency. Sustained MI-induced fetal programming did affect glucose metabolism by altering hindlimb specific glucose oxidation and skeletal muscle glucose utilization and oxidation. Fetal programming induced by our model may not be detrimental to β-cell function as it failed to maintain dysfunction at measurable levels in the absence of the restricted uterine environment, unlike the maternal hyperthermic model for IUGR (Camacho et al., 2017a). Previous studies demonstrated that adrenal demedullation improves functional insulin secretion in IUGR fetuses, but does not

completely alleviate the metabolic deficits caused by IUGR and in fact further impairs β-cell development (Davis et al., 2015; Macko et al., 2016). Thus, fetal programming responses to maternal inflammation likely affect peripheral tissue responsiveness to insulin rather than inducing β-cell dysfunction proper.

Insulin-stimulated hindlimb glucose oxidation rates were impaired in MI-IUGR lambs compared to controls demonstrating the postnatal persistence of fetal programming responses that change insulin responsivity of glucose metabolism and contribute to metabolic dysfunction. *Ex vivo* studies showed that skeletal muscle that glucose uptake was diminished in MI-IUGR neonates but was recovered by daily oral supplement of curcumin. Skeletal muscle glucose oxidation was also impaired in MI-IUGR lambs but was partially recovered by curcumin supplementation. These disparities among experimental groups were observed under both basal and insulin-stimulated conditions. Stimulation with TNFα increased glucose uptake by MI-IUGR muscle but did not have an effect on glucose uptake in skeletal muscle from either of the other two groups. Our previous studies demonstrated that IUGR myoblasts and skeletal muscle have intrinsic adaptations in inflammatory signaling pathways (Posont et al., 2018; Yates et al., 2018), and TNFα increases glucose uptake by acting as an insulin mimetic (Bach et al., 2013) contributing to the pathogenesis of Type II diabetes (Plomgaard et al., 2005; Akash et al., 2018). Increased glucose uptake when MI-IUGR skeletal muscle was stimulated with TNFα may reflect a similar condition. Regardless, it demonstrates that MI-IUGR skeletal muscle responds differently to stimulation with TNFα. The recovery of normal glucose uptake rates and improved oxidation rates associated with curcumin supplementation suggest that curcumin mitigates deficits in skeletal muscle glucose metabolism. This may

be due to its ability to promote insulin sensitivity in peripheral tissues possibly due to the anti-inflammatory effects of this polyphenol, which could suppress inflammatory pathways that have been previously implicated in the development of insulin resistance (Plomgaard et al., 2005; Chen et al., 2015).

From the results of this study, we conclude that sustained maternal inflammation during late gestation restricts fetal growth, yielding IUGR at birth. MI-IUGR lambs develop intrinsic fetal programming that reduces growth and skeletal muscle glucose metabolism at 30 days of age. These programmed changes likely contribute to the deficits in growth and metabolic dysfunction observed in this and other studies. Females in this study exhibited similar growth rates among all experimental groups, which may indicate a possible survival advantage in this model of IUGR, as evidenced by their neonatal body morphometrics compared to males. The mechanistic explanation for this sex-specific advantage, however, is not clear from this study. The fetal programming response to sustained maternal inflammation during late gestation did not produce the β-cell dysfunction observed in other IUGR models or in fetal studies with this model, perhaps due to a lack of fetal hypercatecholaminenia. Fetal programming to maternal inflammation did produce changes in skeletal muscle responsivity to insulin that was consistent with prenatal observations. Primary skeletal muscle from MI-IUGR lambs demonstrated consistent deficits in glucose uptake and oxidation that were improved by daily oral curcumin. Additionally, MI-IUGR skeletal muscle glucose uptake increased in response to TNFα, suggesting that inflammatory programming previously observed in the MI-IUGR fetus modulates skeletal muscle responsivity to cytokines. This represents one example of a possible inflammatory adaptation that confers a survival advantage *in utero*

but contributes to metabolic dysfunction after birth. Future research to determine the mechanisms for inflammatory programming observed in MI-IUGR is warranted to understand how they contribute to the IUGR metabolic phenotype. Supplementation of curcumin in MI-IUGR offspring had minimal benefit on growth and whole-body metabolism of lambs during the first 30 days of life. However, it appeared that curcumin was able to improve glucose uptake and oxidation rates in skeletal muscle. Although these results are encouraging, further research at different dosages, frequency, and routes of administration will better determine the efficacy of curcumin as a treatment for improving outcomes in MI-IUGR offspring.

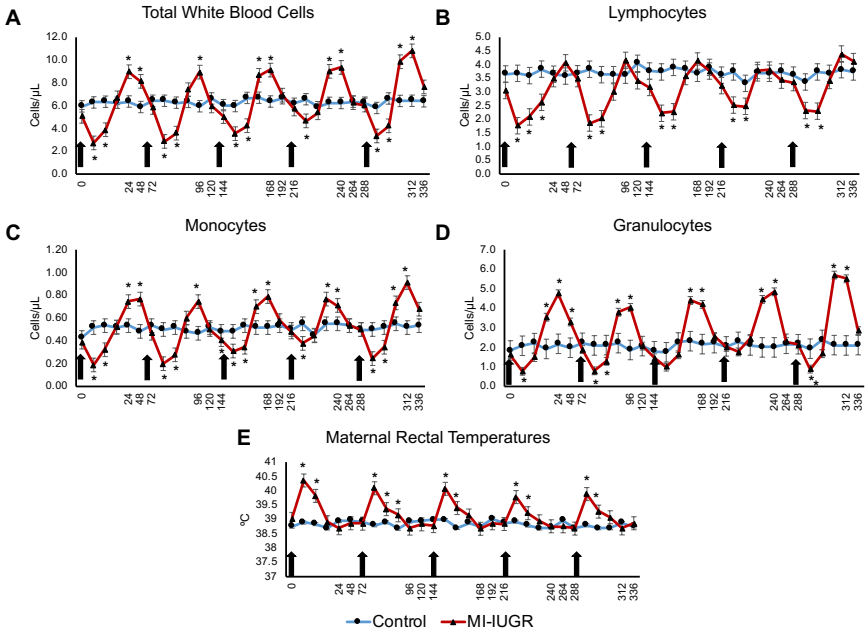

Figure 1

Figure 2-1. **Total (A) and differential white blood cell counts for Lymphocytes (B), Monocytes (C), and Granulocytes (D) and rectal temperatures (E) of pregnant ewes injected with saline (control; n=8) or bacterial endotoxin (MI-IUGR; n=12) every three days from 100-115 dGA. Arrows indicate injection time points and x-axis values are time (hr) after first injection. * Mean differs (P < 0.05) from the mean of the control group.**

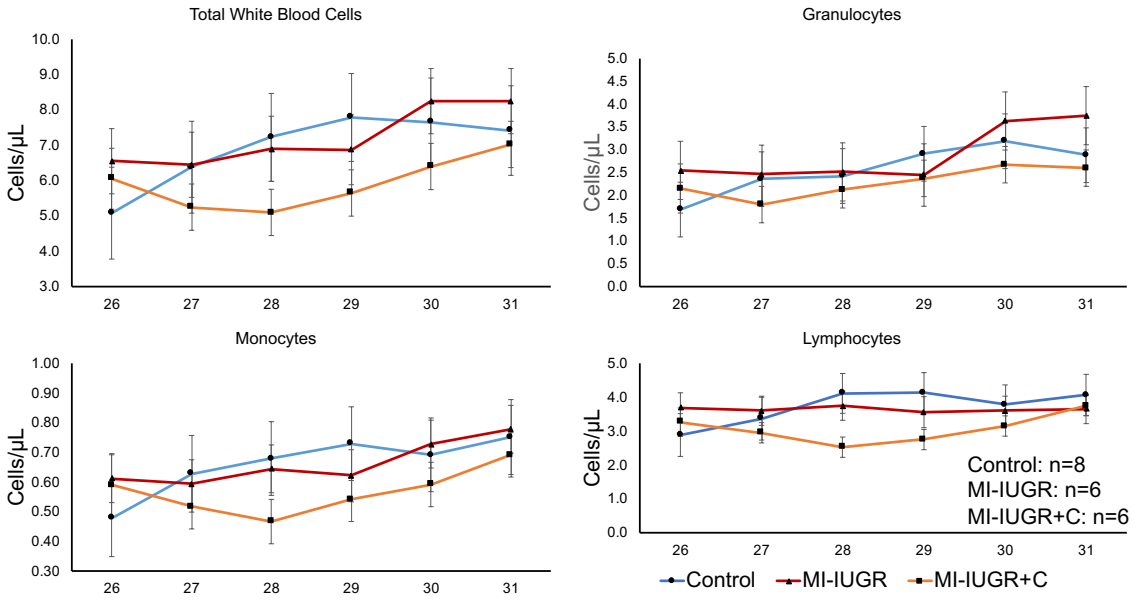

Figure 2

Figure 2-2. **Total and differential (Granulocyte, Monocyte, and Lymphocyte) white blood cell counts for neonates.**

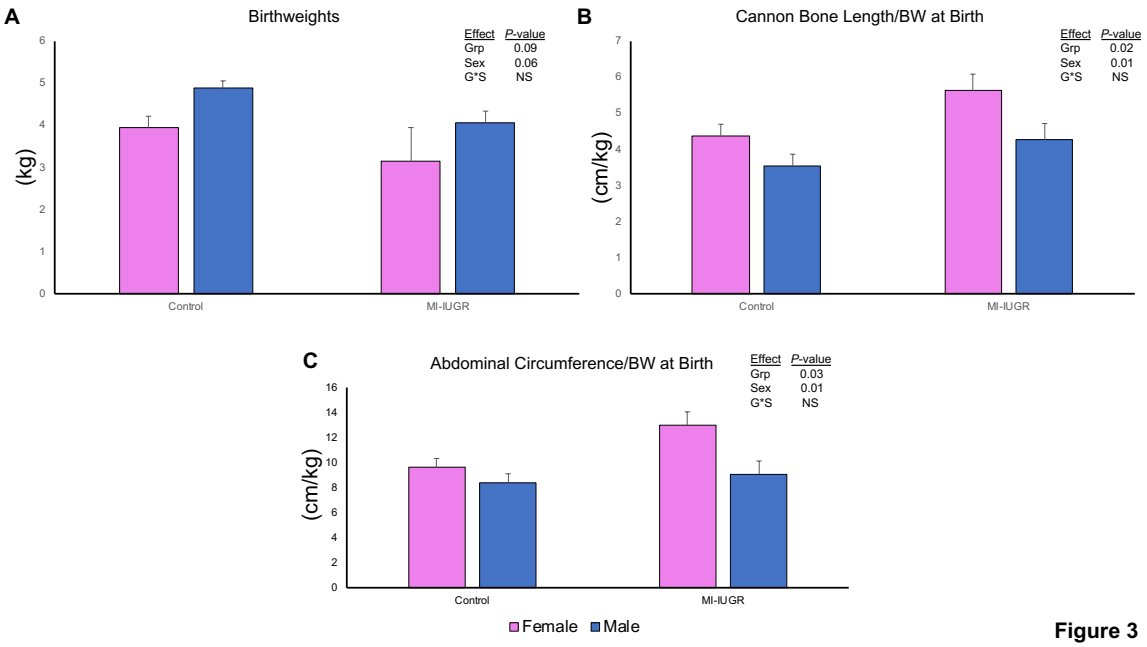

Figure 3

Figure 2-3. **Lamb birthweight (A), measures of cannon bone length (B) and abdominal circumference (C) by birthweight respectively in control (n=8; males=3, females=5) and MI-IUGR (n=12; males=7, females=5) at birth. MI-IUGR lambs weighed less than controls at birth, and demonstrated asymmetrical growth restriction.**

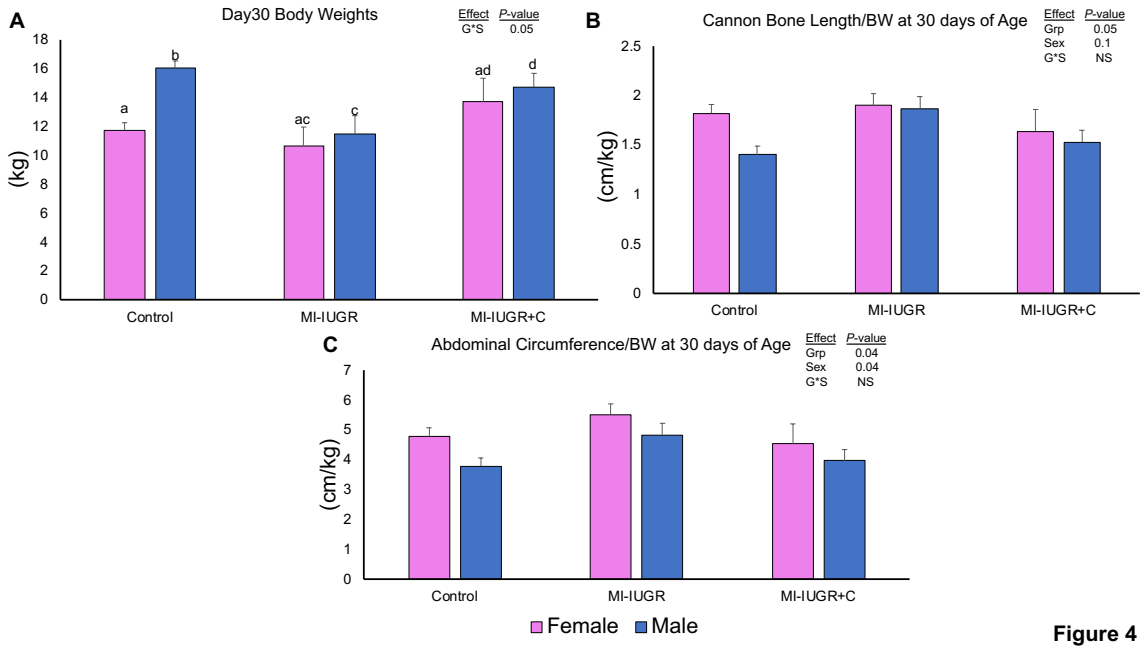

Figure 4

Figure 2-4. **Bodyweight (A), cannon bone length by bodyweight (B) and abdominal circumference by bodyweight (C) at day30 in control (n=8; males=3, females=5), MI-IUGR (n=6; males=4, females=2), and MI-IUGR+C (n=6; males=3, females=3) neonates. MI-IUGR lambs weighed less than control and MI-IUGR+C lambs and demonstrated asymmetrical growth characteristics.**

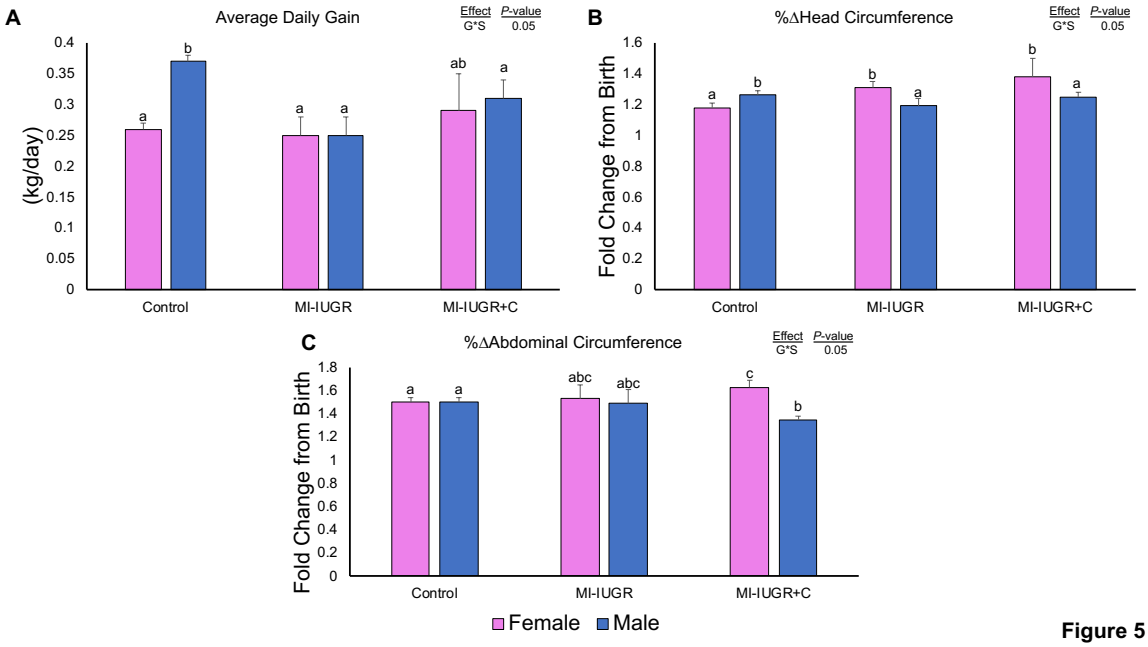

Figure 5

Figure 2-5. **Average daily gain (A), Head circumference growth (B), and Abdominal circumference growth (C) of control (n=8; males=3, females=5), MI-IUGR (n=6; males=4, females=2), and MI-IUGR+C (n=6; males=3, females=3) neonates.[a,b,c] Means with differing superscripts differ.**

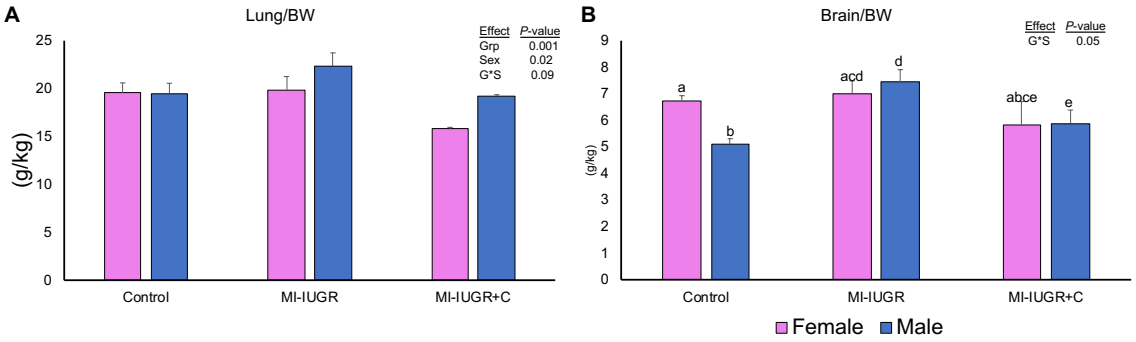

Figure 6

Figure 2-6. **Brainweight by bodyweight (A) and Lung by bodyweight (B) of control (n=8; males=3, females=5), MI-IUGR (n=6; males=4, females=2), and MI-IUGR+C (n=6; males=3, females=3) lambs. Lung by bodyweight was greater in MI-IUGR and less in MI-IUGR+C lambs compared to controls. Brainweight by bodyweight was greater in MI-IUGR and MI-IUGR+C lambs compared to controls.[a,b,c,d,e] Means with differing superscripts differ.**

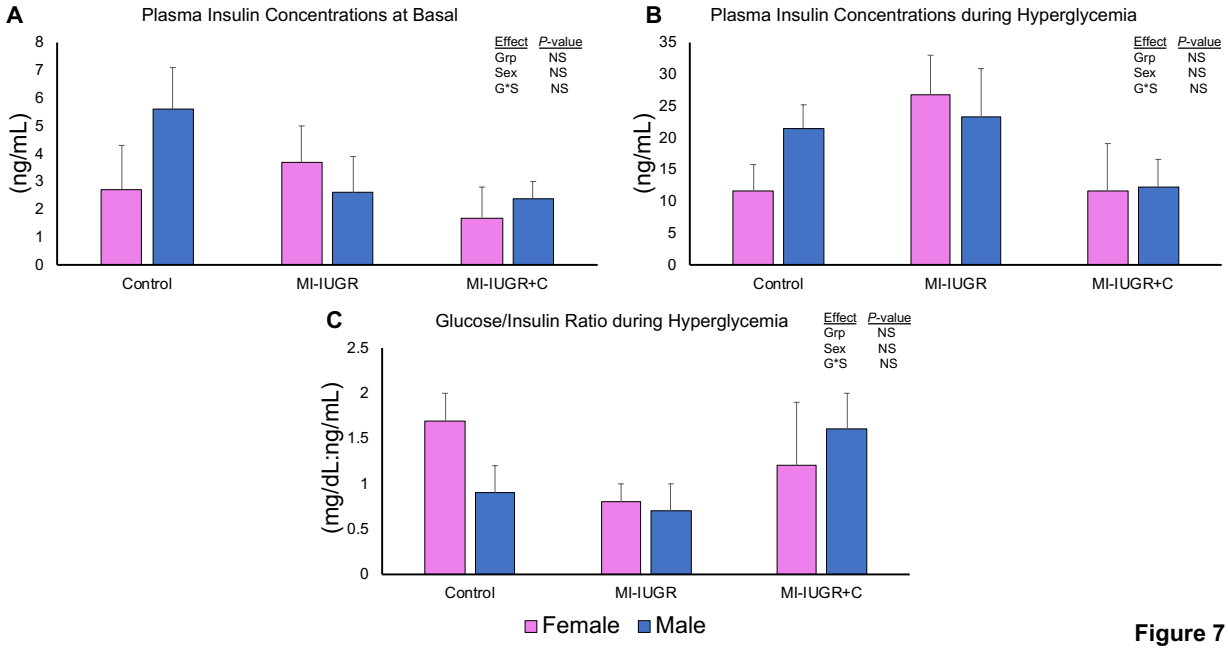

Figure 7

Figure 2-7. **Plasma insulin concentrations (ng/mL) at basal and hyperglycemic states and glucose/insulin ratio (mg/dL:ng/mL) during square-wave hyperglycemic clamp in control (n=8), MI-IUGR (n=6), and MI-IUGR+C (n=6) lambs.**

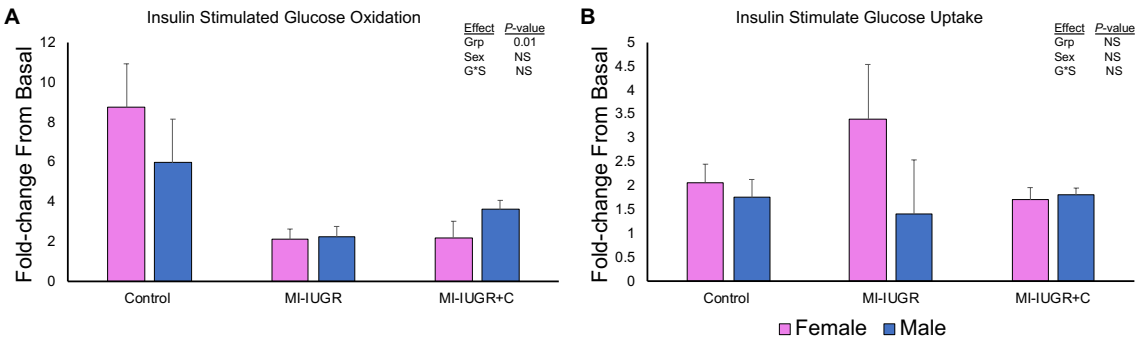

Figure 8

Figure 2-8. **Hindlimb-specific insulin stimulated glucose oxidation (A) and glucose uptake (B) rates, respectively in control (n=8), MI-IUGR (n=6), and MI-IUGR+C (n=6) lambs.**

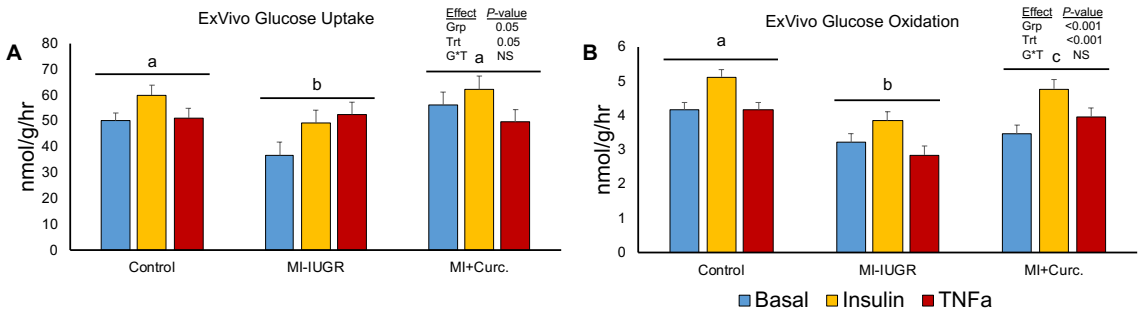

Figure 9

Figure 2-9. ***Ex vivo*** **primary skeletal muscle glucose uptake (A) and oxidation (B) under basal, insulin-stimulated, and TNFα-spiked conditions in control (n=8), MI-IUGR (n=6), and MI-IUGR+C (n=6) lambs.** ^{a,b,c} **Means with differing superscripts report main effect of group and differ.**

Chapter 3: Changes in myoblast responsiveness to TNFα and IL-6 and increased expression of autophagy-associated pathway components contribute to intrinsic myoblast dysfunction in intrauterine growth-restricted fetal sheep.

Abstract

Intrauterine growth restriction (IUGR) is linked to lifelong deficits in muscle mass due to intrinsic functional deficits in myoblasts, but the underlying mechanisms for this dysfunction are unknown. Inflammatory cytokines play a central role in regulating myoblast function and muscle growth, and thus the objective of this study was to assess the functional responsiveness of primary IUGR fetal myoblasts to TNFα and IL-6 in culture and to examine potential changes in growth-regulating pathway components during incubations with an IKK inhibitor (TPCA-1). Maternal hyperthermia was used to induce placental insufficiency and produce IUGR fetuses (n = 7; thermoneutral controls, n = 7) in pregnant sheep. Primary myoblasts were isolated from fetal skeletal muscle at 0.9 of gestation and their functional capacity was assessed after 3d in complete growth media (20% FBS) that was un-spiked (basal) or spiked with TNFα (20ng/ml) in the presence and absence of TPCA-1 (5μM), or spiked with IL-6 (1ng/ml) alone. A fetal experimental group by culture media interaction was observed ($P < 0.05$) for myoblast proliferation. Proliferation rates of IUGR myoblasts were less ($P < 0.05$) than control myoblasts after 3d in basal or IL-6 spiked growth media but did not differ between

groups in TNFα-spiked growth media. Growth media spiked with TNFα decreased ($P < 0.05$) proliferation rates in control myoblasts compared to their rates in basal media. However, proliferation of IUGR myoblasts did not differ among basal, IL-6-spiked and TNF-spiked media all of which were lower ($P < 0.05$) than control myoblasts in basal media. Administration of TPCA-1 decreased ($P < 0.05$) proliferation rates in both control and IUGR myoblasts compared to their respective rates without it. The magnitude of this reduction was greater ($P < 0.05$) in IUGR myoblasts than in controls in both basal and TNFα-spiked media. Fewer ($P < 0.05$) IUGR myoblasts were myogenin$^+$ compared to controls after 3-day incubation in basal, IL-6-spiked, or TNF-spiked differentiation media (2% FBS). In both experiment groups, TNF-spiked differentiation media reduced ($P < 0.05$) myogenin$^+$ myoblasts compared to basal and IL-6 spiked media. After 3d in basal differentiation media, fewer ($P < 0.05$) IUGR myoblasts were desmin$^+$ than controls. However, desmin$^+$ myoblasts did not differ between groups when cultured in IL-6-spiked or TNF-spiked media. Differentiation media spiked with either cytokine reduced ($P < 0.05$) percentages of desmin$^+$ myoblasts compared to basal media in controls but not in IUGR myoblasts, as IUGR myoblasts exhibited low percentages of desmin$^+$ cells in basal media. mRNA expression for Toll-like receptor 4 (TLR4) was increased ($P < 0.05$) in myoblasts from both fetal groups when differentiation media was spiked with TNFα but to a greater ($P < 0.05$) extent in IUGR myoblasts than in controls. Expression for Tumor-necrosis factor receptor 1 (TNFR1) and Unc-like kinase 2 (ULK2) was greater ($P \leq 0.05$) in IUGR myoblasts than in controls in all media types. Myoblast Interleukin 6 receptor (IL6R) mRNA expression was not different between fetal groups or among media types. Semitendinosus muscle collected from IUGR fetuses at the same time as myoblasts

exhibited greater ($P < 0.05$) Interleukin 6 (IL-6) and TNFR1 mRNA expression, less ($P < 0.05$) IκB protein content, and greater ($P < 0.05$) c-Fos protein content than controls. We conclude that multiple inflammatory pathways are enhanced in IUGR muscle/myoblasts, which contributes to the diminished functional capacity of IUGR fetal myoblasts by intrinsically altering their functional regulation. Furthermore, IUGR fetal adaptations increased mRNA expression for key components of mitochondrial autophagy pathways in myoblasts, which are important to cellular survival. Together, these mechanisms may help to explain reduced muscle hypertrophy in the IUGR fetus.

Introduction

Intrauterine growth restriction (IUGR) disproportionately reduces muscle mass in fetuses and offspring (Padoan et al., 2004; Yates et al., 2014; Yates et al., 2018). We recently found that IUGR fetal myoblasts exhibit intrinsic functional deficits (Yates et al., 2016; Yates et al., 2018), but have not previously identified the underlying mechanisms responsible for this dysfunction. Myoblasts are tightly regulated by inflammatory factors (Paulin and Li, 2004; Yates et al., 2018), and programmed changes within this system due to chronic intrauterine stress may represent one underlying molecular mechanisms for impaired IUGR myoblast function (Yates et al., 2014; Cadaret et al., 2017). Tumor Necrosis Factor-alpha (TNFα) and Interleukin-6 (IL-6) are potent multifunctional cytokines involved in systemic and localized inflammatory responses (Tüzün et al., 2006). We recently found that skeletal muscle mRNA expression for TNFR1 (TNFα receptor) and IL6R (IL-6 receptor) were greater in near-term IUGR rat fetuses (Cadaret et al., 2017). Both of these cytokines regulate myoblast proliferation and differentiation (Al-Shanti et al., 2008) and thus are essential factors in normal growth and development of muscle. Therefore, we postulate that developmental changes in inflammatory regulation of IUGR myoblasts contribute to their decreased functional capacity. In addition, the IUGR fetal environment is characterized by nutrient restriction, hypoxia, and chronic exposure to stress factors (Macko et al., 2016; Rozance et al., 2018). Recent studies have implicated the activation of mitophagy and autophagy pathways in response to nutrient deprivation and chronic stress as mediators of metabolic dysfunction and poor muscle growth (Hosokawa et al., 2009; Yan et al., 2012). The Unc-51-like kinase 2 (ULK2)-mediated activity of these pathways after initial activation by TNFα/TNFR1 signaling has

been implicated in the pathology of Type II diabetes via mitochondrial dysfunction in skeletal muscle (Yan et al., 2012; Yang et al., 2015). The activation of the IκB kinase (IKK) complex is a critical step in both the TNFα/TNFR1-mediated activation of NFκB signaling pathways, and in the induction of autophagy and mitophagy in skeletal muscle (Karin, 1999; Mourkioti and Rosenthal, 2008c; Criollo et al., 2010). Thus, the objective of this study was to determine whether programmed changes in inflammatory regulation and in IKK mediated signaling pathways are responsible for the impaired functional capacity of IUGR fetal myoblasts. We further sought to determine if these changes are associated with changes in mRNA expression for key components of mitophagy/autophagy signaling pathways.

Materials and methods

Animals and myoblast isolation

The following experiments were approved by the Institutional Animal Care and Use Committees at the University of Nebraska-Lincoln and The University of Arizona which are both accredited by AAALAC International. Columbia-Rambouillet ewes purchased from Nebeker Ranch (Lancaster, CA, USA) and carrying singleton pregnancies were used to create IUGR fetuses (n = 7). Placental insufficiency was induced by exposing ewes to elevated ambient temperatures (40°C, 35% RH) from the 40th to the 95th day of gestational age (dGA), as previously described (Yates et al., 2014; Yates et al., 2016). Control fetuses (n = 7) were from pair-fed ewes maintained at 25°C. Ewes were euthanized and necropsied at 134 ± 1 dGA and myoblasts were isolated from fetal hindlimb muscle as described (Yates et al., 2014). Briefly, fetal semitendinosus muscles were dissected from the hindlimb of each fetus. Muscles were washed with cold

PBS containing 1% antibiotic-antimycotic (AbAm; Gibco Life Technologies, Grand Island, NY, USA) and 0.5% gentamicin (Gibco) before being finely minced and divided into 50-ml tubes (~5 g tube^{-1}). Minced muscle was then washed, re-suspended in PBS containing 1.25 mg/ml protease type XIV from *Strept. griseus* (Millipore-Sigma, St Louis, MO, USA), and digested at 37ºC for 1 hour to liberate myoblasts. After digestion, samples were serial-centrifuged (500 x g, 10, 8, and 1 minute) and the supernatant was collected and centrifuged (1500 x g, 5 minutes) a final time to pellet the isolated myoblasts. Cellular pellets were re-suspended in DMEM (Gibco) containing 10% fetal bovine serum (FBS, Atlas Biologicals, Ft Collins, CO, USA), 1% AbAm, and 0.5% gentamicin and incubated for 2 hours (37°C; 95% O2, 5% CO2) to remove fibroblasts. Purified myoblasts were grown in complete growth media (DMEM containing 20% FBS, 1% AbAm, and 0.5% gentamicin) on fibronectin-coated culture plates (10 μg ml^{-1}; Millipore-Sigma) for 24 hours, lifted from plates with Accutase (Gibco), re-suspended in complete growth media containing 10% dimethyl sulfoxide (Millipore-Sigma), slowly frozen, and stored in liquid nitrogen.

Myoblast functional studies

Myoblasts were quickly thawed at 37°C and pre-plated in DMEM containing 10% FBS for 2 hours (37°C; 95% O2, 5% CO2) prior to treatment. To determine purity of myoblast isolates, a subsample of cells were stained for the myoblast marker pax7 as previously described (Cadaret et al., 2017), and isolates from all fetuses were ≥96% pax7^{+}. To determine proliferative capacity, myoblasts were plated at 5,000 cells well^{-1} on fibronectin-coated 6-well culture plates, grown for 3 days in complete growth media, and then incubated for 24 hours in complete growth media containing either no additive

(basal), IL-6 (1ng/ml; Sigma) ,or TNFα (20ng/ml; Sigma) in the presence or absence of the I***κ***B kinase inhibitor TPCA-1 (IKKi 5μM; ApexBio Technology, Houston, TX, USA). Myoblasts were then pulse-labelled with EdU (10nM; Thermo Fisher), which is incorporated into replicated DNA for 2 hours. Myoblasts were then cooled on ice for 2 minutes, lifted from plates with Accutase (Sigma), and fixed in suspension with 4% paraformaldehyde (PFA; Millipore Sigma) for 10 minutes. To determine differentiation capacity, a second set of myoblasts were plated at 20,000 cells well^{-1} as described above and cultured for 3 days in differentiation media (DMEM containing 2% FBS, 1% AbAm, and 0.5% gentamicin) that contained no additive (basal), 20ng/ml TNFα, or 1ng/ml IL-6. After 3 days, cells were cooled, lifted from plates, and fixed in 4% PFA as described above. All media were changed daily.

Immunocytochemistry

Proliferation rates were calculated as the percentage of myoblasts incorporating EdU (i.e. undergoing DNA replication) during the 2-hour pulse period. These cells were identified by staining for EdU in suspension using the ClickIT® EdU Alexa Fluor® 555 Cell Proliferation Assay Kit (Life Technologies) according to the manufacturer's recommendations. Briefly, fixed cells were incubated in 200 μL of a permeabilization/blocking buffer comprised of PBS containing 1% bovine serum albumin (BSA; Millipore Sigma), 2% FBS, and 0.5% Triton X-100 (Millipore Sigma) for 10 minutes at 4ºC. Cells were then pelleted by centrifuge (400 x g, 5 minutes) and re-suspended in 100 μL of ClickIT® reaction cocktail prepared according to manufacturer's recommendations. After incubating at room temperature for 30 minutes, cells were pelleted, washed twice, and re-suspended in Moxi Cyte Reagent (ORFLO Technologies,

Ketchum, ID) for analysis. Differentiated myoblasts were identified by staining with antiserum raised in the mouse against myogenin (F5B; 1:50; BD Pharmingen) or desmin (DE-U-10; 1:250; GeneTex). Primary antibodies were diluted in permeabilization / blocking buffer comprised of PBS containing 5% FBS, 0.5% Saponin (Millipore Sigma), and 2% BSA, which was applied for 1 hour at room temperature. Afterward, myoblasts were pelleted, washed, and incubated for 1 hour at room temperature with secondary affinity purified anti-mouse IgG PE-Conjugate antibody (1:250; Cell Signaling). Cells were then washed twice and re-suspended in Moxi Cyte Reagent for analysis. All samples were analyzed on a zEPI flow cytometer (ORFLO Technologies), with gates set from negative controls produced by incubating a subset of cells from each fetus in permeabilization / blocking buffer containing no primary antibody.

RNA extraction and preparation

Transcript expression was measured in differentiated myoblasts from parallel cultures performed for each fetus as described above and in samples of fetal semitendinosus muscle collected and snap frozen at necropsy. Myoblasts were lysed on the plate with 600 µl RLT buffer (Qiagen, Valencia, CA) and stored at -80ºC. Total RNA from myoblast lysates and from homogenized skeletal muscle was isolated with the RNeasy kit (Qiagen), including on-column DNase digestion with the RNase-Free DNase set (Qiagen) according to manufacturer recommendations. To calculated RNA concentrations and quality, isolates were analyzed on a Take3 plate with an Epoch Spectrophotometer System (BioTek, Winooski, VT), and all samples produced a 260/280 ratio $\geq$ 2.0. Isolated RNA was reverse transcribed into cDNA using the QuantiTect

reverse transcription kit (Qiagen). Samples were then diluted at 1:10 in RNase-free water (Qiagen) and stored at -20ºC.

Gene expression

Primer design.

Primers and probes for analysis of myoblast gene expression were designed using the Primer3 system (Untergasser et al., 2012), according to the recommended criteria for use with ddPCR supermix for probe (No dUTP) based assays (Bio-Rad, Hercules CA, USA). These were validated for target specificity using both National Center for Biotechnology and Information primer design tools and the BLAT function of the UCSC genome browser (University of California, Santa Cruz CA). Optimized sequences were purchased as PrimeTime® probe assays from Integrated DNA Technologies (IDT; Coralville, IA), re-suspended in IDTE buffer (IDT) to a stock concentration of 10X, and stored at -20ºC. PrimeTime® probe assays were prepared using the recommended 10X stock concentration protocol (IDT), yielding a final 1X concentration of 500 nM for each primer and 250 nM for probes per reaction. For analysis of skeletal muscle gene expression, oligonucleotide primers were synthesized as previously described (Tüzün et al., 2006; Al-Shanti et al., 2008), and primer pairs were obtained from IDT. The complete list of optimized primers and probes for each target gene is summarized in **Table 3-1**.

Myoblast gene expression.

Droplet digital PCR (ddPCR) analysis was performed in a duplex format by co-amplifying the target gene of interest labelled with FAM and the housekeeping gene ribosomal protein L19 (RPL19) labelled with HEX. Quantification was performed using 11 µl of a 2X concentration of QX200 ddPCR supermix for probe-based assays (Bio-

Rad), yielding a final 1X concentration in each 22-µl reaction. Target gene primers and master mix were added to individual wells of a colorless 96-well PCR plate (Sigma), and 100 ng of cDNA diluted in RNase-free water was added to individual wells to a final volume of 22 µl. RNase-free water was used as the negative template control. Each duplex was analyzed on an individual 96-well plate containing all fetuses and the negative control. Mixtures were vortexed and centrifuged and approximately 20,000 droplets were generated using a QX200 Droplet Digital generator (Bio-Rad). Droplets were transferred to a QX200 compatible ddPCR 96-well plate (Bio-Rad) and thermal cycled on a C1000 Touch Thermo Cycler (Bio-Rad). Conditions were set according to the pre-determined annealing temperatures of designed PrimeTime® assays. The plate was then transferred to a QX200 Droplet Reader (Bio-Rad) and analyzed using QuantaSoft Analysis Pro Software (Bio-Rad). Gene expression was determined in duplicate for each sample.

Skeletal muscle gene expression.

PCR products were cloned into pCR II vectors (Invitrogen) and confirmed with nucleotide sequencing by The University of Arizona Genetics Core as previously described (Macko et al., 2016). Primer efficiency was determined, and standard curves were produced using plasmid DNA. Expression for each gene of interest was determined by qPCR using SYBR Green (Qiagen) with a 7900HT Real-Time PCR Detection System (Life Technologies). Samples were initially denatured (95°C for 15 minutes) and then amplified with 45 cycles of denaturing (96°C for 30 seconds), annealing (60–62°C for 30 seconds), and fluorescence measurement during extension (72°C for 10 seconds). Melt

curves were performed after amplification to confirm product homogeneity. Gene expression was determined in triplicate for each sample.

Western immunoblot

Intracellular protein concentrations for IκBα and c-Fos were determined in snap-frozen fetal semitendinosus muscle. Muscle samples (~100 mg) were homogenized in 200 µl of radioimmunoprecipitation buffer containing manufacturer-recommended concentrations of Protease and Phosphatase Inhibitor (Thermo Fisher). Homogenates were sonicated and centrifuged (14,000 x g for 5 minutes at 4ºC) to separate the supernatant. Total protein concentrations were determined with a Pierce BCA Protein Assay Kit (Thermo Fisher). Protein samples (35 µg) were boiled for 5 minutes at 95°C in BioRad 4x Laemmli Sample Buffer and separated by SDS-polyacrylamide. These gels were transferred to polyvinylidene fluoride low florescence membranes (BioRad) and incubated in Odyssey block solution (Li-Cor Biosciences, Lincoln, NE) for 1 hour at room temperature. They were then washed with 1X TBS-T (20 mM Tris-HCl, 150 mM NaCl, 0.1% Tween-20). Membranes were incubated overnight at 4ºC with antiserum raised in the rabbit against IκBα (1:200; Santa Cruz Biotechnologies, Dallas, TX) or c-Fos (1:200; Santa Cruz) and diluted in Odyssey block solution containing 0.05% Tween-20. An IR800 goat anti-rabbit IgG secondary antibody (1:5000; Li-Cor) diluted in Odyssey block solution with 0.05% Tween-20 and 0.01% SDS was applied for 1 hour at room temperature. Blots were scanned on a Li-Cor Odyssey Infrared Imaging System and analyzed with Li-Cor Image Studio Lite Software.

Statistical analysis

Ex vivo myoblast function and mRNA expression data were analyzed for effects due to fetal experimental group, culture media, and their interaction by ANOVA using the Mixed procedure of SAS (SAS Institute, Cary NC, USA) with the repeated measures function. The subject was fetus and the group was the fetal experimental designation. For myoblast function, two technical replicates per incubation condition were performed and averaged. Data for skeletal muscle mRNA and protein expression were analyzed by one-way ANOVA using the Mixed procedure of SAS. Myoblast mRNA expression analyzed by ddPCR were calculated as the number of transcript copies of target gene per µl normalized to the number of transcript copies of the reference gene RPL19 per µl. Skeletal muscle mRNA expression data measured by qPCR were normalized to expression of ACTB (β actin). Expression of both normalizer genes was steady between groups and among media types. Values are expressed as means ± SE and fetus is the experimental unit for all analyses.

Results

Myoblast proliferation

A fetal group x media type interaction was observed ($P < 0.05$) for myoblast proliferation rates (**Figure 3-1**). Proliferation was less ($P < 0.05$) in IUGR myoblasts compared to controls in basal and IL-6 spiked media but did not differ between control and IUGR myoblasts in TNF-spiked media. In control myoblasts, proliferation was decreased ($P < 0.05$) after incubation in media spiked with TNFα compared to basal media, but rates did not differ between basal and TNF-spiked media. TPCA-1 decreased ($P < 0.05$) proliferation for both groups in basal and TNF-spiked media compared to TPCA-1 free media. IUGR myoblasts incubated in the presence of TPCA-1 had decreased ($P < 0.05$) proliferation compared to controls in both basal and TNF-spiked media. Proliferation rates in IUGR myoblasts were similar among basal, IL-6, and TNF-spiked media, and between basal and TNF-spiked media in the presence of TPCA-1.

Myoblast differentiation

The percentage of myogenin$^+$ myoblasts from IUGR fetuses was less ($P < 0.05$) than the percentage from controls regardless of the type of differentiation media (**Figure 3-2**). In myoblasts from both fetal groups, myogenin$^+$ percentages were similar between basal and IL-6 spiked media and were decreased ($P < 0.05$) in TNF-spiked media. A fetal group x media type interaction was observed ($P < 0.05$) for desmin$^+$ myoblasts (**Figure 3-3**). Percentages of desmin$^+$ myoblasts were less ($P < 0.05$) for IUGR fetuses compared to controls when incubated in basal media but did not differ between groups when incubated in IL-6 or TNFα-spiked media. For control myoblasts, desmin$^+$ percentages were greatest

($P < 0.05$) in basal media and least ($P < 0.05$) in TNFα-spiked media. For IUGR myoblasts, desmin^{+} percentages did not differ among differentiation media types.

Myoblast mRNA expression

A fetal group x media type interaction ($P < 0.05$) was observed for TLR4 expression in differentiated myoblasts (**Figure 3-4A**). TLR4 expression was increased ($P < 0.05$) in myoblast populations from both fetal treatment groups when incubated in TNF-spiked media compared to basal media, but the increase in IUGR myoblasts was of a greater ($P < 0.05$) magnitude than in controls. Myoblast mRNA expression for TLR4 was not different between fetal groups when incubated in basal or IL-6 spiked differentiation media. Expression of TNFR1 was greater ($P < 0.05$) in differentiated myoblasts from IUGR fetuses compared to controls regardless of differentiation media type (**Figure 3-4B**). Similarly, the expression of ULK2 was greater ($P < 0.05$) in myoblasts from IUGR fetuses compared to controls regardless of media type (**Figure 3-4C**). Myoblast mRNA expression for IL6R and USP25 did not differ between fetal groups or among differentiation media (**Figures 3-4D and E**, respectively).

Skeletal muscle gene and protein expression

Expression for TNFA (TNFα) did not differ between control and IUGR fetal semitendinosus muscles (**Figure 3-5A**). However, gene expression for IL6 and TNFR1 was greater ($P < 0.05$) in IUGR fetal semitendinosus than in controls (**Figures 3-5B and C**, respectively). Semitendinosus content of IκBα protein was less ($P = 0.05$) in IUGR fetuses compared to controls (**Figure 3-6A**). Conversely, semitendinosus content of c-Fos protein was greater ($P < 0.05$) in IUGR fetuses compared to controls (**Figure 3-6B**).

Discussion

In this study, we show evidence that IUGR fetal myoblasts may have inherently greater responsiveness to the multifunctional effects of TNFα and IL-6, leading to disruptions in their functional capacity to proliferate and differentiate. These findings help to explain the impaired skeletal muscle growth previously observed in IUGR fetuses (Yates et al., 2014; Cadaret et al., 2018). Incubation with TNFα decreased *ex vivo* proliferation, and both TNFα and IL-6 decreased differentiation rates in control myoblasts. However, IUGR myoblasts proliferated and differentiated at lower rates with or without the addition of exogenous cytokines. Administration of an IKK inhibitor resulted in decreased proliferation in all fetal myoblasts under both basal and TNF-spiked conditions. This indicates inflammatory stimulation was enhanced even under basal conditions. This effect was greater in IUGR myoblasts in both media. Moreover, transcript expression patterns in IUGR myoblasts and semitendinosus muscle were consistent with a change in their responsiveness to inflammatory factors, making them more sensitive to the small amounts of endogenous cytokines either contained in the serum-spiked media or produced by the cells themselves (Podbregar et al., 2013). Enhanced sensitivity and immunomodulatory changes in these IUGR myoblasts may provide the molecular mechanism to explain their previously observed intrinsic functional deficits (Brown, 2014; Yates et al., 2014; Soto et al., 2017). These changes could make IUGR myoblasts respond differently to IL-6 and TNFα-induced inhibition even when the circulating and local expression levels are at resting concentrations. Alternatively, these deficits might be due intrinsic adaptations within inflammatory signaling pathways that render them less responsive to cytokines. A similar phenotype

could manifest due to increased expression of survival elements downstream of NF***κ***B, which has been previously shown to increase TNFR1 expression while simultaneously counteracting its apoptotic signaling pathways (Puimège et al., 2014; Ting and Bertrand, 2016). If this is indeed the case, then the apparent enhanced sensitivity could be a compensatory mechanism to maintain signaling function in the presence of increased NF***κ***B signaling activation (**Figure 3-7**). This would reflect a survival-oriented signaling response to cytokine stimulation, rather than an enhanced sensitivity to these multifunctional signaling molecules. Indeed, when treated with an IKK inhibitor, both control and IUGR myoblasts demonstrated decreased proliferation. IUGR myoblast proliferation was less than controls in TNF-spiked media when IKKi was present indicating that select TNFα signaling pathways are altered in IUGR myoblasts to possibly promote cell survival. Interestingly, our results also indicate that these two cytokines had differing effects on normal myoblast differentiation. TNFα reduced markers of early (myogenin$^+$) and late (desmin$^+$) differentiation in control myoblasts but IL-6 reduced desmin$^+$ myoblasts only, indicating that TNFα may be a more potent inhibitor of fetal myoblast differentiation than IL-6. Together, these findings show that IUGR fetal conditions induce programming responses in skeletal muscle that may modulate the inflammatory regulation of myoblasts, which diminishes their capacity to function and facilitate hypertrophic muscle growth. These altered pathways may represent key molecular mechanisms that help to explain the link between stress-induced fetal adaptations and lifelong reductions in skeletal muscle mass in IUGR-born individuals. Diminished proliferation rates in IUGR myoblasts incubated IKKi in TNF-spiked media indicate that these cells rely in part on NF***κ***B-associated survival pathways

to mitigate the effects of increased inflammatory signaling. However, further analysis of alternative pathways with similar effects on proliferation and differentiation are needed to identify how inflammatory modulation is altered in IUGR-born individuals.

Analyses of specific gene transcripts and proteins involved in canonical inflammatory pathways show for the first time that intrinsic deficits in IUGR myoblasts coincide with molecular changes that may enhance inflammatory signaling pathway coupling. Fetal IUGR myoblasts and skeletal muscle exhibited increased mRNA expression for the well-characterized inflammatory receptor TNFR1, which we postulate augmented TNFα-associated action relative to controls despite similar TNFα concentrations in culture media and similar skeletal muscle mRNA expression for TNFα. The apparent enhancement of TNFα sensitivity was further supported by the greater capacity for TNFα-spiked culture media to induce TLR4 expression in primary IUGR myoblasts compared to controls. Greater TNFα/TNFR1 activity combined with the potential for greater TLR4 activity represents a possible mechanism for increased autophagy and mitophagy within IUGR myoblasts via activation of the IKK complex (Fitzgerald et al., 2004; Criollo et al., 2010). As illustrated in **Figure 3-8**, IKK increases activity of NFκB, a keystone of canonical inflammatory signaling, by facilitating the ubiquitination and degradation of its arrest protein, IκBα (Karin, 1999). It also plays a non-canonical role in stress-associated stimulation of autophagy/mitophagy pathways by increasing ULK2, a key factor in nutrient deprivation-induced autophagy (Lee and Tournier, 2011). Indeed, we observed that IUGR skeletal muscle contained reduced amounts of IκBα and IUGR myoblasts exhibited greater gene expression for ULK2. We further found that IUGR skeletal muscle had increased amounts of c-Fos, which is

induced by TNFα (Haliday et al., 1991; Tu et al., 2013) and has been shown to impair myoblast differentiation by interfering with myoD and myogenin (Li et al., 1992; Trouche et al., 1993; Waskiewicz and Cooper, 1995; Rivard et al., 2000; Wozniak et al., 2005). These observations indicate that IUGR fetal muscle expressed greater inflammatory signaling activity despite the normally immunosuppressive *in utero* conditions during pregnancy (McCracken et al., 2004), which would be consistent with human studies showing greater inflammatory cytokine concentrations in cord blood (Laskowska et al., 2006). The entirety of the changes that occur within these inflammatory pathways has not been fully assessed, but the greater apparent activity of these pathways was not associated with changes in expression of USP25, which mediate both inflammatory responses and skeletal muscle differentiation (Bosch-Comas et al., 2006; Zhong et al., 2013). Moreover, gene expression for the IL-6 receptor remained unchanged between our fetal groups and among incubation conditions, although expression for the ligand itself was increased in IUGR skeletal muscle. Thus, IL-6 signaling activity may have been increased by greater ligand gene expression, whereas TNFα signaling activity was enhanced at the level of its receptor and downstream signaling components. Nevertheless, it appears that enhanced TNFα/TNFR1 affected NFκB-associated and NFκB-independent pathways downstream of IKK, as demonstrated by reduced muscle IκB content and increased myoblast ULK2 gene expression, respectively. These findings implicate adaptive changes in pathways downstream of IKK associated with nutrient sensing, stress responses, and cellular survival in the development of the IUGR phenotype (Limesand et al., 2009; Thorn et al., 2009) and a molecular mechanism for reduced muscle mass and impaired skeletal muscle growth.

Intrinsically-reduced proliferation and differentiation in IUGR myoblasts restricts muscle growth, which is beneficial to fetal survival of intrauterine nutrient deprivation and hypoxia but also predisposes offspring to metabolic health disorders (Yates et al., 2012). Because cytokines play an essential regulatory role in muscle growth and development (Djavaheri-Mergny et al., 2006; Limesand et al., 2007; Al-Shanti et al., 2008), the adaptive mechanisms observed in this study may help to explain smaller muscle fibers and reduced muscle mass in IUGR fetuses (Yates et al., 2014; Yates et al., 2016), which in turn helps explain their impaired glucose homeostasis (Godfrey and Barker, 2000; Cadaret et al., 2018). Although not measured in the present study, this is could perhaps be due to the non-canonical activation of JNK/MAPK by TNFR1-mediated activation of IKK pathways involved in the mitophagy of mitochondria in response to cellular stress (Yan et al., 2012; Yang et al., 2015). TRAF2-mediated activation of JNK/MAPK pathways by stress would explain increases in c-Fos (Fitzgerald et al., 2004; Limesand et al., 2007; Brown et al., 2015) and its associated pathways that are implicit regulators of myoblast-facilitated skeletal muscle growth (Li et al., 1992; Trouche et al., 1993; Rivard et al., 2000). Furthermore, coinciding stimulation of survival-oriented anti-autophagic pathways via canonical IKK-NFκB activation (Reid and Li, 2001; Yan et al., 2012) may help to explain how muscle fiber size and oxidative metabolic phenotypes are reduced without a loss in fiber numbers (Limesand et al., 2007; Yates et al., 2014; Brown et al., 2015; Yates et al., 2016). In TNF-spiked media, IUGR myoblasts demonstrated decreased proliferation rates when only when IKKi was added. This would indicate that some level of IKK-associated signaling within these cells differs from controls allowing them to proliferate at rates similar to control myoblasts in the presence of TNFα in spite

of an enhanced inflammatory signaling response. Increased ULK2 activity would further contribute to IUGR-associated metabolic dysfunction, as increased autophagy and mitochondrial degradation has been implicated in the pathogenesis of Type II diabetes (Yan et al., 2012). These insights implicated the activation of mitophagy/autophagy pathways by an altered inflammatory signaling response in the development of the IUGR phenotype. This represents a promising avenue of further study to fully understand how this complex interaction might be occurring, and whether it is indeed due to an enhanced TNFR1 signaling system. Although TNFR1-associated signaling appears to be responsible for initiating this response in our study, activation of the IKK pathway can occur through a number of different signal transduction systems separate from inflammatory signaling. If inflammatory responsiveness is indeed altered within IUGR-myoblasts then this increase in autophagy could represent a compensatory response to increased NF$\boldsymbol{\kappa}$B-mediated activity, which previous studies have shown TNFR1 signaling to inhibit (Qing et al., 2007; Criollo et al., 2010). Thus, the observed increases in TNFR1 could be due to increased NF$\boldsymbol{\kappa}$B signaling in the absence of altered canonical constitutive TNFR1 signaling downstream of expression (Criollo et al., 2010; Puimège et al., 2014). Alternatively this activation could be due to other, yet unidentified, pathways that are differentially expressed within the IUGR phenotype downstream of IKK such as increases in beta-adrenergic signaling pathways or hypoxic responses both of which have also been implicated in the IUGR phenotype and activation of autophagic pathways (Yan et al., 2012; Farah et al., 2014) It is worth noting that this outcome can be stimulated by TNFα via TRAF2-mediated activation of JNK/MAPK pathways (Yang et al., 2015) and by TLR4 via activation of the IKK complex (Reyna et al., 2008; Criollo et al., 2010).

However, more robust studies need to be conducted to establish if these pathways downstream of IKK are indeed differentially expressed in IUGR myoblasts, and to determine what proteins and genes are responsible for this phenotype. The identification of potential differential activation of autophagy/mitophagy-associated pathways represents a novel avenue of further research, as we continue to attempt to identify the adaptations that occur in IUGR-individuals.

Conclusions

Fetal adaptations that result from IUGR may alter the responsiveness of skeletal muscle stem cells to inflammatory factors, especially cytokines. These programmed changes, which mostly likely follow chronic inflammatory exposure and nutrient restriction *in utero*, may also be linked to cellular autophagy/mitophagy pathways associated with long-term nutrient deprivation. In IUGR myoblasts, changes were observed in pathways associated with the pleiotropic cytokines TNFα and IL-6. These changes appeared to increase pathway components associated with the anti-apoptotic effects of IKK-mediated NFκB activation, pro-mitophaghic and autophagic effects via ULK2 upregulation, and disrupted differentiation via c-Fos upregulation, all of which help to explain reduced hypertrophy in IUGR skeletal muscle fibers without a reduction in fiber number. Our findings in cultured IUGR myoblasts indicate that they could possibly demonstrate altered inflammatory activity independent of their environment, thus providing one potential molecular mechanism to explain their intrinsic dysfunction. Together, our findings show that IUGR fetal skeletal muscle adaptations alter the response of myoblasts to regulatory cytokines by possibly enhancing both canonical and

non-canonical pathways involved in myoblast function, metabolism, and cellular survival.

Table 3-1. Primer and oligo sequences for ddPCR and qPCR.

Gene	Protein	Primer Sequence	Product Size	Accession Number
		ddPCR Primers		
RPL19	60S Ribosomal Protein L19	GCAGACAAGGCTCGCAAG CTAACACAACAGCTGGGCAG HEX-TGGCGTAAGTTCTGAGGCAT-ZEN/IB FQ	100	NC_019468.2
TLR4	Toll-like Receptor 4	CAGATGCAGAGACCAACCCG CACTGAACACACCCTGCATC 6-FAM-TCCACCTGAGGAGGAGAATC-ZEN/IB FQ	100	NM_001135930
TNFR1	TNFα Receptor 1	CACCCGCAAAATAGCACCAT AGAGAAAGAAGCAGGGCCTC 6-FAM-CCAAGTGCCACAAAGGTAGG-ZEN/IB FQ	100	NM_001166185
IL6R	IL-6 Receptor	AACAGAGGCTACTTCTTCCCC GGCAGTGAGGAGCGACTTAT 6-FAM-TAATGGGTAGGCCTAGCAGC-ZEN/IB FQ	100	NC_019458.1
ULK2	Unc51-like Kinase 2	CACCTGTTGCCTGTTCCATC CTGACGGAACTGCTCAGGAA 6-FAM-TTCCTTCTCTCAGTGGGCAC-ZEN/IB FQ	100	NC_019468.2
USP25	Ubiquitin-specific Peptidase 25	ACCAAGGCATCACATGAGCA ATCTCGTGAACATGGATGGGT 6-FAM-TGAAACAGTTTTGCAGTCGGT-ZEN/IB FQ	100	NC_019458.2
		qPCR Primers		
ACTB	β Actin	GCGGCATTCACGAAACTACC CCAGGGCAGTGATCTCTTTCTG	147	NM_001009784
IL6	Interleukin 6 (IL-6)	TTCACAAGCGCCTTCAGTCC TCTGCTTGGGGTGGTGTCAT	120	NM_001009392
TNFA	Tumor necrosis factor α (TNFα)	CATCAAGAGCCCTTGCCACA CGGCAGGTTGATCTCAGCAC	130	NM_001024860
TNFR1	TNFα Receptor 1	CTGGTGATTGTCTTTGGGCTTT AGCGACATGCTAAAACCACAGA	61	NM_001166185

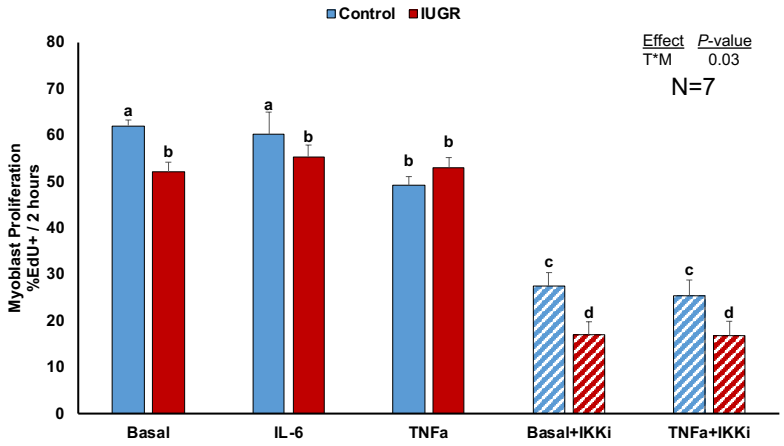

Figure 1

Figure 3-1. **Proliferation rates in primary IUGR fetal myoblasts incubated for 24 hours in complete growth media (20% FBS) containing no additive (basal), TNFα (20 ng ml-1) in the presence or absence of TPCA-1 (5μM) or spiked with IL-6 (1 ng ml-1) alone. Cells were pulsed with 10nM EdU for 2 hours. ^{a,b,c,d} means with different superscripts differ (P < 0.05). N-value represents pairs of one IUGR and one control animal's isolated myoblasts.**

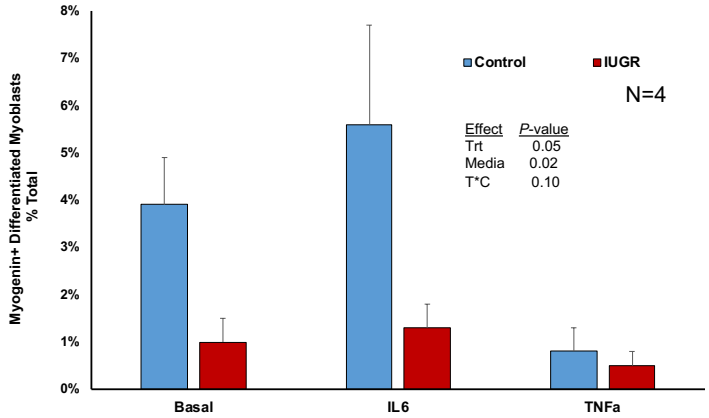

Figure 2

Figure 3-2. **Percentages of myogenin^{+} primary IUGR fetal myoblasts after 4-day differentiation in media containing no additive (basal), TNFα (20 ng ml^{-1}), or IL-6 (1 ng ml^{-1}). Differences ($P \leq 0.05$) were observed for main effects of fetal treatment and differentiation media, but no interaction between these main effects was observed. N-value represents pairs of one IUGR and one control animal's isolated myoblasts.**

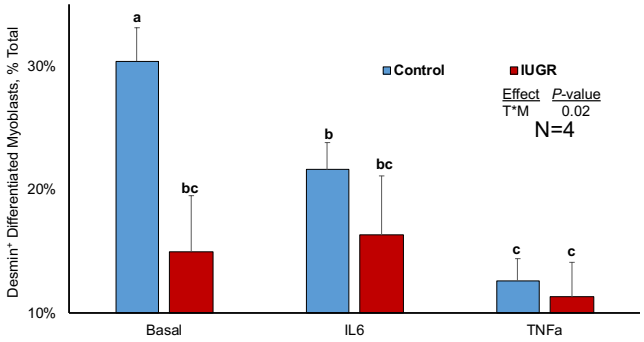

Figure 3

Figure 3-3. **Percentages of desmin^{+} primary IUGR fetal myoblasts after 4-day differentiation in media containing no additive (basal), TNFα (20 ng ml^{-1}), or IL-6 (1 ng ml^{-1}). ^{a,b,c} means with different superscripts differ ($P < 0.05$). N-value represents pairs of one IUGR and one control animal's isolated myoblasts.**

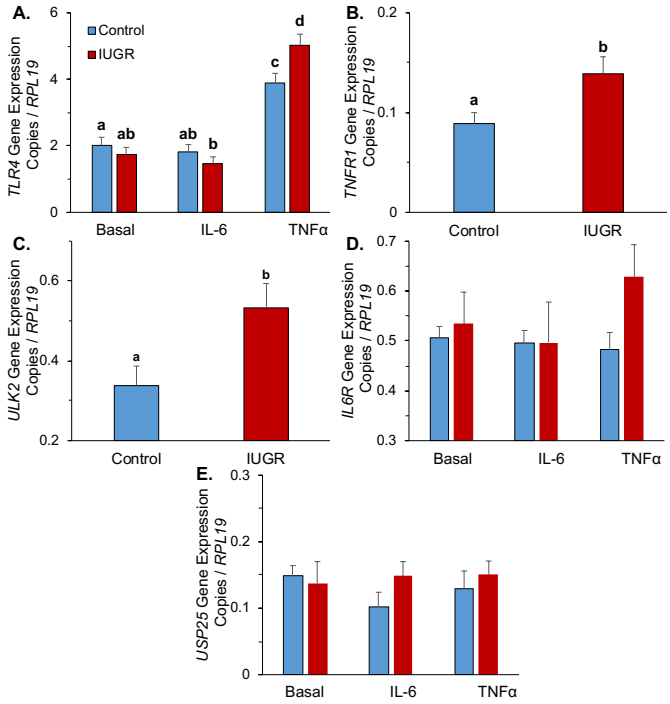

Figure 4

Figure 3-4. **Gene expression (ddPCR) for (A) TLR4, (B) TNFR1, (C) ULK2, (D) IL6R, and (E) USP25 in primary IUGR fetal myoblasts after 4-day differentiation in media containing no additive (basal), TNFα (20 ng ml^{-1}), or IL-6 (1 ng ml^{-1}). ^{a,b,c,d} means with different superscripts differ ($P < 0.05$).**

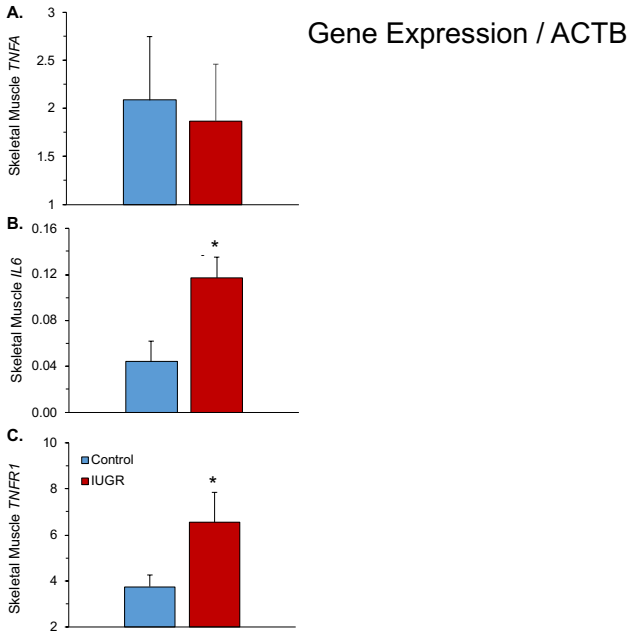

Figure 5

Figure 3-5. **Gene expression (qPCR) for (A) TNFA (TNFα), (B) IL6 (IL-6), and (C) TNFR1 in semitendinosus skeletal muscle from IUGR fetal sheep. * fetal treatment means differ (P < 0.05).**

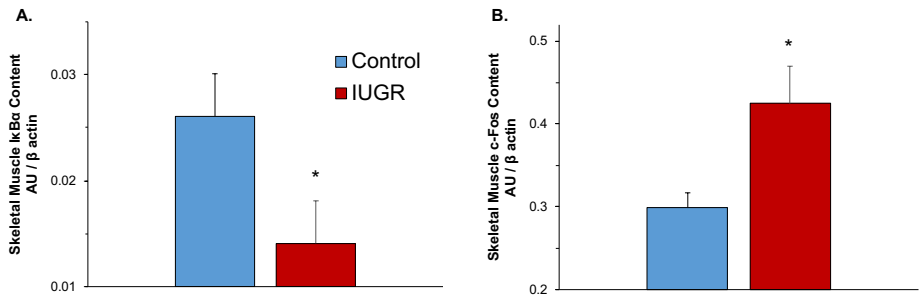

Figure 6

Figure 3-6. **Protein content (western immunoblot) for (A) IκBα and (B) c-Fos in semitendinosus skeletal muscle from IUGR fetal sheep. * fetal treatment means differ ($P < 0.05$).**

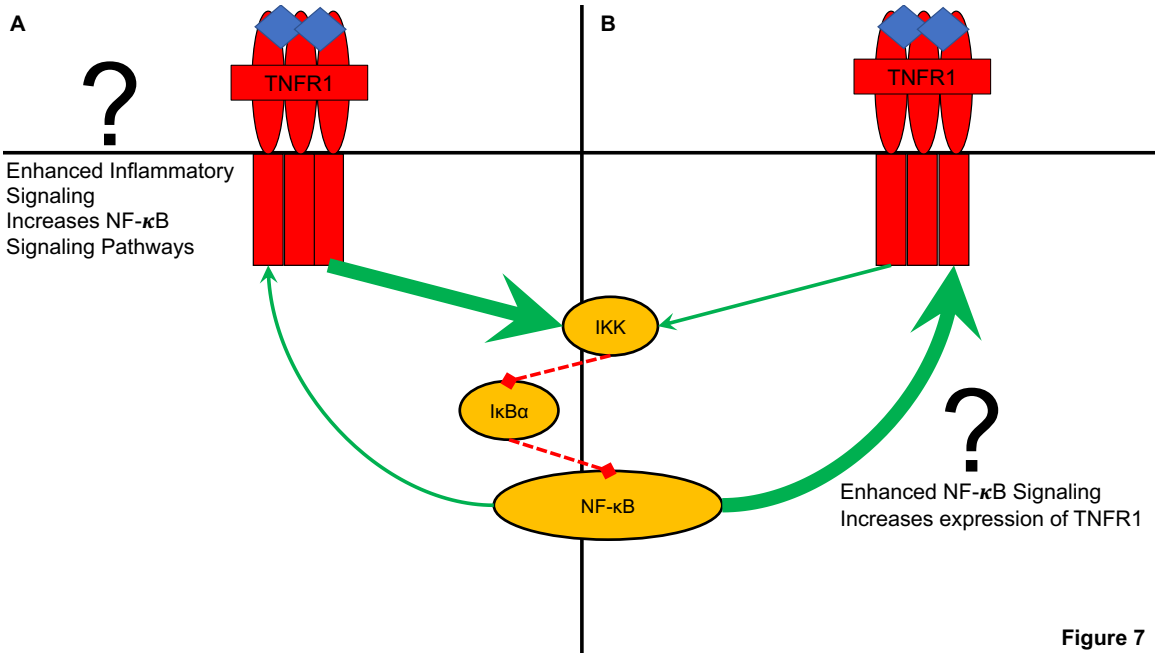

Figure 3-7. **Diagram of two hypothesized inflammatory programming responses that lead to enhanced inflammatory signaling. A) Increased expression of TNFR1 leads to increases in NF-κB signaling via IKK activation. B) Increased intrinsic NF-κB signaling has a positive feedback effect on TNFR1 increasing expression and leading to enhanced inflammatory responsivity.**

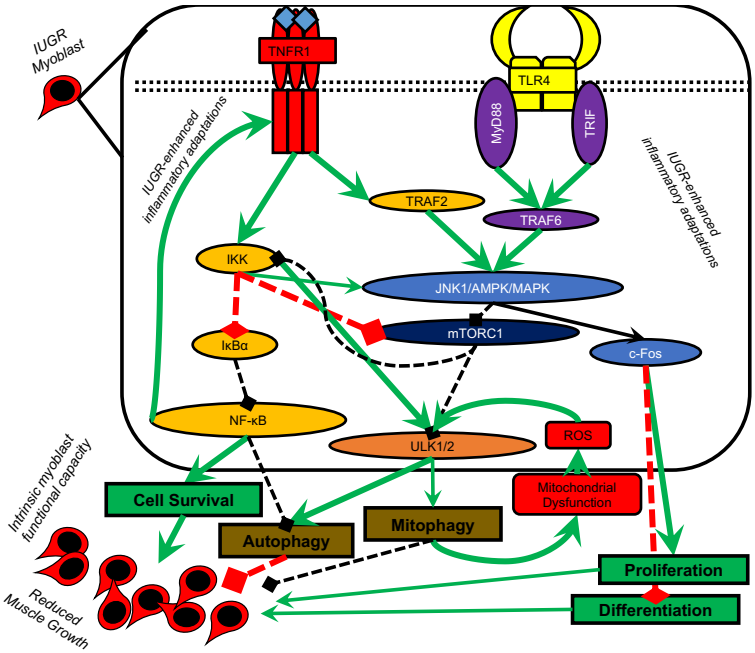

Figure 8

Figure 3-8. **Integrated schematic of the hypothesized adaptive changes in IUGR fetal skeletal muscle and myoblast signaling pathways that enhance the responsiveness to cytokines, impair myoblast functional capacity, and increased autophagy and mitophagy.**

Chapter 4: Blood gene expression of stress-responsive genes as novel biomarkers for assessing stress and wellbeing in rodents & exotic species.

Abstract

Sustained exposure to stress mediators like cytokines and catecholamines ultimately leads to alterations in the cellular expression of their targets. Stressors like maternofetal inflammation have been linked to the development of intrauterine growth restriction (IUGR), which is associated with fetal growth and metabolic adaptations that persist after birth. Our lab previously found that IUGR rat fetuses have increased plasma TNFα and evidence of changes in inflammatory stress responsivity. The objective in Exp. 1 was to assess inflammation-associated gene transcript changes in fetal and maternal blood pellets from Sprague-Dawley rats injected daily with saline, bacterial lipopolysaccharide (LPS) endotoxin, or LPS + the non-steroidal anti-inflammatory drug (NSAID) meloxicam from the 9th day of gestation age (dGA) to the 11th (term = 21 dGA). Maternal samples collected at 0, 6, and 54 hr after onset of LPS injection and fetal samples collected at necropsy on dGA 20, were assessed for *TNFα, TNFR1, IL6R, Fn14, and INFγR1* differential expression using ddPCR. Fetal *TNFR1* tended to be greater ($P < 0.10$) after maternofetal inflammation (MI), but not when meloxicam was given concurrently. Fetal *IL6R* was reduced ($P < 0.05$) by MI and was not rescued by meloxicam. Maternal *TNFR1* was increased ($P < 0.05$) by LPS at 6 hours and was not ameliorated by meloxicam administration. No other gene transcripts differed among

groups. Together, our findings demonstrate that maternofetal inflammation during mid-gestation leads to transient maternal changes and fetal adaptations in cytokine signaling pathways, which are reflected in the transcriptome of circulating leukocytes. We further show that changes were generally not alleviated by concurrent administration of meloxicam. Given our findings in Exp. 1, the objective of Exp. 2 was to determine if differential expression of stress-responsive genes in blood samples from zoo animals analyzed via ddPCR could be potential stress biomarkers. Total RNA was extracted from whole blood of cheetahs, elephants, and giraffes. The ability to measure mRNA for *TNFα, TNFR1, IL6R, IL6, IL10, ADRβ2, NR3C1* was assessed using ddPCR analysis. *RPP30, RPL19,* and *YWHAZ* were assessed as potential normalizers. For elephant and cheetah target transcript analyses, probes were designed using the assemblies published on the National Center for Biotechnology Information (NCBI) database. Giraffes do not have a published assembly available, so an cross-species technique was used to design primers specific to segments of the target transcripts that were predicted to be highly conserved among giraffe, cow, and sheep. In cheetahs (n=2), primers and probers were successfully validated for *ADRβ2, IL10, IL6R, NR3C1, TNFR1, TNFα,* and all three of our potential normalizers. However, only *RPL19* had a relatively low calculated CV (7%) and was thus presumed to be the most suitable for this species as a normalizer. In giraffes (n=1), we successfully designed cross-species primers for *TNFα* and *ADRβ2*, but not for any of our other intended targets. In elephants (n=3), primers and probes were validated for the quantification of *ADRβ2, IL10, NR3C1, TNFR1, TNFα,* with *RPP30* appearing to be the most suitable normalizer (CV = 10%). The mRNA expression patterns appeared to parallel behavioral reports of one elephant displaying consistent high-anxiety. Together,

these findings indicate that differential expression of stress-responsive genes in blood is a promising avenue for better biomarkers capable of tracking stress and assessing wellbeing in zoo animals, which will be important in optimizing health status & reproductive capacity in these animals. This study also demonstrates that it is possible to design on-target primers for specific transcripts in unassembled species, such as giraffes, with whole genome sequences of related species.

Introduction

Multiple models of maternofetal stress including inflammation have been shown to induce intrauterine growth restriction (IUGR), which is linked to lifelong dysfunction in humans and animals (Cadaret et al., 2018; Yates et al., 2018). Inflammation induced by bacterial lipopolysaccharide (LPS) endotoxin have previously been linked to changes in immune cells and specifically with a shift toward a pro-inflammatory phenotype in circulating white blood cells (WBC) (Medzhitov, 2008; Martinez et al., 2014; Yuan et al., 2016). This pro-inflammatory phenotype favors increases in TNFα and IL-6, as well as their respective receptors TNFR1 and IL6R (Duque and Descoteaux, 2014; Martinez et al., 2014) in concert with a marked decrease in the expression of anti-inflammatory cytokines such as IL-10 (Opal and DePalo, 2000; Duque and Descoteaux, 2014). Stress-responsive signaling pathways activated by glucocorticoids and catecholamines have been implicated in exacerbating this pro-inflammatory phenotype under chronic conditions, which further increases inflammation and contributes to the development of chronic diseases (Medzhitov, 2008; Liu et al., 2017). Therefore, the objective of Exp. 1 was to determine the effects of sustained maternofetal inflammation at mid-gestation on maternal and fetal mRNA profiles in whole blood pellets

Modern zoos are expected to maintain high standards for animal wellbeing in a diverse population of wildlife. Zoo animals experiencing novel stressors may be at greater risk for inflammatory diseases, and opportunistic infections in environments that differ from their natural habitat. The most common indicators used to measure the physiological stress of zoo animals is glucocorticoid concentrations in feces, and to lesser extent blood, urine, or saliva. However, this assay is limited by the individual variation

between group-housed animals (Cockram, 2002; Wolfensohn et al., 2018), the natural circadian variations in glucocorticoids, that glucocorticoid release is also associated with non-stress stimuli, and that glucocorticoids are not always elevated by stress (Cockram, 2002). Other measurements, such as the leukocyte or neutrophil activation test have been previously shown to be possible markers of stress levels (Honess et al., 2005). However, these tests only loosely estimate overall stress through leukocyte responsivity. Finally, the majority of published studies on animal wellbeing focus on markers that only apply to mammalian species, which represent one part most zoos taxonomic population (Wolfensohn et al., 2018). The objective of Exp. 2 was to determine if we could measure stress-responsive gene transcripts as potential biomarkers in whole blood from elephants, giraffes, and cheetahs using ddPCR. We further sought to design cross-species primers for a species with only a whole genome sequence available (giraffes), which would allow for the possibility of future research to be applied to a broader range of species.

Materials and Methods

Exp. 1

Animals and experimental design.

All procedures were approved by the Institutional Animal Care and Use Committee at the University of Nebraska-Lincoln. Studies were performed at the University of Nebraska-Lincoln Animal Science Complex, which is an AAALAC International accredited institution. Timed-pregnant Sprague-Dawley rats (Envigo, Indianapolis, IN) were purchased and delivered on day 6 of gestational age (dGA). On dGA 8, rats were moved to individual housing, fed *ad libitum* commercial rat chow, and weighed daily. From dGA 9 to 11, rats were injected (IP) daily with 250µl saline

(control, n=7), 100µg/kg BW of lipopolysaccharide (LPS) from *E. coli* O55:B5 (Sigma-Aldrich, ST. Louis, MO, USA) in 250µl saline to create maternofetal inflammation-induced IUGR (MI-IUGR, n=8), or LPS concurrent with 7.5mg/kg BW of meloxicam (LMX, n=10). Blood samples were collected from dams via saphenous vein puncture at 0, 6, and 54hr after initial injection. On dGA 20, rats were euthanized by decapitation under heavy isoflurane anesthesia after maternal blood samples were collected via heart puncture. Pooled fetal blood samples were collected for each litter via exsanguination. All blood samples were centrifuged (14,000 x *g*, 2 minutes, 4ºC) and blood pellets were re-suspended in TRI Reagent® (Sigma-Aldrich) at a 3:1 ratio to original blood volume, vortexed, and stored at -80ºC.

RNA extraction and preparation.

Gene transcripts were measured in maternal blood samples taken at 0, 6, and 54hr after the first injection. Fetal blood gene transcript expression was measured from samples taken at dGA 20 as described above. To extract RNA, samples suspended in TRI Reagent® were thawed to room temperature and homogenized. Chloroform (160µl) was added to each sample and vortexed for 10-15 seconds before incubating at room temperature for 5 minutes. All samples were then centrifuged (12,000 x *g*, 15 minutes, 4ºC), and the aqueous layer transferred to a QiAmp® shredder column (Qiagen, Germantown, MD, USA). Extraction was then performed using the QiAmp® RNA Blood Mini Kit (Qiagen), including on-column DNase digestion with the RNase-Free DNase set (Qiagen) according to manufacturer recommendations. Isolated RNA concentration and quality was analyzed on a Take3 plate with an Epoch Spectrophotometer System (BioTek, Winooski, VT, USA) to ensure that all samples produced a 260/280 ratio ≥ 2.0.

RNA isolates were reverse transcribed into cDNA using the QuantiTect reverse transcription kit (Qiagen). Samples were diluted at 1:10 in RNase-free water (Qiagen) and stored at -20ºC.

Primer design.

Primers for the analysis of *IL6R, TNFR1,* and *FN14* expression were purchased as PrimePCR ddPCR primers (Bio-Rad, Hercules, CA, USA) specific to the EvaGreen supermix based assay. Primers for the analysis of *TNFA, YWHAZ, and INFGR1* were designed using the Primer3 system (Untergasser et al., 2012), according to the recommended criteria for use with ddPCR Evagreen supermix based assays (Bio-Rad, Hercules CA, USA). These were validated for target specificity using both National Center for Biotechnology and Information primer design tools and the BLAT function of the UCSC genome browser (University of California, Santa Cruz, CA, USA). Optimized sequences were purchased from Integrated DNA Technologies (IDT; Coralville, IA, USA), re-suspended in RNase free water to a concentration of 100µm. Forward and reverse primer solutions were mixed to create a 10µM working solution, which was stored at 20ºC. gBlocks® Gene Fragments were also purchased from IDT for *YWHAZ, TNFR1, FN14,* and *IL6R*.

mRNA quantification.

Droplet digital PCR (ddPCR) analysis was performed in duplicate using the QX200 system (BioRad). EvaGreen Supermix (11µl) at a 2X concentration was added to individual wells of a colorless 96-well PCR plate (Sigma). A 10µM working solution of IDT designed primers (0.22µl), or PrimePCR primers (1µl) for transcripts of interest was added to individual wells before 2µl of 1:10 cDNA sample was added. RNase free water

was then added to the master mix for a total volume of 22µl per well. RNase-free water was used as the negative template control, and gBlocks® Gene Fragments (IDT) for *YWHAZ, TNFR1, Fn14,* and *IL6R* were used as positive controls to determine the expression levels of those target genes. Each gene was analyzed on an individual 96-well plate containing all fetal and maternal samples, with a negative and positive control. Mixtures were vortexed and centrifuged (3,000 x *g*, 3 minutes, 20ºC) before approximately 20,000 droplets were generated using a QX200 Droplet Digital Generator (Bio-Rad). Droplets were transferred to a QX200 compatible ddPCR 96-well plate (Bio-Rad) and thermal cycled on a C1000 Touch Thermo Cycler (Bio-Rad). Conditions were set according to pre-determined annealing temperatures of designed and PrimePCR primers. Expression was quantified using a QX200 Droplet Reader (Bio-Rad), and results analyzed using QuantaSoft Analysis Pro Software (Bio-Rad). The complete list of optimized primers for each target gene is summarized in **Table 4-1**.

Statistical Analysis.

All data were analyzed by ANOVA using the mixed procedure of SAS (SAS Institute, Cary, NC, USA) to determine experimental group effects. Repeated measures were used for serial maternal samples. Gene transcript data are expressed as transcript copies per µl, normalized to copies per µl of *YWHAZ*. Rat (dam) was considered the experimental unit and experimental group was the group for all variables. Fetal values reflect the pooled fetal samples analyzed in each dam's litter. All data are expressed as mean ± standard error.

Exp. 2

Animals and experimental design.

All sample collections were approved by the Institutional Animal Care and Use Committees at the University of Nebraska-Lincoln and Omaha's Henry Doorly Zoo and Aquarium. Giraffe (n=1) and elephant (n=3) samples were collected into Tempus™ blood RNA tubes (Applied Biosystems, Foster City, CA, USA), and stored at 4ºC for a max of 72hr. Cheetah samples (n=2) were collected using the TRI Reagent (Sigma-Aldrich) protocol described in Exp. 1.

RNA extraction and preparation.

Elephant and giraffe samples collected into Tempus™ blood RNA tubes were extracted using manufacturer recommendations. Cheetah samples collected in TRI Reagent® were extracted using the protocol described for Exp. 1. Quality of RNA was determined and extracts were reverse transcribed as in Exp. 1. cDNA was stored at -20ºC as a 1:10 dilution for elephant and cheetah samples, and undiluted for giraffe samples.

Probe design.

Probes for analysis of cheetah and elephant mRNA expression were designed using the Primer3 system (Untergasser et al., 2012), according to the recommended parameters for use with ddPCR supermix for probe (No dUTP) based assays (Bio-Rad). Sequences were validated using the protocol in Exp. 1 are summarized in **Tables 4-2** and **4-3**. Optimized sequences were purchased as PrimeTime® probe assays (IDT), re-suspended in IDTE buffer to a stock concentration of 10X, and stored at -20ºC. Before use, probe assays were prepared using the recommended 10X stock concentration

protocol to yield a final 1X concentration of 500nM for primers and 250nM for probes per reaction.

Cross-species primer design.

Primers for the analysis of giraffe mRNA expression were designed using a cross-species protocol and are summarized **Table 4-4**. Sheep (*Ovis ares*) and cow (*Bos taurus*) assemblies were obtained from the Ensembl database for each target transcript. The coding regions were then paired against the whole genome sequence (NCBI database) for the giraffe (*Giraffa camelopardalis tippelskirchi*) using the BLAST function (NCBI) to determine identity percentage. Sequence segments with at least 99% identity for target coding regions of both sheep and cow were then aligned using MultAlin. Primers were designed using Primer3 (Untergasser et al., 2012) including only sequence segments that had 99% identity across all three species. Primers also included at least one identified exon that was conserved between cow and sheep sequences. Identified sequences for *IL6, ADRB2, TNFA,* and *RPL19* were obtained and validated using the same protocol as described in Exp. 1. Optimized sequences were purchased (IDT) and working solutions were stored at -20ºC.

ddPCR Analysis.

The giraffe sample, was analyzed with the EvaGreen supermix for ddPCR protocol as described in Exp. 1. Cheetah and elephant ddPCR analysis was also performed as described in Exp. 1, with some modifications for probes. Quantification was performed in duplex format by co-amplifying the target transcript of interest labelled with FAM and the normalizer genes (*RPP30, RPL19,* and *YWHAZ*) labelled with HEX. Each target transcript was quantified in duplex with each normalizer gene to accurately

determine fold change and overall expression during analysis. A 2X concentration of QX200 ddPCR supermix (No dUTP) for probe-based assays (Bio-Rad) at a final concentration of 1X in each 22µl was used in place of the EvaGreen supermix. Conditions for thermal cycling were also modified to fit the pre-determined annealing temperatures of designed PrimeTime® assays. Data are analyzed using QuantaSoft Analysis Pro Software (Bio-Rad) with expression determined for each target gene/normalizer gene combination.

Statistical analysis.

Expression for all three species from ddPCR analysis was calculated as the number of transcript copies of target transcript per µl normalized to the number of transcript copies of each available reference transcript per µl. The coefficient of variation (CV) was determined for all references available in each group to determine their suitability as normalizers. The reference used was *RPL19* for cheetahs, *RPP30* for elephants, and *RPL19* was targeted in giraffes.

Results

Exp. 1

Fetal *TNFR1* tended to be increased ($P < 0.10$) but not when meloxicam was concurrently administered (**Figure 4-1A)**. Fetal *IL6R* was reduced ($P < 0.05$) by MI and was not improved by concurrent meloxicam (**Figure 4-1B**). Maternal *TNFR1* was increased ($P < 0.05$) by LPS at 6hr after initial injection and was not affected by meloxicam administration (**Figure 4-2**). No other genes differed among groups.

Exp. 2

In cheetah samples, the expression of *ADRβ2* (β2 Adrenoceptor), *IL10* (Interleukin 10), *IL6R* (Interleukin 6 Receptor), *NR3C1* (Glucocorticoid Receptor), *TNFR1* (TNFα Receptor 1), and *TNFα* (Tumor Necrosis Factor Alpha) was successfully quantified (**Figure 4-3**). Among the three normalizers, *RPL19* (Ribosomal Protein L19) was found to have the lowest CV (7%) among the samples. In elephant samples, the expression of *ADRB2, IL10, NR3C1, TNFR1,* and *TNFA* were successfully quantified (**Figure 4-4**). *RPP30* (Ribonuclease P/MRP Subunit P30) was the reference transcript with the lowest CV (10%). Cross-species primers were able to quantify *ADRB2* and *TNFA* in our giraffe sample, but no other transcript was successfully quantified by our primers.

Discussion

In Exp. 1, we found that injection of LPS endotoxin caused temporal increases in the expression of *TNFA* and its receptor *TNFR1* in circulating leukocytes of pregnant rats. We also demonstrated that MI at mid-gestation leads to lasting inflammatory adaptations in the transcript expression of the cytokine receptors *IL6R* and *TNFR1*, which were observed at term in fetal blood. These results indicate that inflammation and stress lead to changes in the transcriptome of circulating leukocytes, which can be used as biomarkers for stress assessment. They further demonstrate that activation of these pathways during mid-gestation can have lasting effects on the expression patterns of fetal leukocytes.

In Exp. 2 we determined if these biomarkers could be quantified in zoo species as well. We were able to successfully design and implement ddPCR probes for a number of immunological and stress-responsive genes in cheetahs and elephants, which demonstrates the applicability of assays targeting these biomarkers to a broad range of mammals. We were also able to successfully utilize a cross-species primer design approach to target and analyze some but not all transcripts in giraffes. This represents, to our knowledge, the first successful attempt at designing cross-species primers for these targets in this unassembled species.

We chose the biomarkers in this study based off of our previous experiences, and on the complex interactions between the stress, reproductive, and immune systems. We chose to target the receptors for glucocorticoids (NR3C1) and catecholamines (ADRβ2), as these pathways play a role in immunomodulation, the stress response, and even reproductive success in mammals (Padgett and Glaser, 2003; Slavich and Irwin, 2014; Liu et al., 2017; Levine and Muneyyirci-Delale, 2018). The results of Exp. 1 demonstrate

that the blood expression patterns of the cytokines TNFα and IL6, as well as their receptors, are modulated in response to inflammation. Previous studies in mammals also demonstrate these cytokines pleiotropic effects on everything from mental health (Slavich and Irwin, 2014; Vogelzangs et al., 2016) to complex interactions with the reproductive and stress response systems (Morey et al., 2015; Costanza and Pedotti, 2016; Liu et al., 2017). Finally, IL-10 was chosen because it is a major immunoregulatory and anti-inflammatory cytokine (Opal and DePalo, 2000; Couper et al., 2008). Analysis of *IL-10* expression would allow future assays to increase the window for detection of infection and inflammation, as its rise would be concurrent with decreasing levels of pro-inflammatory cytokines. It is worth noting that all of these pathways and biomarkers have also been identified in invertebrates and non-mammals, allowing them to be applicable to a more diverse range of species (Janeway et al., 2001; Müller et al., 2008; Adamo, 2012).

Together, the results of both experiments represent a promising avenue for future research into monitoring animal wellbeing, reproductive programs, and disease detection in zoos with diverse taxonomic populations. The biomarkers and associated pathways we chose to pursue in these experiments are evolutionarily conserved across most vertebrates and invertebrates (Müller et al., 2008; Flajnik and Kasahara, 2010; Adamo, 2012). As demonstrated in experiment 1, some of these stress biomarkers are differentially expressed in whole blood after inflammation which makes them viable targets for assessing disease states in animals. Other studies in mammals and invertebrates have demonstrated these markers are affected by stress, disease, reproductive status, and many other components of overall animal wellbeing (Adamo, 2012; Costanza and Pedotti, 2016; Vogelzangs et al., 2016; Liu et al., 2017). Thus, the ability to analyze these

expression patterns in while blood represents a new opportunity to improve our understanding of wellbeing in a broad range of exotic species.

A high standard of wellbeing in diverse range exotic species is a goal for zoos (Wolfensohn et al., 2018). Proper care requires accurate and reliable assessment of physiological stress and health, which is difficult to tailor to the specific needs of species who may be at greater risk of mortality in these novel environments with current techniques that include the measurement of cortisol from the feces, urine, or saliva of animals and behavioral assessments (Wolfensohn et al., 2018). Both of these measures are limited due to individual variability, circadian variation, complex collection of samples of group housed populations, and their association with other non-stress stimuli (Cockram, 2002; Wolfensohn et al., 2018).

We conclude that whole blood expression of stress-responsive mRNA biomarkers is altered due to inflammation. These and other evolutionarily-conserved biomarkers can be quantified in elephant, cheetah, and giraffe blood samples using species specific ddPCR probes and primers. We were able to design probes specific to most of our intended targets and were also successful in designing cross-species primers capable of quantifying targets in the giraffe, which is currently unassembled. It is of note that we were able to corroborate our findings in elephants with behavioral observations from keepers that indicated a high anxiety female within this family group. The results of our studies represent a promising future for the development of a comprehensive assay that can be used to identify and assess stress in diverse populations of animals housed in zoos. Further research is of course needed to determine the applicability of such assays to other non-mammalian species, and which additional biomarkers might be included.

Table 4-1. Rat primer sequences for ddPCR

Gene	Protein	Primer Sequence	Product Size	Accession Number
TNFA	Tumor necrosis factor alpha	AACTCCCAGAAAAGCAGCA AGAAGAGGCTGAGGCACAGA	200	NM_012675.3
INFGR1	Interferon Gamma Receptor 1	TGAAACATTACAGGAGTGGG GGACGCTATGTTCTGTATGT	48	NM_053783.1
FN14	TWEAK Receptor	CACTGATCCAGTGAGGAGCA GGCAATTAGACACCCTGGAA	88	NM_181086
IL6R	IL-6 Receptor	CACGAGCCATCATGAAGAGA GCCAAGGTGCTTGGATTTTA	96	NM_017020
TNFR1	TNFα Receptor 1	TTGTAGGATTCAGCTCCTGTC CTCTTACAGGTGGCACGAAGTT	109	NM_013091
YWHAZ	14-3-3 protein ζ	CCGAGCTGTCTAACGAGGAG GAGACGACCCTCCAAGATGA	88	NM_013011

Table 4-2. Cheetah primer and oligo sequences for ddPCR.

Cheetah Sequences

Gene	Protein	Primer Sequence	Product Size	Accession Number
		ddPCR Primers		
RPL19	60S Ribosomal Protein L19	CGGGAATGGACAGTCACAGG CGTCAGCAGATCCGGAAACT HEX-ATGGGCTGATCATCCGGAAA-ZEN/IB FQ	100	XM_015078591
TNFα	Tumor necrosis factor alpha	TGGTCTGGTAGGAAACGGCA TCTTCAGGGGCCAAGGATGT 6-FAM-TTCCACACATGTGCTCCTCA-ZEN/IB FQ	100	XM_015082146
TNFR1	TNFα Receptor 1	GTCCCGGTACACTGTGCAAG AGCTGCTCCAAATGCCGAAA 6-FAM-ATGTACCAGGTGGAGATATCTC-ZEN/IB FQ	100	XM_027074099
IL6R	IL-6 Receptor	CTCCGCAGCCAGTGAATTGT GCTGAGTGATGTGGTGACCG 6-FAM-CCAACGTGACCCTGACCTG-ZEN/IB FQ	100	XM_027048711
IL-10	Interleukin 10	GTGCTGTTTGATGTCCGGGT GACTTTAAGGTGAGGGCCCG 6-FAM-TACTTGGAGGAGGTGATGCC-ZEN/IB FQ	100	XM_027074588
NR3C1	Nuclear receptor subfamily 3 group C member 1	GTCTGGGAAAGGAACCGTGC CGAACGGGACAGAAAGGTGG 6-FAM-TCCGAGCACCACGTGATC-ZEN/IB FQ	100	XM_027042531
ADRβ2	Adrenoceptor beta 2	GCTGAGATTTTGGGCGTGGA GGTCTTTCAGGTGGCCCAAA 6-FAM-GATCGACAAATCTGAGGGCC-ZEN/IB FQ	100	XM_015079810
RPP30	Ribonuclease P/MRP subunit p30	CTCTCAGACAGCCCGAACAG TGTCTAGTGCTGCGGAAAGG HEX-AAGAGGCCCATACGATGTGG-ZEN/IB FQ	100	XM_015061888
YWHAZ	Tyrosine 3-monooxygenase/tryptophan 5-monooxygenase activation protein zeta	AAGGGGCCGGCTAACATTTG AGGGGAATTAGTGGTGGGCA HEX-AGTGTCTACCCCAATTCTGGT-ZEN/IB FQ	100	XM_027064119

Table 4-3. Elephant primer and oligo sequences for ddPCR.
Elephant Sequences

Gene	Protein	Primer Sequence	Product Size	Accession Number
		ddPCR Primers		
RPP30	Ribonuclease P/MRP subunit p30	GAGCACTGACAGAGACCGAC CTTCCAGCGTGCAAGAAAGC HEX-AAGTGTGAGGGCTGAGCAG-ZEN/IB FQ	100	XM_003409241
TNFα	Tumor necrosis factor alpha	CTCAACGTCCCGGATCATGC GCTCCACCATCTCCCAGCTA 6-FAM-CCAAAGGACACCATGAGCAC-ZEN/IB FQ	100	XM_023541361
TNFR1	TNFα Receptor 1	GGGAGGGGAAGAGACTGCAT GTAGGGCCAAGAAAGGGTGC 6-FAM-AGGGAAAGGACAAGTGGAGT-ZEN/IB FQ	100	XM_023549042
IL6R	IL-6 Receptor	CCAGGCTTCCATCCCACCTA GTCTCTCTCCTCTGCACCGT 6-FAM-GCTCTCTTTTCCCACAGTGC-ZEN/IB FQ	100	XM_023554017
IL-10	Interleukin 10	CTCTGGGGCCTACTGTTCCA CGGCGCTGTGTGAGTAGAAG 6-FAM-TTTTTCCCCTGGAGGCTGTC-ZEN/IB FQ	100	XM_023548359
NR3C1	Nuclear receptor subfamily 3 group C member 1	AGACTGACCTGGTATGGGGC AAGCCAACACCTCTCCCAGA 6-FAM-ACCTTAGTACAGCAAGGGTTGT-ZEN/IB FQ	100	XM_003404576
ADRβ2	Adrenoceptor beta 2	GCAGGTCTCTTCGGCATAGC ACCTCCTTCTTGCCCATCCA 6-FAM-AATGCACTGGTACCGGGC-ZEN/IB FQ	100	XM_003404840
RPL19	60S Ribosomal Protein L19	AGGCTGTGATACATGTGGCG AGGATGAGAATTCTGCGCCG HEX-CTGCTCAGGAGATACCGTGA-ZEN/IB FQ	100	XM_010594387
YWHAZ	Tyrosine 3-monooxygenase/tryptophan 5-monooxygenase activation protein zeta	TCAACCGCTAGTGGGAGGAC CAGCATGCTCGAGTCCCATC HEX-TGTCATTCCACCTCACCTGA-ZEN/IB FQ	100	XM_010588433

Table 4-4. Giraffe primer sequences for ddPCR.

Giraffe Sequences (Assembly #: GCA_001651235.1)

Gene	Protein	Primer Sequence	Product Size	Accession Number
		ddPCR Primers		
RPL19	60S Ribosomal Protein L19	GGGCCTTGTGTAGAAGAGCA ACACGTTACCCTTCACCTTCA	126	Cow: XM_587778 Sheep: XM_012186026
TNFα	Tumor necrosis factor alpha	TCTACTTTGGGATCATCGCC CAGGCCTCACTTCCCTACAT	201	Cow: XM_005223596 Sheep: XM_012100437
IL-6	Interleukin-6	TCAGCCCTCTAGTGGTGTGA GCATCCATCTTTTTCCTCCA	156	Cow: NM_174674 Sheep: NM_001166185
ADRβ2	Adrenoceptor beta 2	GGGGCAGCTTTGGTTGTTTT AAGCACACTCCAGTCAAGGG	113	Cow: NM_174231 Sheep: NM_001130154

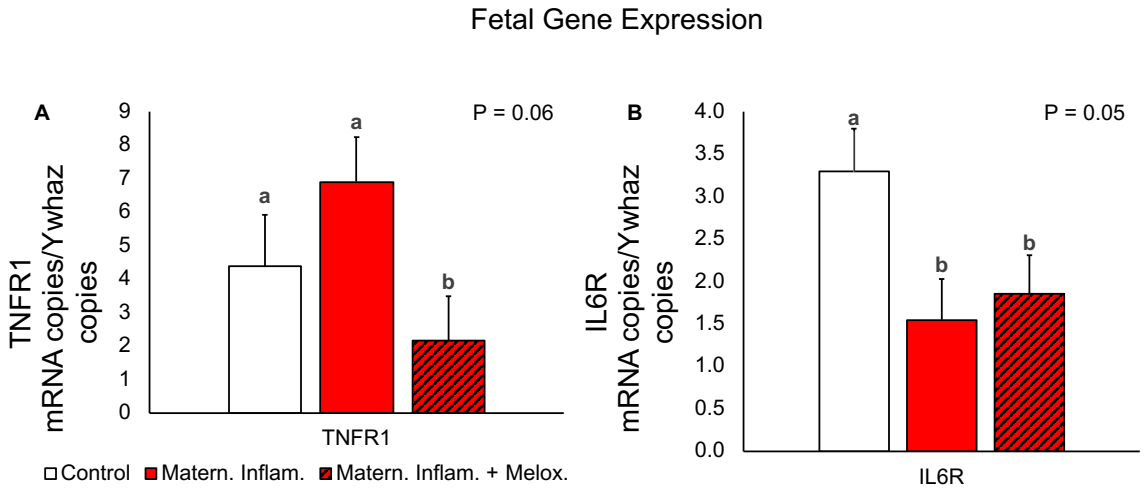

Figure 1

Figure 4-1. **Gene expression (ddPCR) for (A) *TNFR1* and (B) *IL6R* in control (n=7), MI-IUGR (n=8), and MI-IUGR + Meloxicam (n=10) rat fetuses at term. [a,b] means with different superscripts differ.**

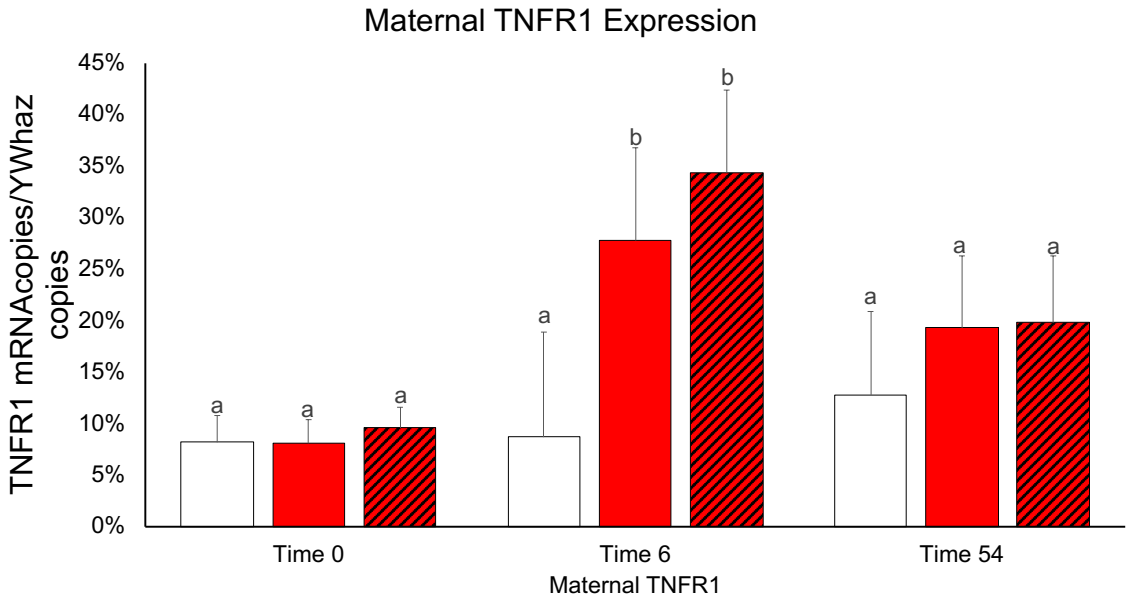

Figure 2

Figure 4-2. **Gene expression (ddPCR) for *TNFR1* in maternal whole blood samples collected at 0, 6, and 54hr after treatment onset of LPS injection. [a,b] means with different superscripts differ (P < 0.05). Control (n=7), MI-IUGR (n=8), MI-IUGR + Meloxicam (n=10).**

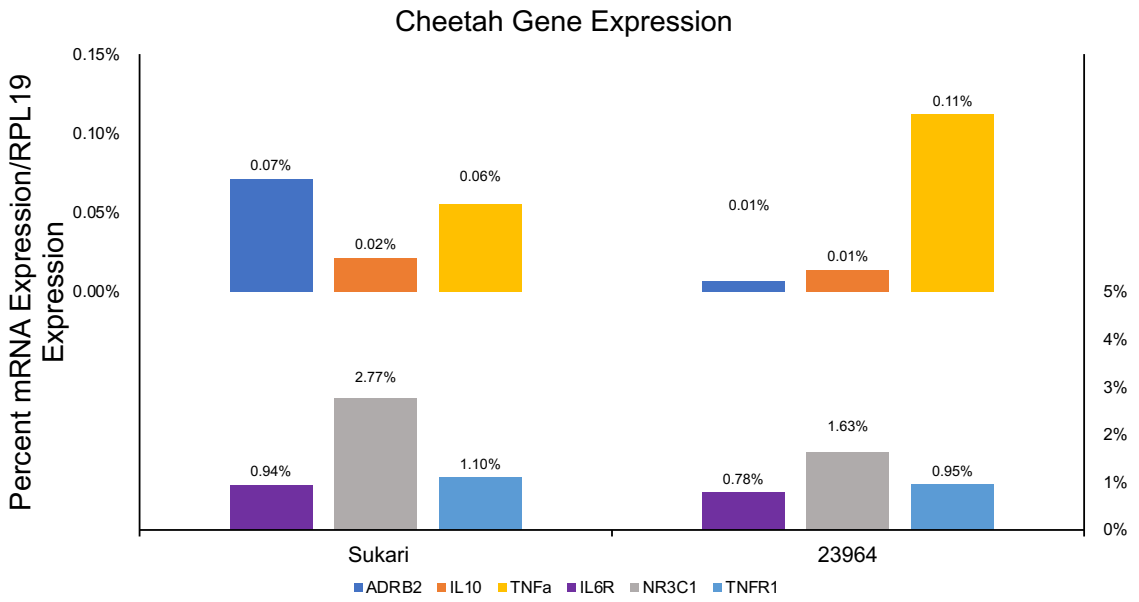

Figure 3

Figure 4-3. **Gene expression (ddPCR) for *ADRB2, IL10, TNFA, IL6R, NR3C1,* and *TNFR1* in whole blood samples collected from cheetahs (n=2).**

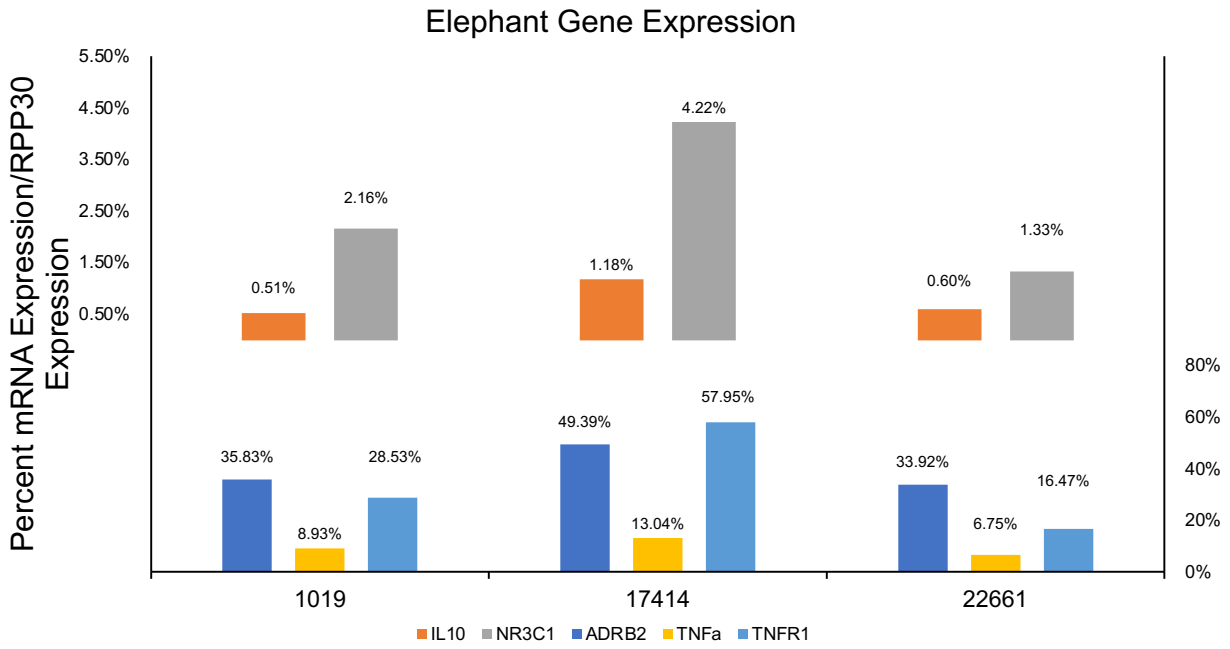

Figure 4

Figure 4-4. **Gene expression (ddPCR) for *ADRB2, IL10, TNFA, NR3C1,* and *TNFR1* in whole blood samples collected from elephants (n=3).**

References

Adamo, S. A. 2012. The effects of the stress response on immune function in invertebrates: An evolutionary perspective on an ancient connection. Horm. Behav. 62:324–330. doi:10.1016/J.YHBEH.2012.02.012. Available from: https://www.sciencedirect.com/science/article/pii/S0018506X12000438?via%3Dihub

Akash, M. S. H., K. Rehman, and A. Liaqat. 2018. Tumor Necrosis Factor-Alpha: Role in Development of Insulin Resistance and Pathogenesis of Type 2 Diabetes Mellitus. J. Cell. Biochem. 119:105–110. doi:10.1002/jcb.26174. Available from: http://doi.wiley.com/10.1002/jcb.26174

Al-Shanti, N., A. Saini, S. H. Faulkner, and C. E. Stewart. 2008. Beneficial synergistic interactions of TNF-α and IL-6 in C2 skeletal myoblasts - Potential cross-talk with IGF system. Growth Factors. 26:61–73. doi:10.1080/08977190802025024. Available from: http://www.tandfonline.com/doi/full/10.1080/08977190802025024

Alberts, B., A. Johnson, J. Lewis, M. Raff, K. Roberts, and P. Walter. 2002. Lymphocytes and the Cellular Basis of Adaptive Immunity. Available from: https://www.ncbi.nlm.nih.gov/books/NBK26921/

Alisi, A., N. Panera, C. Agostoni, and V. Nobili. 2011. Intrauterine growth retardation and nonalcoholic fatty liver disease in children. Int. J. Endocrinol. 2011:269853. doi:10.1155/2011/269853. Available from: http://www.ncbi.nlm.nih.gov/pubmed/22190925

Allen, R. E., R. A. Merkel, and R. B. Young. 1979. Cellular aspects of muscle growth: myogenic cell proliferation. J. Anim. Sci. 49:115–127. doi:10.2527/jas1979.491115x. Available from: https://pdfs.semanticscholar.org/6b4f/0cdcf41c3009ddffb229bb5d1cb2e6155c8f.pdf

Alur, P. 2019. Sex Differences in Nutrition, Growth, and Metabolism in Preterm Infants. Front. Pediatr. 7:22. doi:10.3389/fped.2019.00022. Available from: https://www.frontiersin.org/article/10.3389/fped.2019.00022/full

Anderson, J. E., H. A. McLay, M. Abercromby, and D. Robins. 2006. The satellite cell as a companion in skeletal muscle plasticity: currency, conveyance, clue, connector and colander. J. Exp. Biol. 209:2276–92. doi:10.1242/jeb.02088. Available from: http://www.ncbi.nlm.nih.gov/pubmed/10933998

Andersson, A. K., M. Flodström, and S. Sandler. 2001. Cytokine-Induced Inhibition of Insulin Release from Mouse Pancreatic β-Cells Deficient in Inducible Nitric Oxide Synthase. Biochem. Biophys. Res. Commun. 281:396–403. doi:10.1006/BBRC.2001.4361. Available from: https://www.sciencedirect.com/science/article/pii/S0006291X0194361X

Andrés, V., and K. Walsh. 1996. Myogenin expression, cell cycle withdrawal, and phenotypic differentiation are temporally separable events that precede cell fusion upon myogenesis. J. Cell Biol. 132:657–666. doi:10.1083/jcb.132.4.657. Available from: http://jcb.rupress.org/content/jcb/132/4/657.full.pdf

Aronoff, S. L., K. Berkowitz, B. Shreiner, and L. Want. 2004. Glucose Metabolism and Regulation: Beyond Insulin and Glucagon. Diabetes Spectr. 17:183–190. doi:10.2337/diaspect.17.3.183. Available from: http://spectrum.diabetesjournals.org/cgi/doi/10.2337/diaspect.17.3.183

Babon, J. J., L. N. Varghese, and N. A. Nicola. 2014. Inhibition of IL-6 family cytokines by SOCS3. Semin. Immunol. 26:13–9. doi:10.1016/j.smim.2013.12.004. Available from: http://www.ncbi.nlm.nih.gov/pubmed/24418198

Bach, E., R. R. Nielsen, M. H. Vendelbo, A. B. Møller, N. Jessen, M. Buhl, T. K-Hafstrøm, L. Holm, S. B. Pedersen, H. Pilegaard, R. S. Biensø, J. O. L. Jørgensen, and N. Møller. 2013. Direct effects of TNF-α on local fuel metabolism and cytokine levels in the placebo-controlled, bilaterally infused human leg: increased insulin sensitivity, increased net protein breakdown, and increased IL-6 release. Diabetes. 62:4023–9. doi:10.2337/db13-0138. Available from: http://www.ncbi.nlm.nih.gov/pubmed/23835341

Baker, J., J. P. Liu, E. J. Robertson, and A. Efstratiadis. 1993. Role of insulin-like growth factors in embryonic and postnatal growth. Cell. 75:73–82. doi:10.1016/S0092-8674(05)80085-6. Available from: http://www.ncbi.nlm.nih.gov/pubmed/8402902

Bartoccioni, E., D. Michaelis, and R. Hohlfeld. 1994. Constitutive and cytokine-induced production of interleukin-6 by human myoblasts. Immunol. Lett. 42:135–138. doi:10.1016/0165-2478(94)90076-0. Available from: https://www.sciencedirect.com/science/article/abs/pii/0165247894900760

Baschat, A. A. 2004. Fetal responses to placental insufficiency: An update. BJOG An Int. J. Obstet. Gynaecol. 111:1031–1041. doi:10.1111/j.1471-0528.2004.00273.x. Available from: http://doi.wiley.com/10.1111/j.1471-0528.2004.00273.x

Bellinger, D. L., B. A. Millar, S. Perez, J. Carter, C. Wood, S. ThyagaRajan, C. Molinaro, C. Lubahn, and D. Lorton. 2008. Sympathetic modulation of immunity: Relevance to disease. Cell. Immunol. 252:27–56. doi:10.1016/J.CELLIMM.2007.09.005. Available from: https://www.sciencedirect.com/science/article/pii/S0008874907002511?via%3Dihub#bib213

De Benedetti, F., T. Alonzi, A. Moretta, D. Lazzaro, P. Costa, V. Poli, A. Martini, G. Ciliberto, and E. Fattori. 1997. Interleukin 6 causes growth impairment in transgenic mice through a decrease in insulin-like growth factor-I. A model for stunted growth in children with chronic inflammation. J. Clin. Invest. 99:643–50. doi:10.1172/JCI119207. Available from: http://www.ncbi.nlm.nih.gov/pubmed/9045866

Bentzinger, C. F., Y. X. Wang, and M. A. Rudnicki. 2012. Building muscle: molecular regulation of myogenesis. Cold Spring Harb. Perspect. Biol. 4:a008342. doi:10.1101/cshperspect.a008342. Available from: http://www.ncbi.nlm.nih.gov/pubmed/22300977

Bismuth, K., and F. Relaix. 2010. Genetic regulation of skeletal muscle development. Exp. Cell Res. 316:3081–3086. doi:10.1016/J.YEXCR.2010.08.018. Available from: https://www.sciencedirect.com/science/article/pii/S001448271000412X?via%3Dihub

Boehmer, B. H., S. W. Limesand, and P. J. Rozance. 2017. The impact of IUGR on pancreatic islet development and ß-cell function. J. Endocrinol. 235:R63–R76. doi:10.1530/JOE-17-0076. Available from: http://www.ncbi.nlm.nih.gov/pubmed/28808079

Bonetto, A., T. Aydogdu, X. Jin, Z. Zhang, R. Zhan, L. Puzis, L. G. Koniaris, and T. A. Zimmers. 2012. JAK/STAT3 pathway inhibition blocks skeletal muscle wasting downstream of IL-6 and in experimental cancer cachexia. Am. J. Physiol. Endocrinol. Metab. 303:E410-21. doi:10.1152/ajpendo.00039.2012. Available from:

http://www.ncbi.nlm.nih.gov/pubmed/22669242

Bosch-Comas, A., K. Lindsten, R. Gonzàlez-Duarte, M. G. Masucci, and G. Marfany. 2006. The ubiquitin-specific protease USP25 interacts with three sarcomeric proteins. Cell. Mol. Life Sci. doi:10.1007/s00018-005-5533-1.

Bouché, C., S. Serdy, C. R. Kahn, and A. B. Goldfine. 2004. The Cellular Fate of Glucose and Its Relevance in Type 2 Diabetes. Endocr. Rev. 25:807–830. doi:10.1210/er.2003-0026. Available from: https://academic.oup.com/edrv/article-lookup/doi/10.1210/er.2003-0026

Boucher, J., A. Kleinridders, and C. R. Kahn. 2014. Insulin receptor signaling in normal and insulin-resistant states. Cold Spring Harb. Perspect. Biol. 6. doi:10.1101/cshperspect.a009191. Available from: http://www.ncbi.nlm.nih.gov/pubmed/24384568

Boucher, J., Y.-H. Tseng, and C. R. Kahn. 2010. Insulin and insulin-like growth factor-1 receptors act as ligand-specific amplitude modulators of a common pathway regulating gene transcription. J. Biol. Chem. 285:17235–45. doi:10.1074/jbc.M110.118620. Available from: http://www.ncbi.nlm.nih.gov/pubmed/20360006

Brice, A. L., J. E. Cheetham, V. N. Bolton, N. C. Hill, and P. N. Schofield. 1989. Temporal changes in the expression of the insulin-like growth factor II gene associated with tissue maturation in the human fetus. Development. 106. Available from: http://dev.biologists.org/content/106/3/543.short

Brown, L. D. 2014. Endocrine regulation of fetal skeletal muscle growth: Impact on future metabolic health. J. Endocrinol. 221:R13-29. doi:10.1530/JOE-13-0567. Available from: http://www.ncbi.nlm.nih.gov/pubmed/24532817

Brown, L. D., P. J. Rozance, J. L. Bruce, J. E. Friedman, W. W. Hay, and S. R. Wesolowski. 2015. Limited capacity for glucose oxidation in fetal sheep with intrauterine growth restriction. Am. J. Physiol. Integr. Comp. Physiol. 309:R920–R928. doi:10.1152/ajpregu.00197.2015. Available from: http://www.physiology.org/doi/10.1152/ajpregu.00197.2015

Busch, D. H., I. M. Pilip, S. Vijh, and E. G. Pamer. 1998. Coordinate Regulation of Complex T Cell Populations Responding to Bacterial Infection. Immunity. 8:353–362. doi:10.1016/S1074-7613(00)80540-3. Available from: https://www.sciencedirect.com/science/article/pii/S1074761300805403?via%3Dihub

Busillo, J. M., K. M. Azzams, and J. A. Cidlowski. 2011. Glucocorticoids sensitize the innate immune system through regulation of the NLRP3 inflammasome. J. Biol. Chem. 286:38703–38713. doi:10.1074/jbc.M111.275370. Available from: http://www.ncbi.nlm.nih.gov/pubmed/21940629

Cadaret, C. N., K. A. Beede, H. E. Riley, and D. T. Yates. 2017. Acute exposure of primary rat soleus muscle to zilpaterol HCl (β2 adrenergic agonist), TNFα, or IL-6 in culture increases glucose oxidation rates independent of the impact on insulin signaling or glucose uptake. Cytokine. 96:107–113. doi:10.1016/j.cyto.2017.03.014. Available from: http://linkinghub.elsevier.com/retrieve/pii/S1043466617300777

Cadaret, C. N., E. M. Merrick, T. L. Barnes, K. A. Beede, R. J. Posont, J. L. Petersen, and D. T. Yates. 2018. Sustained maternal inflammation during the early third trimester yields fetal adaptations that impair subsequent skeletal muscle growth and glucose metabolism in sheep1. Transl. Anim. Sci. 2:S14–S18. doi:10.1093/tas/txy047. Available

from: https://academic.oup.com/tas/article/2/suppl_1/S14/5108317

Camacho, L. E., X. Chen, W. W. Hay, and S. W. Limesand. 2017a. Enhanced insulin secretion and insulin sensitivity in young lambs with placental insufficiency-induced intrauterine growth restriction. Am. J. Physiol. Integr. Comp. Physiol. 313:R101–R109. doi:10.1152/ajpregu.00068.2017. Available from: http://www.ncbi.nlm.nih.gov/pubmed/28490449

Camacho, L. E., X. Chen, W. W. Hay, S. W. Limesand, and S. W. Limesand. 2017b. Enhanced insulin secretion and insulin sensitivity in young lambs with placental insufficiency-induced intrauterine growth restriction. Am. J. Physiol. Regul. Integr. Comp. Physiol. 313:R101–R109. doi:10.1152/ajpregu.00068.2017. Available from: http://www.ncbi.nlm.nih.gov/pubmed/28490449

Cassatella, M. A., L. Meda, S. Bonora, M. Ceska, and G. Constantin. 1993. Interleukin 10 (IL-10) inhibits the release of proinflammatory cytokines from human polymorphonuclear leukocytes. Evidence for an autocrine role of tumor necrosis factor and IL-1 beta in mediating the production of IL-8 triggered by lipopolysaccharide. J. Exp. Med. 178:2207–11. doi:10.1084/JEM.178.6.2207. Available from: http://www.ncbi.nlm.nih.gov/pubmed/8245792

Charles A Janeway, J., P. Travers, M. Walport, and M. J. Shlomchik. 2001. Evolution of the innate immune system. Available from: https://www.ncbi.nlm.nih.gov/books/NBK27138/

Chen, L., R. Chen, H. Wang, and F. Liang. 2015. Mechanisms Linking Inflammation to Insulin Resistance. Int. J. Endocrinol. 2015:508409. doi:10.1155/2015/508409. Available from: http://www.ncbi.nlm.nih.gov/pubmed/26136779

Chow, J. C., D. W. Young, D. T. Golenbock, W. J. Christ, and F. Gusovsky. 1999. Toll-like receptor-4 mediates lipopolysaccharide-induced signal transduction. J. Biol. Chem. 274:10689–92. doi:10.1074/JBC.274.16.10689. Available from: http://www.ncbi.nlm.nih.gov/pubmed/10196138

Ciriza, J., H. Thompson, R. Petrosian, J. O. Manilay, and M. E. García-Ojeda. 2013. The migration of hematopoietic progenitors from the fetal liver to the fetal bone marrow: Lessons learned and possible clinical applications. Exp. Hematol. 41:411–423. doi:10.1016/J.EXPHEM.2013.01.009. Available from: https://www.sciencedirect.com/science/article/pii/S0301472X13000131?via%3Dihub#bib38

Cockram, M. S. 2002. The Biology of Animal Stress: Basic Principles and Implications for Animal Welfare. Vet. J. 164:77. doi:10.1053/tvjl.2001.0558. Available from: http://dspace.fudutsinma.edu.ng/jspui/bitstream/123456789/1835/1/THE BIOLOGY OF ANIMAL STRESS %281%29.pdf

Di Cola, G., M. H. Cool, and D. Accili. 1997. Hypoglycemic effect of insulin-like growth factor-1 in mice lacking insulin receptors. J. Clin. Invest. 99:2538–2544. doi:10.1172/JCI119438. Available from: http://www.ncbi.nlm.nih.gov/pubmed/9153298

Constantin, G., M. Majeed, C. Giagulli, L. Piccio, J. Y. Kim, E. C. Butcher, and C. Laudanna. 2000. Chemokines Trigger Immediate β2 Integrin Affinity and Mobility Changes: Differential Regulation and Roles in Lymphocyte Arrest under Flow. Immunity. 13:759–769. doi:10.1016/S1074-7613(00)00074-1. Available from: https://www.sciencedirect.com/science/article/pii/S1074761300000741

Coolican, S. A., D. S. Samuel, D. Z. Ewton, F. J. McWade, and J. R. Florini. 1997. The mitogenic and myogenic actions of insulin-like growth factors utilize distinct signaling pathways. J. Biol. Chem. 272:6653–62. doi:10.1074/JBC.272.10.6653. Available from: http://www.ncbi.nlm.nih.gov/pubmed/9045696

Cori, C. F. 1931. MAMMALIAN CARBOHYDRATE METABOLISM. Physiol. Rev. 11:143–275. doi:10.1152/physrev.1931.11.2.143. Available from: http://www.physiology.org/doi/10.1152/physrev.1931.11.2.143

Costanza, M., and R. Pedotti. 2016. Prolactin: Friend or Foe in Central Nervous System Autoimmune Inflammation? Int. J. Mol. Sci. 17. doi:10.3390/ijms17122026. Available from: http://www.ncbi.nlm.nih.gov/pubmed/27918427

Couper, K. N., D. G. Blount, and E. M. Riley. 2008. Infection IL-10: The Master Regulator of Immunity to. J Immunol Ref. 180:5771–5777. doi:10.4049/jimmunol.180.9.5771. Available from: http://www.jimmunol.org/content/180/9/5771http://www.jimmunol.org/content/180/9/5771.full#ref-list-1

Cox, P., and T. Marton. 2009. Pathological assessment of intrauterine growth restriction. Best Pract. Res. Clin. Obstet. Gynaecol. 23:751–764. doi:10.1016/j.bpobgyn.2009.06.006. Available from: https://www.sciencedirect.com/science/article/pii/S1521693409000820?via%3Dihub

Criollo, A., L. Senovilla, H. Authier, M. C. Maiuri, E. Morselli, I. Vitale, O. Kepp, E. Tasdemir, L. Galluzzi, S. Shen, M. Tailler, N. Delahaye, A. Tesniere, D. De Stefano, A. Ben Younes, F. Harper, G. Pierron, S. Lavandero, L. Zitvogel, A. Israel, V. Baud, and G. Kroemer. 2010. The IKK complex contributes to the induction of autophagy. EMBO J. 29:619–631. doi:10.1038/emboj.2009.364. Available from: http://www.ncbi.nlm.nih.gov/pubmed/19959994

Dan, H. C., R. J. Antonia, and A. S. Baldwin. 2016. PI3K/Akt promotes feedforward mTORC2 activation through IKKα. Oncotarget. 7:21064–75. doi:10.18632/oncotarget.8383. Available from: http://www.ncbi.nlm.nih.gov/pubmed/27027448

Davis, M. A., A. R. Macko, L. V Steyn, M. J. Anderson, and S. W. Limesand. 2015. Fetal adrenal demedullation lowers circulating norepinephrine and attenuates growth restriction but not reduction of endocrine cell mass in an ovine model of intrauterine growth restriction. Nutrients. 7:500–16. doi:10.3390/nu7010500. Available from: http://www.ncbi.nlm.nih.gov/pubmed/25584967

DeFronzo, R. A., E. Jacot, E. Jequier, E. Maeder, J. Wahren, and J. P. Felber. 1981. The effect of insulin on the disposal of intravenous glucose. Results from indirect calorimetry and hepatic and femoral venous catheterization\rEffects of insulin on peripheral and splanchnic glucose metabolism in noninsulin-dependent (type II) diabetes m. Diabetes. 30:1000–1007. doi:10.2337/diab.30.12.1000. Available from: http://diabetes.diabetesjournals.org/content/30/12/1000.full-text.pdf

Djavaheri-Mergny, M., M. Amelotti, J. Mathieu, F. Besançon, C. Bauvy, S. Souquère, G. Pierron, and P. Codogno. 2006. NF-κB activation represses tumor necrosis factor-α-induced autophagy. J. Biol. Chem. 281:30373–30382. doi:10.1074/jbc.M602097200. Available from: http://www.ncbi.nlm.nih.gov/pubmed/16857678

Dupont, J., and D. LeRoith. 2001. Insulin and insulin-like growth factor I receptors:

Similarities and differences in signal transduction. In: Hormone Research. Vol. 55. Karger Publishers. p. 22–26. Available from: http://www.ncbi.nlm.nih.gov/pubmed/11684871

Duque, G. A., and A. Descoteaux. 2014. Macrophage cytokines: Involvement in immunity and infectious diseases. Front. Immunol. 5:491. doi:10.3389/fimmu.2014.00491. Available from: http://www.ncbi.nlm.nih.gov/pubmed/25339958

Düvel, K., J. L. Yecies, S. Menon, P. Raman, A. I. Lipovsky, A. L. Souza, E. Triantafellow, Q. Ma, R. Gorski, S. Cleaver, M. G. Vander Heiden, J. P. MacKeigan, P. M. Finan, C. B. Clish, L. O. Murphy, and B. D. Manning. 2010. Activation of a Metabolic Gene Regulatory Network Downstream of mTOR Complex 1. Mol. Cell. 39:171–183. doi:10.1016/J.MOLCEL.2010.06.022. Available from: https://www.sciencedirect.com/science/article/pii/S1097276510004636?via%3Dihub

Ebeling, P., H. A. Koistinen, and V. A. Koivisto. 1998. Insulin-independent glucose transport regulates insulin sensitivity. FEBS Lett. 436:301–303. doi:10.1016/S0014-5793(98)01149-1. Available from: http://doi.wiley.com/10.1016/S0014-5793%2898%2901149-1

Edwards, J. P., X. Zhang, K. A. Frauwirth, and D. M. Mosser. 2006. Biochemical and functional characterization of three activated macrophage populations. J. Leukoc. Biol. 80:1298–1307. doi:10.1189/jlb.0406249. Available from: http://doi.wiley.com/10.1189/jlb.0406249

Fan, X., and A. Y. Rudensky. 2016. Hallmarks of Tissue-Resident Lymphocytes. Cell. 164:1198–1211. doi:10.1016/j.cell.2016.02.048. Available from: http://www.ncbi.nlm.nih.gov/pubmed/26967286

Farah, B. L., R. A. Sinha, Y. Wu, B. K. Singh, J. Zhou, B.-H. Bay, and P. M. Yen. 2014. β-Adrenergic agonist and antagonist regulation of autophagy in HepG2 cells, primary mouse hepatocytes, and mouse liver. PLoS One. 9:e98155. doi:10.1371/journal.pone.0098155. Available from: http://www.ncbi.nlm.nih.gov/pubmed/24950230

Felber, J. P., E. Jacot, J. Wahren, E. Jequier, R. A. DeFronzo, and E. Maeder. 2013. The Effect of Insulin on the Disposal of Intravenous Glucose: Results from Indirect Calorimetry and Hepatic and Femoral Venous Catheterization. Diabetes. 30:1000–1007. doi:10.2337/diab.30.12.1000. Available from: http://www.ncbi.nlm.nih.gov/pubmed/7030826

Fitzgerald, K. A., D. C. Rowe, and D. T. Golenbock. 2004. Endotoxin recognition and signal transduction by the TLR4/MD2-complex. Microbes Infect. 6:1361–1367. doi:10.1016/J.MICINF.2004.08.015. Available from: https://www.sciencedirect.com/science/article/pii/S1286457904002977

Flajnik, M. F., and M. Kasahara. 2010. Origin and evolution of the adaptive immune system: genetic events and selective pressures. Nat. Rev. Genet. 11:47–59. doi:10.1038/nrg2703. Available from: http://www.ncbi.nlm.nih.gov/pubmed/19997068

Fu, Z., E. R. Gilbert, and D. Liu. 2013. Regulation of insulin synthesis and secretion and pancreatic Beta-cell dysfunction in diabetes. Curr. Diabetes Rev. 9:25–53. Available from: http://www.ncbi.nlm.nih.gov/pubmed/22974359

Garbers, C., S. Aparicio-Siegmund, and S. Rose-John. 2015. The IL-6/gp130/STAT3

signaling axis: Recent advances towards specific inhibition. Curr. Opin. Immunol. 34:75–82. doi:10.1016/j.coi.2015.02.008. Available from: https://www.sciencedirect.com/science/article/pii/S0952791515000370#bib0330

Gleeson, M., A. W. Cripps, R. L. Clancy, A. J. Husband, M. J. Hensley, and S. R. Leeder. 1982. Ontogeny of the secretory immune system in man. Aust. N. Z. J. Med. 12:255–8. Available from: http://www.ncbi.nlm.nih.gov/pubmed/6753816

Godfrey, K. M., and D. J. Barker. 2000. Fetal nutrition and adult disease. [Review] [85 refs]. Am. J. Clin. Nutr. 71:1344S–1352S. doi:10.1111/j.1365-277X.2005.00612.x. Available from: https://academic.oup.com/ajcn/article/71/5/1344S/4729552

Greenwood, P. L., A. S. Hunt, J. W. Hermanson, and A. W. Bell. 2000. Effects of birth weight and postnatal nutrition on neonatal sheep: II. Skeletal muscle growth and development. J. Anim. Sci. 78:50–61. Available from: http://www.ncbi.nlm.nih.gov/pubmed/10682802

Guttridge, D. C., C. Albanese, J. Y. Reuther, R. G. Pestell, and A. S. Baldwin. 1999. NF-kappaB controls cell growth and differentiation through transcriptional regulation of cyclin D1. Mol. Cell. Biol. 19:5785–99. Available from: http://www.ncbi.nlm.nih.gov/pubmed/10409765

Hales, C. N., and D. J. Barker. 1992. Type 2 (non-insulin-dependent) diabetes mellitus: the thrifty phenotype hypothesis. Diabetologia. 35:595–601. Available from: http://www.ncbi.nlm.nih.gov/pubmed/1644236

Hales, C. N., and D. J. P. Barker. 2013. Type 2 (non-insulin-dependent) diabetes mellitus: the thrifty phenotype hypothesis. Int. J. Epidemiol. 42:1215–1222. doi:10.1093/ije/dyt133. Available from: http://link.springer.com/10.1007/BF00400248

Haliday, E. M., C. S. Ramesha, and G. Ringold. 1991. TNF induces c-fos via a novel pathway requiring conversion of arachidonic acid to a lipoxygenase metabolite. Embo J. 10:109–115. Available from: http://www.ncbi.nlm.nih.gov/pubmed/1899225

Hammond, M. E., G. R. Lapointe, P. H. Feucht, S. Hilt, C. A. Gallegos, C. A. Gordon, M. A. Giedlin, G. Mullenbach, and P. Tekamp-Olson. 1995. IL-8 induces neutrophil chemotaxis predominantly via type I IL-8 receptors. J. Immunol. 155:1428–33. Available from: http://www.ncbi.nlm.nih.gov/pubmed/7636208

Hansen, D., P. Dendale, M. Beelen, R. A. M. Jonkers, A. Mullens, L. Corluy, R. Meeusen, and L. J. C. van Loon. 2010. Plasma adipokine and inflammatory marker concentrations are altered in obese, as opposed to non-obese, type 2 diabetes patients. Eur. J. Appl. Physiol. 109:397–404. doi:10.1007/s00421-010-1362-5. Available from: http://link.springer.com/10.1007/s00421-010-1362-5

Hansen, G., T. R. Hercus, B. J. McClure, F. C. Stomski, M. Dottore, J. Powell, H. Ramshaw, J. M. Woodcock, Y. Xu, M. Guthridge, W. J. McKinstry, A. F. Lopez, and M. W. Parker. 2008. The Structure of the GM-CSF Receptor Complex Reveals a Distinct Mode of Cytokine Receptor Activation. Cell. 134:496–507. doi:10.1016/J.CELL.2008.05.053. Available from: https://www.sciencedirect.com/science/article/pii/S0092867408008131?via%3Dihub

Hashimoto, D., A. Chow, C. Noizat, P. Teo, M. B. Beasley, M. Leboeuf, C. D. Becker, P. See, J. Price, D. Lucas, M. Greter, A. Mortha, S. W. Boyer, E. C. Forsberg, M. Tanaka, N. van Rooijen, A. García-Sastre, E. R. Stanley, F. Ginhoux, P. S. Frenette, and M. Merad. 2013. Tissue-Resident Macrophages Self-Maintain Locally throughout Adult Life

with Minimal Contribution from Circulating Monocytes. Immunity. 38:792–804. doi:10.1016/J.IMMUNI.2013.04.004. Available from: https://www.sciencedirect.com/science/article/pii/S107476131300157X?via%3Dihub

Hay, W. W., H. K. Meznarich, J. E. Digiacomo, K. Hirst, and G. Zerbe. 1988. Effects of Insulin and Glucose Concentrations on Glucose Utilization in Fetal Sheep. Pediatr. Res. 23:381–387. doi:10.1203/00006450-198804000-00008. Available from: http://www.nature.com/doifinder/10.1203/00006450-198804000-00008

Heidemann, J., H. Ogawa, M. B. Dwinell, P. Rafiee, C. Maaser, H. R. Gockel, M. F. Otterson, D. M. Ota, N. Lügering, W. Domschke, and D. G. Binion. 2003. Angiogenic Effects of Interleukin 8 (CXCL8) in Human Intestinal Microvascular Endothelial Cells Are Mediated by CXCR2. J. Biol. Chem. 278:8508–8515. doi:10.1074/jbc.M208231200. Available from: http://www.ncbi.nlm.nih.gov/pubmed/12496258

Heinrich, P. C., I. Behrmann, S. Haan, H. M. Hermanns, G. Uller-Newen, and F. Schaper. 2003. Biochem. J. (2003) 374, 1-20 - P.C. Heinrich and others - Principles of interleukin (IL)-6-type cytokine signalling and its regulation. biochemj.org. 374:1–20. doi:10.1042/BJ20030407. Available from: https://www.ncbi.nlm.nih.gov/pmc/articles/PMC1223585/pdf/12773095.pdf

Hemmann, U., C. Gerhartz, B. Heesel, J. Sasse, G. Kurapkat, J. Grötzinger, A. Wollmer, Z. Zhong, J. E. Darnell, L. Graeve, P. C. Heinrich, and F. Horn. 1996. Differential activation of acute phase response factor/Stat3 and Stat1 via the cytoplasmic domain of the interleukin 6 signal transducer gp130. II. Src homology SH2 domains define the specificity of stat factor activation. J. Biol. Chem. 271:12999–3007. doi:10.1074/JBC.271.22.12999. Available from: http://www.ncbi.nlm.nih.gov/pubmed/8662795

Henningsen, J., K. T. G. Rigbolt, B. Blagoev, B. K. Pedersen, and I. Kratchmarova. 2010. Dynamics of the skeletal muscle secretome during myoblast differentiation. Mol. Cell. Proteomics. 9:2482–96. doi:10.1074/mcp.M110.002113. Available from: http://www.ncbi.nlm.nih.gov/pubmed/20631206

Henry, C. J., Y. Huang, A. Wynne, M. Hanke, J. Himler, M. T. Bailey, J. F. Sheridan, and J. P. Godbout. 2008. Minocycline attenuates lipopolysaccharide (LPS)-induced neuroinflammation, sickness behavior, and anhedonia. J. Neuroinflammation. 5:15. doi:10.1186/1742-2094-5-15. Available from: http://jneuroinflammation.biomedcentral.com/articles/10.1186/1742-2094-5-15

Hewlings, S., and D. Kalman. 2017. Curcumin: A Review of Its' Effects on Human Health. Foods. 6:92. doi:10.3390/foods6100092. Available from: http://www.ncbi.nlm.nih.gov/pubmed/29065496

Ho, A. S., Y. Liu, T. A. Khan, D. H. Hsu, J. F. Bazan, and K. W. Moore. 1993. A receptor for interleukin 10 is related to interferon receptors. Proc. Natl. Acad. Sci. U. S. A. 90:11267–71. doi:10.1073/PNAS.90.23.11267. Available from: http://www.ncbi.nlm.nih.gov/pubmed/8248239

Holzlechner, M., K. Strasser, E. Zareva, L. Steinhäuser, H. Birnleitner, A. Beer, M. Bergmann, R. Oehler, and M. Marchetti-Deschmann. 2017. In Situ Characterization of Tissue-Resident Immune Cells by MALDI Mass Spectrometry Imaging. J. Proteome Res. 16:65–76. doi:10.1021/acs.jproteome.6b00610. Available from: http://pubs.acs.org/doi/10.1021/acs.jproteome.6b00610

Honess, P. E., C. Marin, A. P. Brown, and S. E. Wolfensohn. 2005. Assessment of stress in non-human primates: Application of the neutrophil activation test. Anim. Welf. 14:291–295. Available from: https://www.ingentaconnect.com/content/ufaw/aw/2005/00000014/00000004/art00004

Horowitz, J. F., S. W. Coppack, and S. Klein. 2001. Whole-body and adipose tissue glucose metabolism in response to short-term fasting in lean and obese women. Am. J. Clin. Nutr. 73:517–522. doi:10.1093/ajcn/73.3.517. Available from: https://academic.oup.com/ajcn/article/73/3/517/4737345

Hosokawa, N., T. Hara, T. Kaizuka, C. Kishi, A. Takamura, Y. Miura, S. Iemura, T. Natsume, K. Takehana, N. Yamada, J.-L. Guan, N. Oshiro, and N. Mizushima. 2009. Nutrient-dependent mTORC1 Association with the ULK1–Atg13–FIP200 Complex Required for Autophagy. S. L. Schmid, editor. Mol. Biol. Cell. 20:1981–1991. doi:10.1091/mbc.e08-12-1248. Available from: http://www.molbiolcell.org/doi/10.1091/mbc.e08-12-1248

Hsu, H., H.-B. Shu, M.-G. Pan, and D. V Goeddel. 1996. TRADD–TRAF2 and TRADD–FADD Interactions Define Two Distinct TNF Receptor 1 Signal Transduction Pathways. Cell. 84:299–308. doi:10.1016/S0092-8674(00)80984-8. Available from: https://www.sciencedirect.com/science/article/pii/S0092867400809848?via%3Dihub#BIB20

Hunter, D. S., S. J. Hazel, K. L. Kind, H. Liu, D. Marini, L. C. Giles, M. J. De Blasio, J. A. Owens, J. B. Pitcher, and K. L. Gatford. 2015. Placental and fetal growth restriction, size at birth and neonatal growth alter cognitive function and behaviour in sheep in an age- and sex-specific manner. Physiol. Behav. 152:1–10. doi:10.1016/J.PHYSBEH.2015.08.042. Available from: https://www.sciencedirect.com/science/article/abs/pii/S0031938415300962

Janeway Jr., C. A., P. Travers, M. Walport, and M. J. Shlomchik. 2001. Immunobiology: the immune system in health and disease. 5th ed. (S. Gibbs, M. Dtizel, E. Hunt, M. Morales, and L. Cegielka, editors.). Garland Publishing, New York. Available from: http://www.mta.ca/pshl/docs/janewayimmunobiology8.pdf

Jenkins, T. C., and N. Fotouhi. 1990. Effects of lecithin and corn oil on site of digestion, ruminal fermentation and microbial protein synthesis in sheep. J. Anim. Sci. 68:460–6. Available from: http://www.ncbi.nlm.nih.gov/pubmed/2312434

Jensen, T. E., and E. A. Richter. 2012. Regulation of glucose and glycogen metabolism during and after exercise. J. Physiol. 590:1069–76. doi:10.1113/jphysiol.2011.224972. Available from: http://www.ncbi.nlm.nih.gov/pubmed/22199166

Jones, D. L., and A. J. Wagers. 2008. No place like home: anatomy and function of the stem cell niche. Nat. Rev. Mol. Cell Biol. 9:11–21. doi:10.1038/nrm2319. Available from: http://www.nature.com/doifinder/10.1038/nrm2319

Joyce, B. J., S. Louey, M. G. Davey, M. L. Cock, S. B. Hooper, and R. Harding. 2001. Compromised Respiratory Function in Postnatal Lambs after Placental Insufficiency and Intrauterine Growth Restriction. Pediatr. Res. 50:641–649. doi:10.1203/00006450-200111000-00018. Available from: http://www.nature.com/doifinder/10.1203/00006450-200111000-00018

Karin, M. 1999. How NF-κB is activated: The role of the IκB kinase (IKK) complex. Oncogene. 18:6867–6874. doi:10.1038/sj.onc.1203219. Available from:

http://www.nature.com/articles/1203219

Kayagaki, N., M. T. Wong, I. B. Stowe, S. R. Ramani, L. C. Gonzalez, S. Akashi-Takamura, K. Miyake, J. Zhang, W. P. Lee, A. Muszyński, L. S. Forsberg, R. W. Carlson, and V. M. Dixit. 2013. Noncanonical inflammasome activation by intracellular LPS independent of TLR4. Science. 341:1246–9. doi:10.1126/science.1240248. Available from: http://www.ncbi.nlm.nih.gov/pubmed/23887873

Keller, C., A. Steensberg, A. K. Hansen, C. P. Fischer, P. Plomgaard, and B. K. Pedersen. 2005. Effect of exercise, training, and glycogen availability on IL-6 receptor expression in human skeletal muscle. J. Appl. Physiol. 99:2075–2079. doi:10.1152/japplphysiol.00590.2005. Available from: http://www.physiology.org/doi/10.1152/japplphysiol.00590.2005

Kemppainen, J., T. Fujimoto, K. K. Kalliokoski, T. Viljanen, P. Nuutila, and J. Knuuti. 2002. Myocardial and skeletal muscle glucose uptake during exercise in humans. J. Physiol. 542:403–12. doi:10.1113/JPHYSIOL.2002.018135. Available from: http://www.ncbi.nlm.nih.gov/pubmed/12122141

Krook, A., M. Björnholm, D. Galuska, X. J. Jiang, R. Fahlman, M. G. Myers, H. Wallberg-Henriksson, and J. R. Zierath. 2000. Characterization of signal transduction and glucose transport in skeletal muscle from type 2 diabetic patients. Diabetes. 49:284–292. doi:10.2337/diabetes.49.2.284. Available from: http://diabetes.diabetesjournals.org/content/diabetes/49/2/284.full.pdf

Larsson, L., L. Edström, B. Lindegren, L. Gorza, and S. Schiaffino. 1991. MHC composition and enzyme-histochemical and physiological properties of a novel fast-twitch motor unit type. Am. J. Physiol. 261:C93–C101. Available from: https://www.physiology.org/doi/pdf/10.1152/ajpcell.1991.261.1.C93

Laskowska, M., B. Leszczyńska-Gorzelak, K. Laskowska, and J. Oleszczuk. 2006. Evaluation of maternal and umbilical serum TNFα levels in preeclamptic pregnancies in the intrauterine normal and growth-restricted fetus. J. Matern. Neonatal Med. 19:347–351. doi:10.1080/14767050600637937. Available from: http://www.tandfonline.com/doi/full/10.1080/14767050600637937

Lata, S., and G. P. S. Raghava. 2008. CytoPred: a server for prediction and classification of cytokines. Protein Eng. Des. Sel. 21:279–282. doi:10.1093/protein/gzn006. Available from: https://academic.oup.com/peds/article-lookup/doi/10.1093/protein/gzn006

Lavin, Y., D. Winter, R. Blecher-Gonen, E. David, H. Keren-Shaul, M. Merad, S. Jung, and I. Amit. 2014. Tissue-Resident Macrophage Enhancer Landscapes Are Shaped by the Local Microenvironment. Cell. 159:1312–1326. doi:10.1016/J.CELL.2014.11.018. Available from: https://www.sciencedirect.com/science/article/pii/S0092867414014494?via%3Dihub

Lee, E. J., and C. Tournier. 2011. The requirement of uncoordinated 51-like kinase 1 (ULK1) and ULK2 in the regulation of autophagy. Autophagy. 7:689–695. doi:10.4161/auto.7.7.15450. Available from: http://www.ncbi.nlm.nih.gov/pubmed/21460635

Leney, S. E., and J. M. Tavaré. 2009. The molecular basis of insulin-stimulated glucose uptake: signalling, trafficking and potential drug targets. J. Endocrinol. 203:1–18. doi:10.1677/JOE-09-0037. Available from: http://www.ncbi.nlm.nih.gov/pubmed/19389739

Levine, S., and O. Muneyyirci-Delale. 2018. Stress-Induced Hyperprolactinemia: Pathophysiology and Clinical Approach. Obstet. Gynecol. Int. 2018:1–6. doi:10.1155/2018/9253083. Available from: http://www.ncbi.nlm.nih.gov/pubmed/30627169

Li, L., J. C. Chambard, M. Karin, and E. N. Olson. 1992. Fos and Jun repress transcriptional activation by myogenin and MyoD: The amino terminus of Jun can mediate repression. Genes Dev. 6:676–689. doi:10.1101/gad.6.4.676. Available from: http://www.ncbi.nlm.nih.gov/pubmed/1313772

Li, Y.-P., and M. B. Reid. 2000. NF-κB mediates the protein loss induced by TNF-α in differentiated skeletal muscle myotubes. Am. J. Physiol. - Regul. Integr. Comp. Physiol. 279:R1165–R1170. doi:10.1152/ajpregu.2000.279.4.R1165. Available from: http://www.physiology.org/doi/10.1152/ajpregu.2000.279.4.R1165

Limesand, S. W., P. J. Rozance, L. D. Brown, W. W. Hay, and Jr. 2009. Effects of chronic hypoglycemia and euglycemic correction on lysine metabolism in fetal sheep. Am. J. Physiol. Endocrinol. Metab. 296:E879-87. doi:10.1152/ajpendo.90832.2008. Available from: http://www.ncbi.nlm.nih.gov/pubmed/19190258

Limesand, S. W., P. J. Rozance, D. Smith, and W. W. Hay. 2007. Increased insulin sensitivity and maintenance of glucose utilization rates in fetal sheep with placental insufficiency and intrauterine growth restriction. AJP Endocrinol. Metab. 293:E1716–E1725. doi:10.1152/ajpendo.00459.2007. Available from: http://www.ncbi.nlm.nih.gov/pubmed/17895285

Liu, Y.-Z., Y.-X. Wang, and C.-L. Jiang. 2017. Inflammation: The Common Pathway of Stress-Related Diseases. Front. Hum. Neurosci. 11:316. doi:10.3389/fnhum.2017.00316. Available from: http://www.ncbi.nlm.nih.gov/pubmed/28676747

Macko, A. R., D. T. Yates, X. Chen, L. A. Shelton, A. C. Kelly, M. A. Davis, L. E. Camacho, M. J. Anderson, and S. W. Limesand. 2016. Adrenal Demedullation and Oxygen Supplementation Independently Increase Glucose-Stimulated Insulin Concentrations in Fetal Sheep With Intrauterine Growth Restriction. Endocrinology. 157:2104–2115. doi:10.1210/en.2015-1850. Available from: http://www.ncbi.nlm.nih.gov/pubmed/26937714

Mariely Jaguezeski, A., G. Perin, R. Boaretto Crecencio, M. Dellaméa Baldissera, L. Moura Stefani, and A. Schafer da Silva. 2018. Pub. 297 Addition of Curcumin in Dairy Sheep Diet in the Control of Subclinical Mastitis. 46:297. Available from: http://www.ufrgs.br/actavet/46-suple-1/CR_297.pdf

Martinez, F. O., and S. Gordon. 2014. The M1 and M2 paradigm of macrophage activation: time for reassessment. F1000Prime Rep. 6:13. doi:10.12703/P6-13. Available from: http://www.ncbi.nlm.nih.gov/pubmed/24669294

Martinez, F. O., R. E. Jonkers, M. N. Hylkema, J. Hamann, B. N. Melgert, and M. D. B. van de Garde. 2014. Chronic Exposure to Glucocorticoids Shapes Gene Expression and Modulates Innate and Adaptive Activation Pathways in Macrophages with Distinct Changes in Leukocyte Attraction. J. Immunol. 192:1196–1208. doi:10.4049/jimmunol.1302138. Available from: http://www.ncbi.nlm.nih.gov/pubmed/24395918

McCarthy, J. J., J. Mula, M. Miyazaki, R. Erfani, K. Garrison, A. B. Farooqui, R. Srikuea, B. A. Lawson, B. Grimes, C. Keller, G. Van Zant, K. S. Campbell, K. A. Esser,

E. E. Dupont-Versteegden, and C. A. Peterson. 2011. Effective fiber hypertrophy in satellite cell-depleted skeletal muscle. Development. 138:3657–66. doi:10.1242/dev.068858. Available from: http://www.ncbi.nlm.nih.gov/pubmed/21828094

McCracken, S. A., E. Gallery, and J. M. Morris. 2004. Pregnancy-specific down-regulation of NF-kappa B expression in T cells in humans is essential for the maintenance of the cytokine profile required for pregnancy success. J. Immunol. 172:4583–91. doi:10.4049/JIMMUNOL.172.7.4583. Available from: http://www.ncbi.nlm.nih.gov/pubmed/15034076

Medzhitov, R. 2008. Origin and physiological roles of inflammation. Nature. 454:428–435. doi:10.1038/nature07201. Available from: http://www.nature.com/articles/nature07201

Meshkani, R., and S. Vakili. 2016. Tissue resident macrophages: Key players in the pathogenesis of type 2 diabetes and its complications. Clin. Chim. Acta. 462:77–89. doi:10.1016/J.CCA.2016.08.015. Available from: https://www.sciencedirect.com/science/article/pii/S0009898116303552?via%3Dihub#bb0025

MIKKOLA, H., C. GEKAS, S. ORKIN, and F. DIETERLENLIEVRE. 2005. Placenta as a site for hematopoietic stem cell development. Exp. Hematol. 33:1048–1054. doi:10.1016/j.exphem.2005.06.011. Available from: http://www.ncbi.nlm.nih.gov/pubmed/16140153

Mikkola, H. K. A., S. H. Orkin, A. Kazarov, J. C. Papadimitriou, and G. Keller. 2006. The journey of developing hematopoietic stem cells. Development. 133:3733–44. doi:10.1242/dev.02568. Available from: http://www.ncbi.nlm.nih.gov/pubmed/9435292

Mitchell, P. J., S. E. Johnson, and K. Hannon. 2002. Insulin-like growth factor I stimulates myoblast expansion and myofiber development in the limb. Dev. Dyn. 223:12–23. doi:10.1002/dvdy.1227. Available from: http://doi.wiley.com/10.1002/dvdy.1227

Mizgier, M. L., M. Casas, A. Contreras-Ferrat, P. Llanos, and J. E. Galgani. 2014. Potential role of skeletal muscle glucose metabolism on the regulation of insulin secretion. Obes. Rev. 15:587–597. doi:10.1111/obr.12166. Available from: http://doi.wiley.com/10.1111/obr.12166

Molkentin, J. D., B. L. Black, J. F. Martin, and E. N. Olson. 1995. Cooperative activation of muscle gene expression by MEF2 and myogenic bHLH proteins. Cell. 83:1125–1136. doi:10.1016/0092-8674(95)90139-6. Available from: https://www.sciencedirect.com/science/article/pii/0092867495901396

Morey, J. N., I. A. Boggero, A. B. Scott, and S. C. Segerstrom. 2015. Current Directions in Stress and Human Immune Function. Curr. Opin. Psychol. 5:13–17. doi:10.1016/j.copsyc.2015.03.007. Available from: http://www.ncbi.nlm.nih.gov/pubmed/26086030

Morgan, J. E., and T. A. Partridge. 2003. Muscle satellite cells. Int. J. Biochem. Cell Biol. 35:1151–1156. doi:10.1016/S1357-2725(03)00042-6. Available from: https://www.sciencedirect.com/science/article/pii/S1357272503000426?via%3Dihub

Moser, B., M. Wolf, A. Walz, and P. Loetscher. 2004. Chemokines: multiple levels of leukocyte migration control☆. Trends Immunol. 25:75–84.

doi:10.1016/J.IT.2003.12.005. Available from: https://www.sciencedirect.com/science/article/pii/S1471490603003867

Mosmann, T. R., H. Cherwinski, M. W. Bond, M. A. Giedlin, and R. L. Coffman. 1986. Two types of murine helper T cell clone. I. Definition according to profiles of lymphokine activities and secreted proteins. J. Immunol. 136:2348–57. Available from: http://www.ncbi.nlm.nih.gov/pubmed/2419430

Mourkioti, F., and N. Rosenthal. 2008a. NF-κB signaling in skeletal muscle: prospects for intervention in muscle diseases. J. Mol. Med. 86:747–759. doi:10.1007/s00109-008-0308-4. Available from: http://link.springer.com/10.1007/s00109-008-0308-4

Mourkioti, F., and N. Rosenthal. 2008b. NF-kappaB signaling in skeletal muscle: prospects for intervention in muscle diseases. J. Mol. Med. (Berl). 86:747–59. doi:10.1007/s00109-008-0308-4. Available from: http://www.ncbi.nlm.nih.gov/pubmed/18246321

Mourkioti, F., and N. Rosenthal. 2008c. NF-κB signaling in skeletal muscle: prospects for intervention in muscle diseases. J. Mol. Med. 86:747–759. doi:10.1007/s00109-008-0308-4. Available from: http://link.springer.com/10.1007/s00109-008-0308-4

Müller, U., P. Vogel, G. Alber, and G. Schaub. 2008. The innate immune system of mammals and insects. Contrib. Microbiol. 15:21–44. doi:10.1159/000135684. Available from: http://www.ncbi.nlm.nih.gov/pubmed/18511854

Muñoz-Cánoves, P., C. Scheele, B. K. Pedersen, and A. L. Serrano. 2013. Interleukin-6 myokine signaling in skeletal muscle: a double-edged sword? FEBS J. 280:4131–4148. doi:10.1111/febs.12338. Available from: http://doi.wiley.com/10.1111/febs.12338

Na, L.-X., Y. Li, H.-Z. Pan, X.-L. Zhou, D.-J. Sun, M. Meng, X.-X. Li, and C.-H. Sun. 2013. Curcuminoids exert glucose-lowering effect in type 2 diabetes by decreasing serum free fatty acids: a double-blind, placebo-controlled trial. Mol. Nutr. Food Res. 57:1569–1577. doi:10.1002/mnfr.201200131. Available from: http://www.ncbi.nlm.nih.gov/pubmed/22930403

Nelms, K., A. D. Keegan, J. Zamorano, J. J. Ryan, and W. E. Paul. 1999. THE IL-4 RECEPTOR: Signaling Mechanisms and Biologic Functions. Annu. Rev. Immunol. 17:701–738. doi:10.1146/annurev.immunol.17.1.701. Available from: http://www.annualreviews.org/doi/10.1146/annurev.immunol.17.1.701

Nelson, D. L., M. M. Cox, and A. L. Lehninger. 2008. Lehninger Principles of Biochemistry. Macmillan Learning. Available from: http://www.esalq.usp.br/lepse/imgs/conteudo_thumb/mini/Principles-of-Biochemistry-by-ALbert-Leningher.pdf

Nikolovski, J., G. N. Stamatas, N. Kollias, and B. C. Wiegand. 2008. Barrier Function and Water-Holding and Transport Properties of Infant Stratum Corneum Are Different from Adult and Continue to Develop through the First Year of Life. J. Invest. Dermatol. 128:1728–1736. doi:10.1038/SJ.JID.5701239. Available from: https://www.sciencedirect.com/science/article/pii/S0022202X15339439?via%3Dihub

Oehler, L., O. Majdic, W. F. Pickl, J. Stöckl, E. Riedl, J. Drach, K. Rappersberger, K. Geissler, and W. Knapp. 1998. Neutrophil granulocyte-committed cells can be driven to acquire dendritic cell characteristics. J. Exp. Med. 187:1019–28. doi:10.1084/JEM.187.7.1019. Available from: http://www.ncbi.nlm.nih.gov/pubmed/9529318

Ogilvy-Stuart, A. L., S. J. Hands, C. J. Adcock, J. M. P. Holly, D. R. Matthews, V. Mohamed-Ali, J. S. Yudkin, A. R. Wilkinson, and D. B. Dunger. 1998. Insulin, Insulin-Like Growth Factor I (IGF-I), IGF-Binding Protein-1, Growth Hormone, and Feeding in the Newborn. J. Clin. Endocrinol. Metab. 83:3550–3557. doi:10.1210/jcem.83.10.5162. Available from: http://www.ncbi.nlm.nih.gov/pubmed/9768663

Opal, S. M., and V. A. DePalo. 2000. Anti-Inflammatory Cytokines. Chest. 117:1162–1172. doi:10.1378/CHEST.117.4.1162. Available from: https://www.sciencedirect.com/science/article/pii/S0012369215328208

Padgett, D. A., and R. Glaser. 2003. How stress influences the immune response. Trends Immunol. 24:444–8. doi:10.1016/S1471-4906(03)00173-X. Available from: http://www.ncbi.nlm.nih.gov/pubmed/12909458

Padoan, A., S. Rigano, E. Ferrazzi, B. L. Beaty, F. C. Battaglia, and H. L. Galan. 2004. Differences in fat and lean mass proportions in normal and growth-restricted fetuses. In: American Journal of Obstetrics and Gynecology. Vol. 191. Mosby. p. 1459–1464. Available from: https://www.sciencedirect.com/science/article/pii/S0002937804006453?via%3Dihub

Pagenkemper, M., and A. Diemert. 2014. Monitoring fetal immune development in human pregnancies: current concepts and future goals. J. Reprod. Immunol. 104–105:49–53. doi:10.1016/J.JRI.2014.06.001. Available from: https://www.sciencedirect.com/science/article/pii/S0165037814000618#bib0020

Paulin, D., and Z. Li. 2004. Desmin: a major intermediate filament protein essential for the structural integrity and function of muscle. Exp. Cell Res. 301:1–7. doi:10.1016/J.YEXCR.2004.08.004. Available from: https://www.sciencedirect.com/science/article/pii/S0014482704004501?via%3Dihub

Pearce, L. R., D. Komander, and D. R. Alessi. 2010. The nuts and bolts of AGC protein kinases. Nat. Rev. Mol. Cell Biol. 11:9–22. doi:10.1038/nrm2822. Available from: http://www.nature.com/articles/nrm2822

Pedersen, B. K., and M. A. Febbraio. 2008. Muscle as an Endocrine Organ: Focus on Muscle-Derived Interleukin-6. Physiol. Rev. 88:1379–1406. doi:10.1152/physrev.90100.2007. Available from: http://www.ncbi.nlm.nih.gov/pubmed/18923185

Peng, Y.-L., Y.-N. Liu, L. Liu, X. Wang, C.-L. Jiang, and Y.-X. Wang. 2012. Inducible nitric oxide synthase is involved in the modulation of depressive behaviors induced by unpredictable chronic mild stress. J. Neuroinflammation. 9:564. doi:10.1186/1742-2094-9-75. Available from: http://jneuroinflammation.biomedcentral.com/articles/10.1186/1742-2094-9-75

Petersen, K. F., and G. I. Shulman. 2002. Pathogenesis of skeletal muscle insulin resistance in type 2 diabetes mellitus. Am. J. Cardiol. 90:11–18. doi:10.1016/S0002-9149(02)02554-7. Available from: https://www.sciencedirect.com/science/article/pii/S0002914902025547

Pinto-Junior, D. C., K. S. Silva, M. L. Michalani, C. Y. Yonamine, J. V. Esteves, N. T. Fabre, K. Thieme, S. Catanozi, M. M. Okamoto, P. M. Seraphim, M. L. Corrêa-Giannella, M. Passarelli, and U. F. Machado. 2018. Advanced glycation end products-induced insulin resistance involves repression of skeletal muscle GLUT4 expression. Sci. Rep. 8:8109. doi:10.1038/s41598-018-26482-6. Available from:

http://www.nrcresearchpress.com/doi/10.1139/H09-047

Plomgaard, P., K. Bouzakri, R. Krogh-Madsen, B. Mittendorfer, J. R. Zierath, and B. K. Pedersen. 2005. Tumor necrosis factor-alpha induces skeletal muscle insulin resistance in healthy human subjects via inhibition of Akt substrate 160 phosphorylation. Diabetes. 54:2939–45. Available from: http://www.ncbi.nlm.nih.gov/pubmed/16186396

Podbregar, M., M. Lainscak, O. Prelovsek, and T. Mars. 2013. Cytokine response of cultured skeletal muscle cells stimulated with proinflammatory factors depends on differentiation stage. ScientificWorldJournal. 2013:617170. doi:10.1155/2013/617170. Available from: http://www.ncbi.nlm.nih.gov/pubmed/23509435

Posont, R. J., K. A. Beede, S. W. Limesand, and D. T. Yates. 2018. Changes in myoblast responsiveness to TNFα and IL-6 contribute to decreased skeletal muscle mass in intrauterine growth restricted fetal sheep. Transl. Anim. Sci. 2:S44–S47. doi:10.1093/tas/txy038. Available from: http://www.ncbi.nlm.nih.gov/pubmed/30627704

Puimège, L., C. Libert, and F. Van Hauwermeiren. 2014. Regulation and dysregulation of tumor necrosis factor receptor-1. Cytokine Growth Factor Rev. 25:285–300. doi:10.1016/J.CYTOGFR.2014.03.004. Available from: https://www.sciencedirect.com/science/article/pii/S1359610114000240?via%3Dihub

Punch, V. G., A. E. Jones, and M. A. Rudnicki. 2009. Transcriptional networks that regulate muscle stem cell function. Wiley Interdiscip. Rev. Syst. Biol. Med. 1:128–140. doi:10.1002/wsbm.11. Available from: http://doi.wiley.com/10.1002/wsbm.11

Qing, G., P. Yan, Z. Qu, H. Liu, and G. Xiao. 2007. Hsp90 regulates processing of NF-κB2 p100 involving protection of NF-κB-inducing kinase (NIK) from autophagy-mediated degradation. Cell Res. 17:520–530. doi:10.1038/cr.2007.47. Available from: http://www.nature.com/articles/cr200747

Quinn, K. E., S. Z. Prosser, K. K. Kane, and R. L. Ashley. 2017. Inhibition of chemokine (C-X-C motif) receptor four (CXCR4) at the fetal-maternal interface during early gestation in sheep: alterations in expression of chemokines, angiogenic factors and their receptors1. J. Anim. Sci. 95:1144–11153. doi:10.2527/jas.2016.1271. Available from: https://academic.oup.com/jas/article/95/3/1144/4703735

Reichardt, H. M., J. P. Tuckermann, M. Göttlicher, M. Vujic, F. Weih, P. Angel, P. Herrlich, and G. Schütz. 2001. Repression of inflammatory responses in the absence of DNA binding by the glucocorticoid receptor. EMBO J. 20:7168–7173. doi:10.1093/emboj/20.24.7168. Available from: http://www.ncbi.nlm.nih.gov/pubmed/11742993

Reid, M. B., and Y. P. Li. 2001. Cytokines and oxidative signalling in skeletal muscle. In: Acta Physiologica Scandinavica. Vol. 171. Wiley/Blackwell (10.1111). p. 225–232. Available from: http://doi.wiley.com/10.1046/j.1365-201x.2001.00824.x

Reyna, S. M., S. Ghosh, P. Tantiwong, C. S. R. M. Meka, P. Eagan, C. P. Jenkinson, E. Cersosimo, R. A. Defronzo, D. K. Coletta, A. Sriwijitkamol, and N. Musi. 2008. Elevated toll-like receptor 4 expression and signaling in muscle from insulin-resistant subjects. Diabetes. 57:2595–2602. doi:10.2337/db08-0038. Available from: http://www.ncbi.nlm.nih.gov/pubmed/18633101

Rivard, A., N. Principe, and V. Andrés. 2000. Age-dependent increase in c-fos activity and cyclin A expression in vascular smooth muscle cells A potential link between aging, smooth muscle cell proliferation and atherosclerosis. Cardiovasc. Res. 45:1026–1034.

doi:10.1016/S0008-6363(99)00385-5. Available from: https://academic.oup.com/cardiovascres/article-lookup/doi/10.1016/S0008-6363(99)00385-5

Rose-John, S. 2012. IL-6 trans-signaling via the soluble IL-6 receptor: importance for the pro-inflammatory activities of IL-6. Int. J. Biol. Sci. 8:1237–47. doi:10.7150/ijbs.4989. Available from: http://www.ncbi.nlm.nih.gov/pubmed/23136552

Rosenthal, S. M., and Z. Q. Cheng. 1995. Opposing early and late effects of insulin-like growth factor I on differentiation and the cell cycle regulatory retinoblastoma protein in skeletal myoblasts. Proc. Natl. Acad. Sci. U. S. A. 92:10307–11. Available from: http://www.ncbi.nlm.nih.gov/pubmed/7479773

Rozance, P. J., L. Zastoupil, S. R. Wesolowski, D. A. Goldstrohm, B. Strahan, M. Cree-Green, M. Sheffield-Moore, G. Meschia, W. W. Hay, R. B. Wilkening, and L. D. Brown. 2018. Skeletal muscle protein accretion rates and hindlimb growth are reduced in late gestation intrauterine growth-restricted fetal sheep. J. Physiol. 596:67–82. doi:10.1113/JP275230. Available from: http://doi.wiley.com/10.1113/JP275230

Rudnicki, M. A., P. N. J. Schnegelsberg, R. H. Stead, T. Braun, H.-H. Arnold, and R. Jaenisch. 1993. MyoD or Myf-5 is required for the formation of skeletal muscle. Cell. 75:1351–1359. doi:10.1016/0092-8674(93)90621-V. Available from: https://www.sciencedirect.com/science/article/pii/009286749390621V?via%3Dihub

Sambasivan, R., and S. Tajbakhsh. 2007. Skeletal muscle stem cell birth and properties. Semin. Cell Dev. Biol. 18:870–882. doi:10.1016/J.SEMCDB.2007.09.013. Available from: https://www.sciencedirect.com/science/article/pii/S1084952107001553

Sano, H., S. Kane, E. Sano, C. P. Mîinea, J. M. Asara, W. S. Lane, C. W. Garner, and G. E. Lienhard. 2003. Insulin-stimulated phosphorylation of a Rab GTPase-activating protein regulates GLUT4 translocation. J. Biol. Chem. 278:14599–602. doi:10.1074/jbc.C300063200. Available from: http://www.ncbi.nlm.nih.gov/pubmed/12637568

Sarbassov, D. D., D. A. Guertin, S. M. Ali, and D. M. Sabatini. 2005. Phosphorylation and regulation of Akt/PKB by the rictor-mTOR complex. Science. 307:1098–101. doi:10.1126/science.1106148. Available from: http://www.ncbi.nlm.nih.gov/pubmed/15718470

Sassoon, D. A., I. Garner, M. Buckingham, H. Arnold, and M. Buckingham. 1988. Transcripts of alpha-cardiac and alpha-skeletal actins are early markers for myogenesis in the mouse embryo. Development. 104:155–64. Available from: http://www.ncbi.nlm.nih.gov/pubmed/3075543

Schiaffino, S., and C. Reggiani. 2011. Fiber Types in Mammalian Skeletal Muscles. Physiol. Rev. 91:1447–1531. doi:10.1152/physrev.00031.2010. Available from: http://www.physiology.org/doi/10.1152/physrev.00031.2010

Schnyder, S., and C. Handschin. 2015. Skeletal muscle as an endocrine organ: PGC-1α, myokines and exercise. Bone. 80:115–125. doi:10.1016/j.bone.2015.02.008. Available from: http://www.ncbi.nlm.nih.gov/pubmed/26453501

Schroers, A., O. Hecht, K. Kallen, M. Pachta, S. Rose-John, and J. Grötzinger. 2005. Dynamics of the gp130 cytokine complex: A model for assembly on the cellular membrane. Protein Sci. 14:783–790. doi:10.1110/ps.041117105. Available from: http://doi.wiley.com/10.1110/ps.041117105

Seale, P., L. A. Sabourin, A. Girgis-Gabardo, A. Mansouri, P. Gruss, and M. A. Rudnicki. 2000. Pax7 Is Required for the Specification of Myogenic Satellite Cells. Cell. 102:777–786. doi:10.1016/S0092-8674(00)00066-0. Available from: https://www.sciencedirect.com/science/article/pii/S0092867400000660?via%3Dihub

Sharma, D., S. Shastri, and P. Sharma. 2016. Intrauterine Growth Restriction: Antenatal and Postnatal Aspects. Clin. Med. Insights. Pediatr. 10:67–83. doi:10.4137/CMPed.S40070. Available from: http://www.ncbi.nlm.nih.gov/pubmed/27441006

Shoba, G., D. Joy, T. Joseph, M. Majeed, R. Rajendran, and P. Srinivas. 1998. Influence of Piperine on the Pharmacokinetics of Curcumin in Animals and Human Volunteers. Planta Med. 64:353–356. doi:10.1055/s-2006-957450. Available from: http://www.thieme-connect.de/DOI/DOI?10.1055/s-2006-957450

Silverstein, A. M. 2002. The Clonal Selection Theory: what it really is and why modern challenges are misplaced. Nat. Immunol. 3:793–796. doi:10.1038/ni0902-793. Available from: http://www.nature.com/articles/ni0902-793

Simon, A. K., G. A. Hollander, and A. McMichael. 2015. Evolution of the immune system in humans from infancy to old age. Proceedings. Biol. Sci. 282:20143085. doi:10.1098/rspb.2014.3085. Available from: http://www.ncbi.nlm.nih.gov/pubmed/26702035

Sironi, M., F. O. Martinez, D. D'Ambrosio, M. Gattorno, N. Polentarutti, M. Locati, A. Gregorio, A. Iellem, M. A. Cassatella, J. Van Damme, S. Sozzani, A. Martini, F. Sinigaglia, A. Vecchi, and A. Mantovani. 2006. Differential regulation of chemokine production by Fc receptor engagement in human monocytes: association of CCL1 with a distinct form of M2 monocyte activation (M2b, Type 2). J. Leukoc. Biol. 80:342–349. doi:10.1189/jlb.1005586. Available from: http://doi.wiley.com/10.1189/jlb.1005586

Slavich, G. M., and M. R. Irwin. 2014. From stress to inflammation and major depressive disorder: a social signal transduction theory of depression. Psychol. Bull. 140:774–815. doi:10.1037/a0035302. Available from: http://www.ncbi.nlm.nih.gov/pubmed/24417575

Soto, S. M., A. C. Blake, S. R. Wesolowski, P. J. Rozance, K. B. Barthel, B. Gao, B. Hetrick, C. E. McCurdy, N. G. Garza, W. W. Hay, L. A. Leinwand, J. E. Friedman, and L. D. Brown. 2017. Myoblast replication is reduced in the IUGR fetus despite maintained proliferative capacity in vitro. J. Endocrinol. 232:475–491. doi:10.1530/JOE-16-0123. Available from: http://www.ncbi.nlm.nih.gov/pubmed/28053000

Spangenburg, E. E., and F. W. Booth. 2003. Molecular regulation of individual skeletal muscle fibre types. Acta Physiol. Scand. 178:413–424. doi:10.1046/j.1365-201X.2003.01158.x. Available from: http://doi.wiley.com/10.1046/j.1365-201X.2003.01158.x

Stahl, N., T. G. Boulton, T. Farruggella, N. Y. Ip, S. Davis, B. A. Witthuhn, F. W. Quelle, O. Silvennoinen, G. Barbieri, and S. Pellegrini. 1994. Association and activation of Jak-Tyk kinases by CNTF-LIF-OSM-IL-6 beta receptor components. Science. 263:92–5. Available from: http://www.ncbi.nlm.nih.gov/pubmed/8272873

Sun, L., K. Ma, H. Wang, F. Xiao, Y. Gao, W. Zhang, K. Wang, X. Gao, N. Ip, and Z. Wu. 2007. JAK1-STAT1-STAT3, a key pathway promoting proliferation and preventing premature differentiation of myoblasts. J. Cell Biol. 179:129–38. doi:10.1083/jcb.200703184. Available from:

http://www.ncbi.nlm.nih.gov/pubmed/17908914

Takaishi, H., H. Konishi, H. Matsuzaki, Y. Ono, Y. Shirai, N. Saito, T. Kitamura, W. Ogawa, M. Kasuga, U. Kikkawa, and Y. Nishizuka. 1999. Regulation of nuclear translocation of forkhead transcription factor AFX by protein kinase B. Proc. Natl. Acad. Sci. U. S. A. 96:11836–41. doi:10.1073/PNAS.96.21.11836. Available from: http://www.ncbi.nlm.nih.gov/pubmed/10518537

Talmage, D. W. 1957. Allergy and Immunology. Annu. Rev. Med. 8:239–256. doi:10.1146/annurev.me.08.020157.001323. Available from: http://www.annualreviews.org/doi/10.1146/annurev.me.08.020157.001323

Thorn, S. R., T. R. H. Regnault, L. D. Brown, P. J. Rozance, J. Keng, M. Roper, R. B. Wilkening, W. W. Hay, J. E. Friedman, and J. E. Friedman. 2009. Intrauterine growth restriction increases fetal hepatic gluconeogenic capacity and reduces messenger ribonucleic acid translation initiation and nutrient sensing in fetal liver and skeletal muscle. Endocrinology. 150:3021–30. doi:10.1210/en.2008-1789. Available from: http://www.ncbi.nlm.nih.gov/pubmed/19342452

Thorn, S. R., P. J. Rozance, L. D. Brown, and W. W. Hay. 2011. The intrauterine growth restriction phenotype: Fetal adaptations and potential implications for later life insulin resistance and diabetes. Semin. Reprod. Med. 29:225–236. doi:10.1055/s-0031-1275516. Available from: http://www.ncbi.nlm.nih.gov/pubmed/21710398

Ting, A. T., and M. J. M. Bertrand. 2016. More to Life than NF-kB in TNFR1 Signaling. doi:10.1016/j.it.2016.06.002. Available from: http://dx.doi.org/10.1016/j.it.2016.06.002

Triozzi, P. L., and W. Aldrich. 1997. Phenotypic and functional differences between human dendritic cells derived in vitro from hematopoietic progenitors and from monocytes/macrophages. J. Leukoc. Biol. 61:600–608. doi:10.1002/jlb.61.5.600. Available from: http://doi.wiley.com/10.1002/jlb.61.5.600

Trouche, D., M. Grigoriev, J.-L. Lenormand, P. Robin, S. Alexandre Leibovitch, P. Sassone-Corsi, and A. Harel-Bellan. 1993. Repression of c-fos promoter by MyoD on muscle cell differentiation. Nature. 363:79–82. doi:10.1038/363079a0. Available from: http://www.nature.com/doifinder/10.1038/363079a0

Tu, Y. C., D. Y. Huang, S. G. Shiah, J. S. Wang, and W. W. Lin. 2013. 1DUMMY Regulation of c-Fos gene expression by NF-κB: A p65 homodimer binding site in mouse embryonic fibroblasts but not human HEK293 cells. S. Mummidi, editor. PLoS One. 8:e84062. doi:10.1371/journal.pone.0084062. Available from: http://dx.plos.org/10.1371/journal.pone.0084062

Turner, M. D., B. Nedjai, T. Hurst, and D. J. Pennington. 2014. Cytokines and chemokines: At the crossroads of cell signalling and inflammatory disease. Biochim. Biophys. Acta - Mol. Cell Res. 1843:2563–2582. doi:10.1016/J.BBAMCR.2014.05.014. Available from: https://www.sciencedirect.com/science/article/pii/S0167488914001967#bb0405

Tüzün, E., J. Li, N. Wanasen, L. Soong, and P. Christadoss. 2006. Immunization of mice with T cell-dependent antigens promotes IL-6 and TNF-α production in muscle cells. Cytokine. 35:100–106. doi:10.1016/j.cyto.2006.05.009. Available from: https://www.sciencedirect.com/science/article/pii/S1043466606002122?via%3Dihub

Untergasser, A., I. Cutcutache, T. Koressaar, J. Ye, B. C. Faircloth, M. Remm, and S. G. Rozen. 2012. Primer3—new capabilities and interfaces. Nucleic Acids Res. 40:e115–

e115. Available from: http://dx.doi.org/10.1093/nar/gks596

Valsamakis, G., C. Kanaka-Gantenbein, A. Malamitsi-Puchner, and G. Mastorakos. 2006. Causes of intrauterine growth restriction and the postnatal development of the metabolic syndrome. In: Annals of the New York Academy of Sciences. Vol. 1092. p. 138–147. Available from: http://www.ncbi.nlm.nih.gov/pubmed/17308140

Vogelzangs, N., P. de Jonge, J. H. Smit, S. Bahn, and B. W. Penninx. 2016. Cytokine production capacity in depression and anxiety. Transl. Psychiatry. 6:e825. doi:10.1038/tp.2016.92. Available from: http://www.ncbi.nlm.nih.gov/pubmed/27244234

Wang, Y., and J. E. Pessin. 2013. Mechanisms for fiber-type specificity of skeletal muscle atrophy. Curr. Opin. Clin. Nutr. Metab. Care. 16:243–50. doi:10.1097/MCO.0b013e328360272d. Available from: http://www.ncbi.nlm.nih.gov/pubmed/23493017

Waskiewicz, A. J., and J. A. Cooper. 1995. Mitogen and stress response pathways: MAP kinase cascades and phosphatase regulation in mammals and yeast. Curr. Opin. Cell Biol. 7:798–805. doi:10.1016/0955-0674(95)80063-8. Available from: https://www.sciencedirect.com/science/article/pii/0955067495800638?via%3Dihub

Westwood, M., J. M. Gibson, S. R. Sooranna, S. Ward, J. P. Neilson, and R. Bajoria. 2001. Genes or placenta as modulator of fetal growth: evidence from the insulin-like growth factor axis in twins with discordant growth. Mol. Hum. Reprod. 7:387–395. doi:10.1093/molehr/7.4.387. Available from: https://academic.oup.com/molehr/article-lookup/doi/10.1093/molehr/7.4.387

Wilson, S. J., J. C. McEwan, P. W. Sheard, and A. J. Harris. 1992. Early stages of myogenesis in a large mammal: Formation of successive generations of myotubes in sheep tibialis cranialis muscle. J. Muscle Res. Cell Motil. 13:534–550. doi:10.1007/BF01737996. Available from: http://link.springer.com/10.1007/BF01737996

Wolf, J., S. Rose-John, and C. Garbers. 2014. Interleukin-6 and its receptors: A highly regulated and dynamic system. Cytokine. 70:11–20. doi:10.1016/J.CYTO.2014.05.024. Available from: https://www.sciencedirect.com/science/article/pii/S1043466614001574#b0020

Wolfensohn, S., J. Shotton, H. Bowley, S. Davies, S. Thompson, and W. S. M. Justice. 2018. Assessment of Welfare in Zoo Animals: Towards Optimum Quality of Life. Anim. an open access J. from MDPI. 8. doi:10.3390/ani8070110. Available from: http://www.ncbi.nlm.nih.gov/pubmed/29973560

Wozniak, A. C., J. Kong, E. Bock, O. Pilipowicz, and J. E. Anderson. 2005. Signaling satellite-cell activation in skeletal muscle: Markers, models, stretch, and potential alternate pathways. Muscle and Nerve. 31:283–300. doi:10.1002/mus.20263. Available from: http://doi.wiley.com/10.1002/mus.20263

Yan, J., Z. Feng, J. Liu, W. Shen, Y. Wang, K. Wertz, P. Weber, J. Long, and J. Liu. 2012. Enhanced autophagy plays a cardinal role in mitochondrial dysfunction in type 2 diabetic Goto–Kakizaki (GK) rats: ameliorating effects of (−)-epigallocatechin-3-gallate. J. Nutr. Biochem. 23:716–724. doi:10.1016/J.JNUTBIO.2011.03.014. Available from: https://www.sciencedirect.com/science/article/pii/S0955286311001112?via%3Dihub

Yang, K.-C., X. Ma, H. Liu, J. Murphy, P. M. Barger, D. L. Mann, and A. Diwan. 2015. Tumor Necrosis Factor Receptor-Associated Factor 2 Mediates Mitochondrial Autophagy. Circ. Hear. Fail. 8:175–187.

doi:10.1161/CIRCHEARTFAILURE.114.001635. Available from: http://www.ncbi.nlm.nih.gov/pubmed/25339503

Yates, D. T., C. N. Cadaret, K. A. Beede, H. E. Riley, A. R. Macko, M. J. Anderson, L. E. Camacho, and S. W. Limesand. 2016. Intrauterine growth-restricted sheep fetuses exhibit smaller hindlimb muscle fibers and lower proportions of insulin-sensitive Type I fibers near term. Am. J. Physiol. - Regul. Integr. Comp. Physiol. 310:R1020–R1029. doi:10.1152/ajpregu.00528.2015. Available from: http://www.ncbi.nlm.nih.gov/pubmed/27053651

Yates, D. T., D. S. Clarke, A. R. Macko, M. J. Anderson, L. A. Shelton, M. Nearing, R. E. Allen, R. P. Rhoads, and S. W. Limesand. 2014. Myoblasts from intrauterine growth-restricted sheep fetuses exhibit intrinsic deficiencies in proliferation that contribute to smaller semitendinosus myofibres. J. Physiol. 592:3113–3125. doi:10.1113/jphysiol.2014.272591. Available from: http://www.ncbi.nlm.nih.gov/pubmed/24860171

Yates, D. T., A. R. Macko, M. Nearing, X. Chen, R. P. Rhoads, and S. W. Limesand. 2012. Developmental programming in response to intrauterine growth restriction impairs myoblast function and skeletal muscle metabolism. J. Pregnancy. 2012:631038. doi:10.1155/2012/631038. Available from: http://www.ncbi.nlm.nih.gov/pubmed/22900186

Yates, D. T., J. L. Petersen, T. B. Schmidt, C. N. Cadaret, T. L. Barnes, R. J. Posont, and K. A. Beede. 2018. ASAS-SSR Triennnial Reproduction Symposium: Looking back and moving forward—how reproductive physiology has evolved: Fetal origins of impaired muscle growth and metabolic dysfunction: Lessons from the heat-stressed pregnant ewe. J. Anim. Sci. 96. doi:10.1093/jas/sky164.

Ygberg, S., and A. Nilsson. 2012. The developing immune system - from foetus to toddler. Acta Paediatr. 101:120–127. doi:10.1111/j.1651-2227.2011.02494.x. Available from: http://doi.wiley.com/10.1111/j.1651-2227.2011.02494.x

Yuan, R., S. Geng, and L. Li. 2016. Molecular Mechanisms That Underlie the Dynamic Adaptation of Innate Monocyte Memory to Varying Stimulant Strength of TLR Ligands. Front. Immunol. 7:497. doi:10.3389/fimmu.2016.00497. Available from: http://www.ncbi.nlm.nih.gov/pubmed/27891130

Zammit, P. S., J. P. Golding, Y. Nagata, V. Hudon, T. A. Partridge, and J. R. Beauchamp. 2004. Muscle satellite cells adopt divergent fates: a mechanism for self-renewal? J. Cell Biol. 166:347–57. doi:10.1083/jcb.200312007. Available from: http://www.ncbi.nlm.nih.gov/pubmed/15277541

Zammit, P. S., T. A. Partridge, and Z. Yablonka-Reuveni. 2006. The Skeletal Muscle Satellite Cell: The Stem Cell That Came in From the Cold. J Histochem Cytochem. 54:1177–1191. doi:10.1369/jhc.6R6995.2006. Available from: http://journals.sagepub.com/doi/pdf/10.1369/jhc.6R6995.2006

Zhong, B., X. Liu, X. Wang, X. Liu, H. Li, B. G. Darnay, X. Lin, S. C. Sun, and C. Dong. 2013. Ubiquitin-specific protease 25 regulates TLR4-dependent innate immune responses through deubiquitination of the adaptor protein TRAF3. Sci. Signal. 6:ra35. doi:10.1126/scisignal.2003708. Available from: http://www.ncbi.nlm.nih.gov/pubmed/23674823

Zhu, J., H. Yamane, and W. E. Paul. 2010. Differentiation of effector CD4 T cell

populations (*). Annu. Rev. Immunol. 28:445–89. doi:10.1146/annurev-immunol-030409-101212. Available from: http://www.ncbi.nlm.nih.gov/pubmed/20192806

ZINKERNAGEL, R. M. 1978. Thymus and Lymphohemopoietic Cells: Their Role in T Cell Maturation in Selection of T Cells' H-2-Restriction-Specificity and in H-2 Linked Ir Gene Control. Immunol. Rev. 42:224–270. doi:10.1111/j.1600-065X.1978.tb00264.x. Available from: http://doi.wiley.com/10.1111/j.1600-065X.1978.tb00264.x